CHALMERS
UNIVERSITY OF TECHNOLOGY

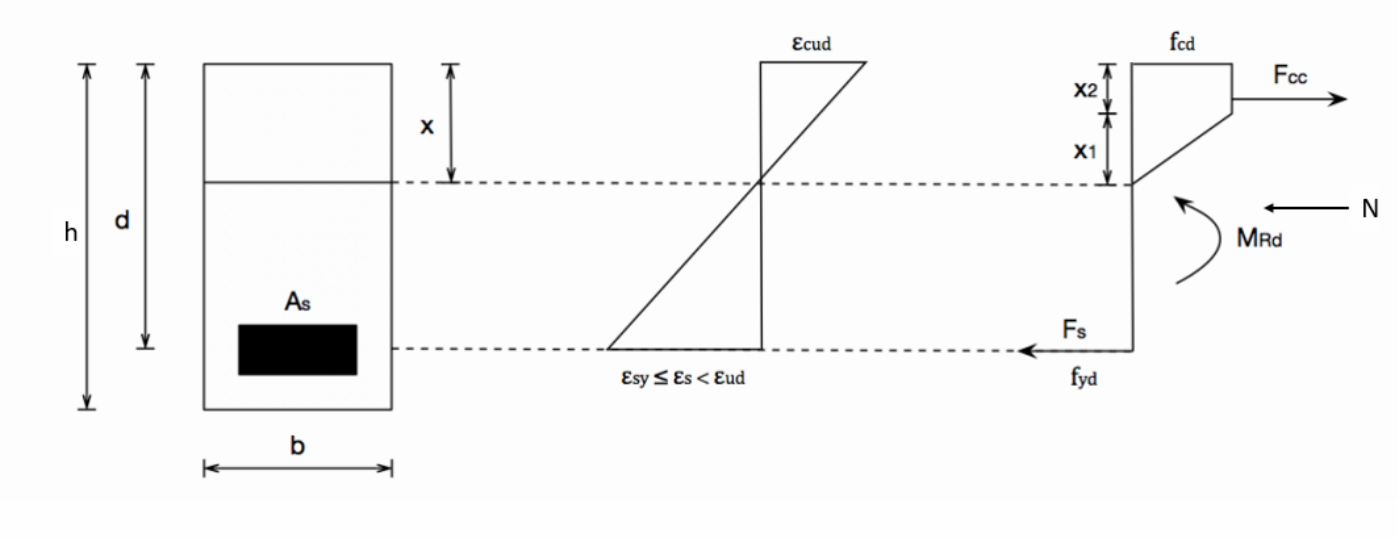

Implementation of High/ Ultra high-Performance Concrete in Design & Production of Conventional Bridge Structures

Master's thesis in Structural Engineering and Building Technology

ABDULRAZAK ALABRASH
KHALED ALYOUSSEF

Department of Architecture and Civil Engineering
Division of Structural Engineering
CHALMERS UNIVERSITY OF TECHNOLOGY
Master's Thesis ACEX30
Gothenburg, Sweden 2022

MASTER'S THESIS ACEX30

Implementation of High/ Ultra high-Performance Concrete in Design & Production of Conventional Bridge Structures

Master's thesis in Structural Engineering and Building Technology

ABDULRAZAK ALABRASH
KHALED ALYOUSSEF

CHALMERS
UNIVERSITY OF TECHNOLOGY

Department of Architecture and Civil Engineering
Division of Structural Engineering
Concrete Structures
CHALMERS UNIVERSITY OF TECHNOLOGY
Göteborg, Sweden 2022

Implementation of High/ Ultra high-Performance Concrete in Design & Production of Conventional Bridge Structures

Master's thesis in Structural Engineering and Building Technology

ABDULRAZAK ALABRASH

KHALED ALYOUSSEF

Examiner: Prof. Ignasi Fernandez, Architecture and Civil Engineering
Supervisor: Ludwig Lundberg, Structural Engineer at AFRY
Supervisor: Thomas Lechner, Dr. tekn at AFRY

Examensarbete ACEX30
Institutionen för arkitektur och samhällsbyggnadsteknik
Chalmers tekniska högskola, 2022

Department of Architecture and Civil Engineering
Division of Structural Engineering
Concrete Structures
Chalmers University of Technology
SE-412 96 Göteborg
Sweden
Telephone: + 46 (0)31-772 1000

Cover:
The cover picture describes the stress and strain distribution of a cross-section made from UHPC.
Department of Architecture and Civil Engineering
Göteborg,Sweden,2022

Implementation of High/ Ultra high-Performance Concrete in Design & Production of Conventional Bridge Structures

Master's thesis in Structural Engineering and Building Technology

ABDULRAZAK ALABRASH

KHALED ALYOUSSEF

Department of Architecture and Civil Engineering
Division of Structural Engineering
Concrete Structures
Chalmers University of Technology

ABSTRACT

Concrete has been used in various applications in civil engineering projects for a long time, and it has also developed over time regarding its strength, durability and performance. The development of concrete technology could achieve new types of concrete, such as high-performance and ultra high-performance concrete (HPC)/(UHPC). Since the 1980s, HPC/UHPC has been widely used in bridge construction worldwide because of its superior properties compared to normal strength reinforced concrete in terms of strength and durability. HPC/UHPC could provide bridges with substantial savings such as longer service life, more slender, higher cross-section capacity, and better durability. However, HPC/UHPC are delayed in Sweden, where only two bridges are built with HPC while no application of UHPC can be found. The lack of standards and experience are among the reasons behind this delayed.

This thesis aims to give a general overview of HPC/UHPC to increase the knowledge about HPC/UHPC from material and design perspectives in Sweden. HPC/UHPC will be used to design a concrete bridge to compare the differences in design between HPC/UHPC and an exciting bridge made from conventional concrete C35/45. The calculation will consider the gaining of moment capacity that can be provided to the cross-section using HPC/UHPC respectively while keeping the same reinforcement. Moreover, the cross-section will be optimised by reducing the thickness and comparing the amount of reinforcement, crack width and deflection. Two case studies are carried out to make a comparison. Case 1 considers the design with HPC (C 90/105) and compares the results with the existing bridge, while case 2 considers the design of UHPC.

Keywords:
High-performance concrete (HPC), ultra-high-performance concrete (UHPC), ultra high-performance fibre reinforced concrete (UHPFRC), normal strength concrete (NC), bridge design, sustainable concrete bridge, cement, moment capacity.

Implementering av hög/ultra högpresterande betong i design och tillverkning av konventionella brokonstruktioner

ABDULRAZAK ALABRASH

KHALED ALYOUSSEF

Institutionen för arkitektur och samhällsbyggnadsteknik
Avdelningen för Konstruktionsteknik och Byggnadsteknologi
Chalmers tekniska högskola

SAMMANFATTNING

Betong har använts i olika applikationer i infrastrukturprojekt under lång tid, och det har också utvecklats över tiden vad gäller dess hållfasthet, hållbarhet och prestanda. Utvecklingen av betongteknik kunde åstadkomma nya typer av betong, såsom högpresterande och ultrahögpresterande betong (HPC)/(UHPC). Sedan 1980-talet har HPC/UHPC använts i stor utsträckning i brokonstruktioner över hela världen på grund av dess överlägsna egenskaper jämfört med normalhållfast armerad betong vad gäller hållfasthet och hållbarhet. HPC/UHPC skulle kunna bidra för broar till betydande besparingar såsom längre livslängd, slimmade, högre tvärsnittskapacitet och bättre hållbarhet. HPC/UHPC är dock försenade i Sverige, där endast två broar byggdes med HPC medan ingen tillämpning av UHPC kan hittas i Sverige. Bristen på standarder och erfarenhet är en av orsakerna bakom detta försenade.

Detta examensarbete syftar till att ge en allmän översikt över HPC/UHPC för att öka kunskapen om HPC/UHPC ur material- och designperspektiv i Sverige. HPC/UHPC kommer att användas för att konstruera en plattrambro för att jämföra skillnaderna i design mellan HPC/UHPC och en bro gjord av konventionell betong C35/45. Beräkningen kommer att beakta ökningen av momentkapacitet som kan tillhandahållas till tvärsnittet med HPC/UHPC respektive samtidigt som samma armering bibehålls. Dessutom kommer tvärsnittet att optimeras genom att minska tjockleken och jämföra mängden förstärkning, sprickbredd och nedböjning. Två fallstudier genomförs för att göra en jämförelse. Fall 1 överväger designen med HPC C 90/105 och jämför resultaten med den befintliga bron, medan fall 2 tar hänsyn till designen av UHPC.

Nyckelord:
Högpresterande betong (HPC), ultrahögpresterande betong (UHPC), ultrahögpresterande fiberarmerad betong (UHPFRC), normalhållfast betong (NC), brodesign, hållbar betongbro, cement, momentkapacitet.

Contents

Preface

The thesis has been carried out from January 2022 to June 2022 at the Department of Structural Engineering, Concrete Structures, Chalmers University of Technology, in collaboration with AFRY, Gothenburg, Sweden.

The authors would like to express gratitude to AFRY for giving this exciting proposal to work with and for their support and guidance. We would like to extend our gratitude to Associate Professor Ignasi Fernandez for the assistance and advice during this work. We would also like to thank our supervisors from AFRY, Thomas Lechner and Ludwig Lundberg, for their help and guidance.

Finally, we would like to thank our families for their encouragement and patience during this long journey.

Göteborg June 2022

Abdulrazak Alabrash & Khaled Alyoussef

Notations

Roman upper-case letters

A_c	Gross area of the cross-section
$A_{c,eff}$	Effective cross-sectional area
A_f	Fracture energy
A_{fv}	Area of rectangular cross section
A_s	Longitudinal reinforcement area
$A_{s,bot}$	Area of reinforcement in the bottom side of the bridge
$A_{s.top}$	Area of reinforcement in the top side of the bridge
$A_{s.w}$	Area of shear reinforcement
$A_{sw,erq}$	Required shear reinforcement
CO_2	Carbon dioxide emissions
E	Young's modulus
E_{cm}	Concrete modulus of elasticity (mean value)
E_s	Steel modulus of elasticity
F_{cc}	Concrete force in compression at ULS
F_s	Tensile force of reinforcement
G_f	Facture energy
I_c	Moment of inertia
I_{tr}	Transformed moment of inertia
K	Orientation factor expressing the mechanical effect of the fibres
K_c	Critical stress intensity factor
K_{global}	Orientation factor related to global effects
L	Total length of the bridge
L_c	Characteristic length that relates the crack width to deformation
L_f	Fibre length
L_s	Crack width
M_c	Moment from the dead load
M_{cr}	Cracking moment
M_{Ed}	Design moment
$M_{Ed,ch}$	Characteristic moment from LM71 (train load)
$M_{Ed,sw,UHPC}$	Moment due to self-weight of UHPC cross section
M_{Rd}	Design moment resistance

Q	Applied load
V_c	Shear force from dead load
V_{Ed}	Design shear force at ULS
V_{Rd}	Total shear force resistance
$V_{Rd,c}$	Contribution to the shear force resistance without shear reinforcement
$V_{Rd,f}$	Contribution to the shear force resistance from the fibers
$V_{Rd,max}$	Maximum shear force
$V_{Rd,s}$	Contribution to the shear force resistance from the shear reinforcement
W_K	Max allowed crack width

Roman lower-case letters

b	Bridge width
c_m	Cement content
c_{min}	Minimum concrete cover
$c_{min,b}$	Minimum concrete cover with bond
$c_{min,dur}$	Minimum concrete cover regarding environmental conditions
$c_{min,p}$	Minimum concrete cover considering compliance with concreting conditions
c_{nom}	Concrete cover
d	Distance from top of the cross-section to center of the reinforcement
e	Eccentricity, distance from the axial force and the neutral axis
f_{cd}	Design value for the compressive strength of the concrete
f_{ck}	Characteristic cylinder compressive strength for concrete
f_{ctm}	Mean value of axial tensile strength of concrete
f_{cm}	Mean value of concrete cylinder compressive strength
f_{ctk}	Characteristic axial tensile strength of concrete
$f_{ct,el}$	Tensile limit of elasticity
$f_{ctk,el}$	Characteristic value of the tensile limit of elasticity
$f_{ctm,el}$	Mean value of the tensile limit of elasticity
$f_{ctm,fl}$	Mean flexural tensile strength
$f_{ctf,d}$	Design value of post-cracking strength
f_{yk}	Characteristic value for the yield strength of the reinforcement
f_{yd}	Design value for the yield strength of the reinforcement
$G_{s.con}$	Self-weight of conventional cross section
$G_{s.UHPC}$	Self-weight of UHPC cross section

h	Hight of cross section
q_{c1}	Load coming from conventional concrete
$s_{r,max}$	Maximum crack spacing of concrete
w_k	Maximum crack width requirement
x	Compressed depth at ULS
x_1	Height from the natural to the strain
x_2	Height between the strains ε_{c0d} and ε_{cud}
x_{cc}	Lever arm to the neutral axis for UHPFRC

Greek upper-case letters

Δc_{dev}	Allowance in design for deviation
$\Delta c_{dur,add}$	Reduction of minimum cover for use of additional protection
$\Delta c_{dur,st}$	Reduction of minimum cover for use of stainless steel
$\Delta c_{dur,y}$	Additive safety margin

Greek lower-case letters

α_{cc}	Coefficient that accounts for long-term effects on compressive strength
β	Adjustment coefficient
γ_c	Partial factor for compressed concrete
γ_{cf}	Partial factor for UHPFRC under tension
γ_s	Partial factor for reinforcing steel
δ_1	Deflection factor
δ_{max}	Max deflection
δ_{tot}	Total deflection
ε_{c0d}	Maximum design elastic shortening strain at ULS
ε_{cc}	Compressive strain of concrete
ε_{cm}	Mean strain of concrete
$\varepsilon_{cm,f}$	Mean strain of UHPC
ε_{ct}	Tensile strain of UHPC
ε_{cud}	Maximum design shortening strain at ULS
ε_{el}	Strain at the maximum limit of elasticity of UHPFRC at SLS
ε_s	Steel strain
ε_u	Maximum elongation of UHPFRC in bending
$\varepsilon_{u,el}$	Strain at maximum limit of elasticity of UHPFRC
ε_{ud}	Design ultimate strain of reinforcement
ε_{uk}	Characteristic value for the elongation in reinforcement
ζ_f	Contribution from the fibers
η	Utilization ratio

θ	angle
κ	Scale factor
ν	Strength reduction factor
ξ_p	Slump value
ρ_c	Concrete density
ρ_s	Steel density
σ_{cc}	Concrete stress under compression
σ_{ct}	Concrete stress under tension
ϕ	Diameter of reinforcement bar
φ_{ef}	Creep coefficient
ψ	Factors that define representative values of variable loads

Abbreviations

CO2	Carbon dioxide
FA	Fly ash
GGBS	Granulated blast-furnace slag
GP	Glass powder
LCA	Life-cycle analysis
LCCA	Life-cycle cost analysis
LM1	Load Model 1
QP	Quasi-permanent
RH	Relative humidity
SCC	Self-compacting concrete
SF	Silica fume
SLS	Serviceability Limit State
SP	Superplasticizer
UHPC	Ultra High-Performance Concrete
UHPFRC	Ultra High-Performance Fibre Reinforced Concrete
ULS	Ultimate Limit State
w/b	water/ binder ratio
w/c	water / cement ratio

1 Introduction

Today, developing and building new infrastructure is necessary due to the high expansion of transport pathways. Current bridges cannot always meet the demand of increased traffic volumes and load-carrying capacities. The usage of bridges for traffic, railway, and pedestrian, is essential for covering the need for transportation and shortening journey times.

Since concrete has improved properties such as strength, durability, low cost and so forth, this motivates the wide use of concrete in the construction field. Considering bridge construction, concrete is the main building material used in the bridge industry (Meyer, 2005). On the other hand, concrete has always faced challenges due to high environmental impact and sustainability concerns (Martin, 2004). According to Lehne & Preston (2018) cement manufacturing contributes approximately 8% of the total global CO2 emissions due to high energy consumption and extraction of natural resources. Since concrete bridges are the cornerstone of infrastructure, there is a need to improve concrete bridge construction by using other types and classes of concrete that can be more durable and environmentally friendly to ensure a sustainable future

1.1 Background

Concrete has developed in many different stages throughout history regarding its strength and durability. There was a considerable change in the compressive strength of concrete during history, and this change is still ongoing nowadays (Duggal, 2017). In the mid of 1960s, concrete with compressive strength of 15 to 30 MPa was commonly used in the design and construction of concrete structures because it was well understood and economic (Aïtcin, 1998). In the early 1970s, the concrete could achieve 45-60 MPa by reducing the water-cement ratio (w/c) to 0.35-0.45, and this type of concrete was called *"high strength concrete"* (Aïtcin, 1998). During the 1980s, the high strength concrete was optimised by adding a superplasticizer and reducing the w/c ratio to 0.23 achieving a compressive strength of 130MPa (Aïtcin, 1998). Moreover, a low w/c ratio could provide concrete improved characteristic properties such as higher modulus of elasticity, higher flexural strength, and better durability (Aïtcin, 1998). In the early 1990s, a big jump was achieved where more than 150MPa in compressive strength. This type was called Ultra high-performance concrete (UHPC) (Shafieifar et al., 2017).

HPC/UHPC are widely used in more slender structures and high-rise towers, and in European countries like France and Netherlands, there have been traffic bridges built with UHPC (Schmidt & Fehling, 2005). However, the implementation of HPC and UHPC in the bridge industry in Sweden is still limited. In this Master thesis, the focus is on studying the mechanical properties and possible design approaches for bridges made from HPC/UHPC in order to investigate whether HPC/UHPC would be a promising alternative to conventional concrete to reduce the environmental impact of bridge construction and to address the gains with HPC/UHPC implementation.

1.2 Aim

This research aims to expand the knowledge about HPC and UHPC in Sweden regarding manufacturing possibilities, mechanical properties, and design approaches and study the behaviour of HPC/UHPC in the design of concrete bridges. The research highlights the differences in design between bridges made from HPC /UHPC and conventional concrete. Moreover, investigating the benefits of structural behaviour, environmental efficiency, and durability can be gained by using HPC/UHPC instead of conventional concrete in bridge construction.

1.3 Scope and limitation

This thesis focuses on the design and applications of HPC/UHPC in bridge construction and considers the following scopes:

- The case study compares an excited conventional concrete bridge (C35/45) and similar fictitious bridges made from HPC/UHPC.
- The results focus on the design phase, not on the whole service life of the bridge, where other researchers like LCA and LCC are required to obtain the actual results of the whole service life, and they can not be carried out due to time constraints.
- The scope of the results focuses on bridges of type Rigid frame with normal reinforcement and short span.

The limitations of the thesis are

- The literature review focuses on the applications of HPC/UHPC in bridge construction, while other possible applications of HPC/HUPC are not considered.
- This thesis considers the material properties from a theoretical perspective, not experimental.
- The economic aspect is not considered due to the limited timeframe.

- The durability properties of HPC/UHPC are described in the literature review, while durability aspects are not considered in the case study.
- Only the bridge's superstructure was considered in the calculation, where no calculation for the bridge legs or wings is included

1.4 Methodology

The master's thesis begans with a comprehensive literature study on high-performance concrete (HPC) and ultra-high performance concrete (UHPC) to provide the state of the art of materials. Then case studies were conducted to apply the knowledge obtained from the literature study to analyse and study the differences in design between conventional concrete and HPC/ UHPC.

AFRY had provided materials as input data for the case study. These materials consisted of design calculations and drawings of an existed rigid-frame bridge. The geometry, load combinations and reinforcement amount were used to carry out another two case studies. The main aim of the case studies was to calculate the bending moment and shear capacities of the cross-section obtained by using HPC and UHPC, respectively, instead of normal strength

concrete. The bending moment calculation considered the middle of the span. In contrast, shear capacity was checked close to the support where the maximum shear force occurs.

Moreover, a new design for the cross-section will be made using HPC and UHPC, where the aim is to design a cross-section that can carry the applied loads and fulfil the requirement in service limit state (SLS). Hence, crack width and deflection were controlled and compared with the cross-section where normal strength concrete was used. The reduction of cross-section height and changing of reinforcement amount was compared with the normal strength concrete cross-section to see the gains of using HPC and UHPC.

The applied loads on the structure are retrieved from the case study provided by AFRY. In other words, there was no need to calculate the loads acting on the bridge or make any load combination.

1.5 Targeted stakeholders

- The Chalmers University of Technology.
- AFRY
- Construction companies working in bridge industry.
- Swedish Transport Administration.

2 Literature study

This chapter presents a comprehensive literature review to offer a deeper understanding of HPC/UHPC mechanical and durability properties and present some application areas where HPC/UHPC is applied worldwide and in Sweden. Moreover, mixed proportion examples are suggested where some properties are reviewed to show the differences between conventional and HPC/UHPC. Further, standards and design guidelines published in different countries are reviewed.

2.1 Overview of high-performance concrete (HPC) and ultra high-performance concrete (UHPC)

Concrete has developed continuously over time. This development has considered various aspects such as concrete mechanical properties and durability performance. During the 1970s, the concrete used in some high-rise buildings was improved more than the normal-strength concrete used in other construction types, e.g., infrastructure. This improved concrete was named "high strength concrete" due to its higher strength than the normal strength concrete. High-strength concrete was made using the same methods as normal concrete, except that some ingredients were selected carefully to increase concrete strength. When superplasticisers started to be implemented in concrete manufacturing to reduce water/binder ratio, concrete could acquire improved properties such as significant higher compressive and flexural strength, good flowability, higher elastic module, lower permeability, and improved durability, and abrasion resistance (Aïtcin, 1998). During the 1980s, the term "High-performance concrete (HPC)" appeared, and the expression high strength concrete was no longer suitable due to the overall development of concrete properties, especially the durability performance t al., 2008). The service life of structures made from HPC could be considerably longer than other structures made from normal concrete, which made the usage of HPC concrete preferable for contractors (Aitcin, 1998). Moreover, HPC could offer designers better alternatives than conventional concrete because of its higher strength properties (Dybel, et al. 2019). HPC has superior properties in terms of strength (Compared to conventional concrete), and it also has considerable high durability properties that give HPC this name (Aitcin, 1998; Gustafsson et al., 2011; Persson, 1992; Sofia Utsi, 2008).

HPC has developed forward to reach a higher strength, which was done by reducing the water-cement ratio and adding more robust aggregates than what was used for HPC (Tang, 2004). This optimised concrete is called "Ultra high-performance concrete (UHPC)". UHPC has higher strength, durability, and more ductile behaviour than conventional HPC. These improved properties could be achieved because of the low permeability and very dense concrete by optimising the mix proportion and adding steel fibre of different sizes, shapes and strengths (Fehling et al., 2014; Sofia Utsi, 2008).

2.1.1 Classification of HPC and UHPC

It is worth mentioning that there is no clear point when the development of HPC and UHPC started. This process took place in different parts of the world, e.g. (France, Japan, Canada, Denmark, the U.S, and the UK). These countries had no standard definition of HPC and UHPC, where the compressive strength was a vital parameter to classify the HPC and UHPC.

However, the reviewed literature has found a different definition of HPC/UHPC depending on the source's origin.
EC 2 lists 14 strength classes from class 12/15 to class 90/105, where concrete class C12/15 – C55/67 refers to normal strength concrete, while classes C55/67- C90/105 correspond HPC (Al-Emrani et al., 2013). According to the old Swedish handbook (2000), the HPC is defined as a concrete that has a water-binder ratio of less than 0.35 and compressive strength at 28 days higher than 80 MPa (Byggtjänst, 2000), while in the new version of the Swedish handbook there is no definition of HPC. Moreover, any concrete that fulfils the requirements to overcome the limitations of usual concrete can be called HPC. The appropriate categorisation of HPC depends on several levels of performance standards, where the water/cement ratio should be between 0.2 and 0.3, the compressive strength between 60 MPa-150 MPa, and the durability factor 80% at 28 days(Kumar et al., 2017). Aïtcin (1998) has concluded a definition for high-performance concrete *"high-performance concrete is nothing more than some concrete with a very low porosity".* To reach a low porosity concrete, a much lower cement/water ratio than conventional concrete must be used. Concrete strength increases when the porosity decrease (Aïtcin, 1998).

Consequently, according to the reviewed literature, there is no common precise limitation of the strength of HPC/UHPC. However, it is observed that there is a widespread understanding that UHPC has a compressive strength of a minimum of 150 MPa. It can reach 280 MPa and higher by reducing the w/b ratio to a value between 0.16 and 0.2 and adding a significant dosage of superplasticiser and cementitious material (Eide & Hisd(Eide & Hisdal, 2012)HPC have been in the developing stage in latest five decades. At present, the concrete technology could establish a new generation of concrete and achieve a significant high quality, strength, and durability of concrete (Eide & Hisdal, 2012).

2.1.2 Applications

This sub-chapter presents a general description of the different applications of HPC/ UHPC. The literature covers a comprehensive review of applications both internationally and in Sweden. Considering the application of bridge construction, it is noticed that UHPC with fibre is applied to a large extent internationally while HPC is utilised at a lower rate.

2.1.2.1 Worldwide

UHPC is widely used internationally due to its various advantages, such as allowing designers to design more slender structures, reducing the structures' self-weight, increasing the lifespan by enhancing higher durability, and so forth (Eide & Hisdal, 2012). It is chosen to review some applications in different countries and focus more on bridge constructions while less attention was paid to HPC/UHPC applications on building, e.g. high, rise buildings, offshore.

USA

First-time UHPC became commercially available in the United States was in 2000. Since then, great attention has been paid to investigating the capability of this material to replace the conventional concrete and be utilised in infrastructure projects Russell & Graybeal, 2013). Federal Highway Administration in the USA (corresponding to Trafikverket in Sweden) has actively integrated UHPC in various infrastructure applications because of many beneficial properties obtained by using UHPC. Besides its improved and high compressive strength (more than 150MPa), the durability performance of UHPC is superior compared to conventional and high-performance concrete(Russell & Graybeal, 2013)

The Water Tower Place" in Chicago (1970)

An example of a high-rise building built in the USA using high-performance concrete is "The Water Tower Place" in Chicago in 1970 (Aïtcin, 1998). It is a building with 86 stories and maximum compressive strength of 60 MPa when the superplasticiser was not used yet. The only way to reach a high strength concrete was to reduce the water/cement ratio and select a high-quality cement type to get the best mechanical properties. The compressive strength of the used concrete differs between stories depending on the applied loads. This 262 m building was built from HPC on the lowest floors only (Aïtcin, 1998).

Figure 2.1 Water tower place in Chicago (Aïtcin, 1998).

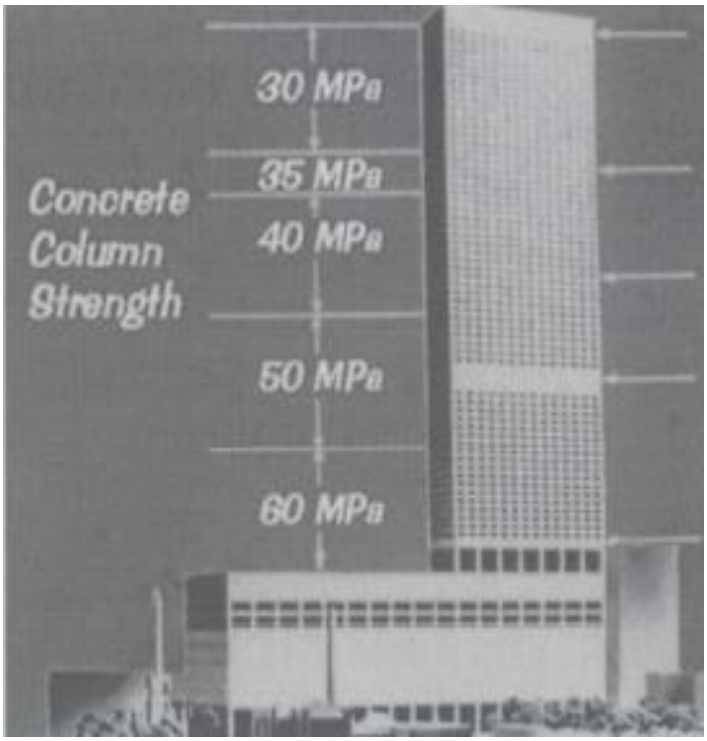

Figure 2.2 Water Tower Place, (Aïtcin, 1998).

Mars Hill bridge

The first bridge built with UHPC in the USA is the Mars Hill bridge in Wapello county, built in 2006 (Russell & Graybeal, 2013). It is a single-span precast prestressed bridge with a length of 33.5 m. The bridge consists of three modified Bulb-tees girders with a deep of 1.14 m and a length of 24.8 m covered with 20.3 cm cast-in-situ concrete decks (Russell & Graybeal, 2013). Steel fibres content of 2% by volume has been included in order to eliminate the non-prestressed reinforcement (Wayne, 2007)

Figure 2.3 Mars Hill Bridge, Wapello County, IA (Wayne, 2007).

The cross-section dimensions could be reduced compared to conventional lowa Bulb tees. The web thickness could be reduced from 165 mm to 114.3 mm, the bottom flange from 190.5 mm to 139.7 mm, and the top flange from 95.25 mm to 69.85 mm (Wayne, 2007).

Forty-nine low relaxation prestressing strands with a diameter of 15.2 mm have been used for each beam where no shear reinforcement has been added (Russell, 2013). Distribution of pre-stressing strands is shown in Figure 2.4. The compressive strength was 83 MPa at releasing the strands and 159 MPa for design (Russell & Graybeal, 2013).

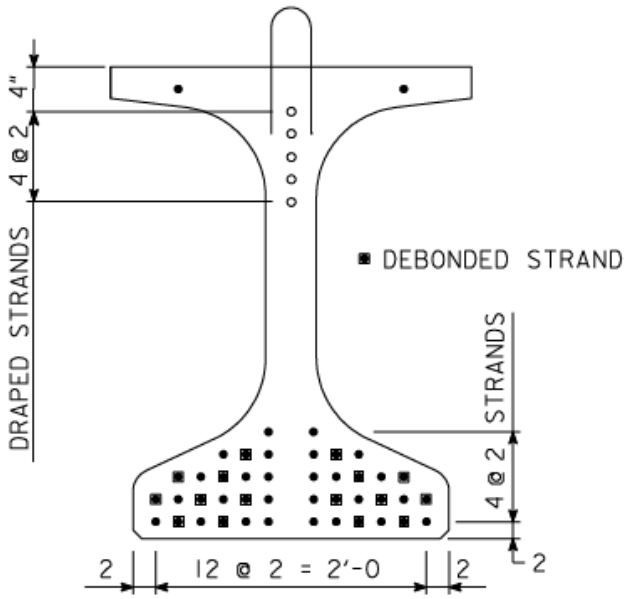

Figure 2.4 Cross-section of Bulb-bees girder with an illustration of the number and distribution of the prestressed strands (Wayne, 2007).

Figure 2.5 Distribution of prestressing strands (Wayne, 2007).

The main challenge was the lack of design specification where no other similar bridges had been built with UHPC at that time in the USA (Wayne, 2007). However, the exploring process took three years as the material behaviour was unique. Therefore, various tests were performed to establish and determine the mechanical properties of these girders made from UHPC (Wayne, 2007).

By using UHPC, the designer could achieve a lighter weight structure with a more slender cross-section, reducing the material usage. Another benefit is the provided durability of the low permeability properties of the UHPC, which reduces the risk of corrosion (Wayne, 2007).

Jakway Park Bridge, Buchanan County, IA, U.S

A three-span bridge length of 35.5 m was completed in 2008 and was the first pre-stressed UHPC π - girder bridge built in the U.S (Graybeal, 2009a; Russell & Graybeal, 2013). Due to a limited budget, only the bridge's centre spans are made from UHPC π- girder and consist of three π -girders connected by longitudinal joints resulting in total width of 7.62 m and length of 15.24 m (Graybeal, 2009a; Rouse et al., 2011). Figure 2.6 shows the overall view of the bridge.

Figure 2.6 Jakway Park Bridge, Buchanan County, IA, USA (Russell & Graybeal, 2013).

The final cross-section of the π -girder is illustrated in Figure 2.7. This final shape was optimised from an initial π - girder, where an analytical study was carried out to investigate the capability of the cross-section properties (Rouse et al., 2011).

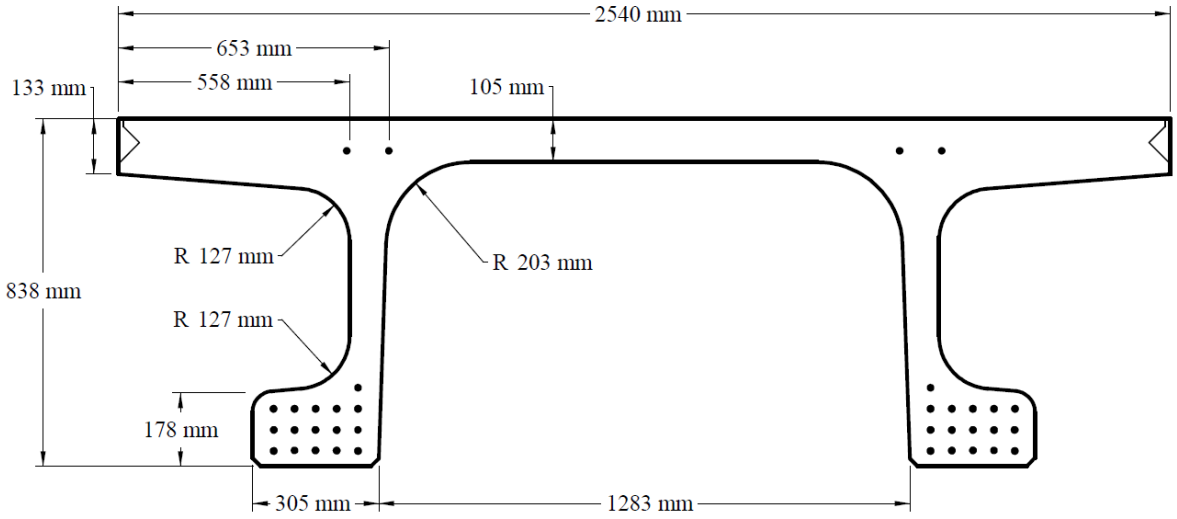

Figure 2.7 Illustration of π -girder cross-section (Russell & Graybeal, 2013).

Reinforcement

Twenty-two low-relaxation prestressing strands with a diameter of 15.24 mm were used. Each Bulb contains nine strands distributed into two layers, the lower layer contains five strands, and the upper layer contains four strands. All the strands were tensioned to a total force of 3407 kN, while the other four strands located in the upper flange were tensioned to (756 kN)(Rouse et al., 2011). The distribution of pre-stressing strands is shown in Figure 2.8.

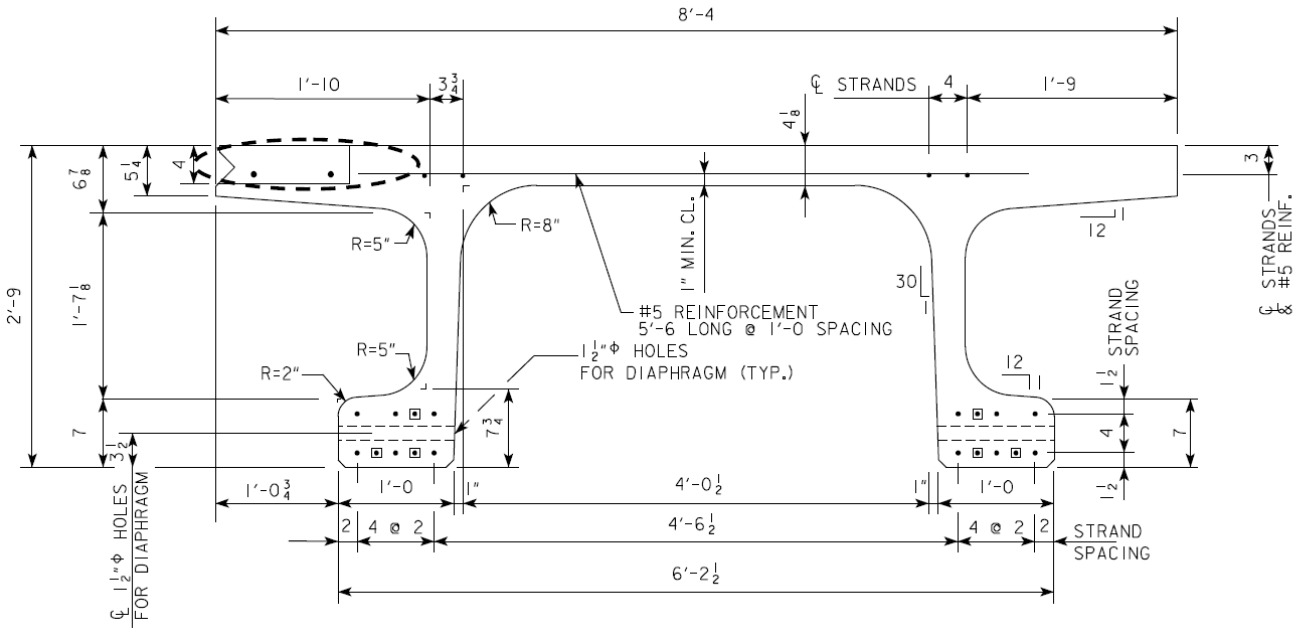

Figure 2.8 Distribution of pre-stressing strands in optimised π -girder (units is inch) (Rouse et al., 2011).

UHPC with steel fibre content has been used. The mix used was Ductal® provided by LaFarge construction materials supplier (Rouse et al., 2011). The mix proportion used for this bridge is presented in Table 2-1.

Table 2-1 UHPC mix proportion (Graybeal, 2009b).

Material	Amount (kg/m^3 (lb/yd^3))	Percent by Weight
Portland Cement	712 (1,200)	28.5
Fine Sand	1020 (1,720)	40.8
Silica Fume	231 (390)	9.3
Ground Quartz	211 (355)	8.4
Superplasticizer	30.7 (51.8)	1.2
Accelerator	30.0 (50.5)	1.2
Steel Fibers	156 (263)	6.2
Water	109 (184)	4.4

1 kg/m^3 = 1.686 lb/yd^3
RDM = relative dynamic modulus (see p. 134)

The mechanical properties of the materials were obtained from the UHPC research program performed by the Federal Highway Administration (FHWA). The results are shown in Table 2-2 UHPC material properties (Graybeal, 2009b).

Table 2-2 UHPC material properties (Graybeal, 2009b).

Material Characteristic	Average Result
Compressive Strength (ASTM C39; 28-day strength)	193 MPa
Modulus of Elasticity (ASTM C469; 28-day modulus)	52.4 GPa
Split Cylinder Cracking Strength (ASTM C496)	11.7 MPa
Prism Flexure Cracking Strength (ASTM C1018; 305-mm span; corrected)	9.0 MPa
Mortar Briquette Cracking Strength (AASHTO T132)	8.3 MPa
Direct Tension Cracking Strength (Axial tensile load)	9.7–11.0 MPa
Prism Flexural Tensile Toughness (ASTM C1018; 305-mm span)	$I_{30} = 53$
Long-Term Creep Coefficient (ASTM C512; 77 MPa sustained load)	0.29
Long-Term Shrinkage (ASTM C157; initial reading after set)	766 microstrain
Total Shrinkage (Embedded vibrating wire gage)	850 microstrain
Coefficient of Thermal Expansion (AASHTO TP60–00)	15.6×10^{-6}
Chloride Ion Penetrability (ASTM C1202; 28-day test)	18 coulombs
Chloride Ion Permeability (AASHTO T259; 12.7-mm depth)	< 0.06 kg/m^3
Scaling Resistance (ASTM C672)	No Scaling
Abrasion Resistance (ASTM C944 2x weight; ground surface)	0.17 grams lost
Freeze-Thaw Resistance (ASTM C666A; 600 cycles)	RDM = 96%
Alkali-Silica Reaction (ASTM C1260; tested for 28 days)	Innocuous

1 MPa = 145 psi
1 kg/m^3 = 1.69 lb/yd^3
1 g = 0.035 ounce

France

Île de Ré bridge, France (1989)

The implementations of high-performance concrete are not limited to high rise buildings. Instead, during the end of the 1980s, high-performance concrete started to be used in bridge construction. One of the first bridges built in Europe with high-performance concrete is "Île de Ré bridge" in France which connects Charente-Maritime cities, see Figure 2.9. Box-girders construct the bridge with external prestressing. The compressive strength at 28 days is 67,7 MP (Aïtcin, 1998) a. Another bridge was built in France at that time was "The Joigny bridge", southeast of Paris in 1989. The reached compressive strength of the bridge was 78 MPa after 28 days and 102 MPa after one year.

Figure 2.9 Île de Ré bridge in France (Aïtcin, 1998).

Bourg-lès-Valence bridge (2001)

The first road bridge built with UHPC in the world is the Bourg-lès-Valence bridge. It is located in France and was completed in 2001 (HAJAR et al., 2004; Russell & Graybeal, 2013). The bridge consists of two spans with a span length of 20.50 m and 22.50 m. The cross-section has a π-shaped profile with a height of 900 mm and a width of 2400 mm. The web thickness is (110 mm). The total width is 12700 mm, obtained by assembling five π-shaped pre-stressed beams connected using cast-in-situ UHPC (HAJAR et al., 2004). An illustration of the cross-section can be shown in Figure 2.10.

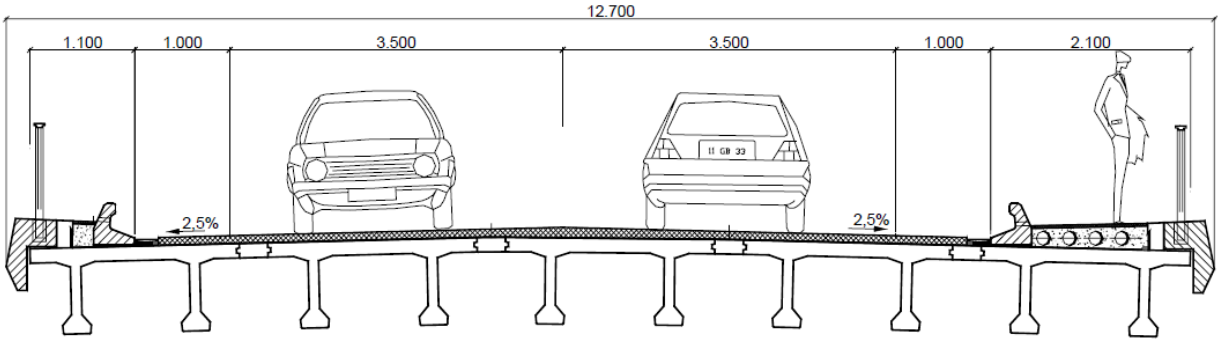

Figure 2.10 Cross-section of Bourg-lès-Valence bridge (Schmidt et al., 2004).

Figure 2.11 View of the bridge's central pier(Schmidt et al., 2004).

The material used for building "*Béton Spécial Industriel (BSI)"* is concrete, which is UHPC characterised by a significant amount of cement, use of silica fume, fine aggregates, very low w/c ratio and 3% fibre content by total volume (Schmidt et al., 2004). The mix design of BSI UHPC is presented in Table 2-3.

Table 2-3 Mix design proportion of BSI concrete(Schmidt et al., 2004).

cement	kg/m³	1114
silica fume	kg/m³	169
0 - 6 mm aggregate	kg/m³	1072
fibres	kg/m³	234
superplasticizer	kg/m³	40
water	kg/m³	209
w/c ratio		0.19

Because of the high fibre content used in this mix design, there was no need for passive reinforcement (Schmidt et al., 2004). Reinforcement was only used in the joints between the decks and the pavements (Fehling et al., 2014; Schmidt et al., 2004). Very low relaxation strands with 1860 MPa strength class were used. According to Fehling et al. (2014), a considerable saving on materials could be gained thanks to utilising UHPC solutions. The thickness of the decks could be reduced to (250 mm) instead of (750 mm) compared to the structure built with conventional concrete(Schmidt et al., 2004). The self-weight of the superstructure could be reduced to 328 tons instead of 975 tons compared to a bridge built with conventional concrete (Fehling et al., 2014). The mechanical properties of BSI concrete are presented in Table 2.4

Table 2-4 Characteristics of BSI Concrete (Fehling et al., 2014).

28-day characteristic compressive strength	175 MPa
28-day characteristic direct tensile strength of the matrix	8 MPa
28-day characteristic post-cracking direct tensile strength	9.1 MPa
Modulus of elasticity	64 GPa
Density	2.8 tons/m^3

Pont du Diable footbridge (2005)

This (70 m) long footbridge is not an arch or a suspension footbridge. Rather, it is a prestressed bridge constructed of two bone-shaped beams with cross-section dimensions of (1800 mm) deep and (120 mm) thick prestressed bridge constructed of two bone-shaped beams with cross-section dimensions of

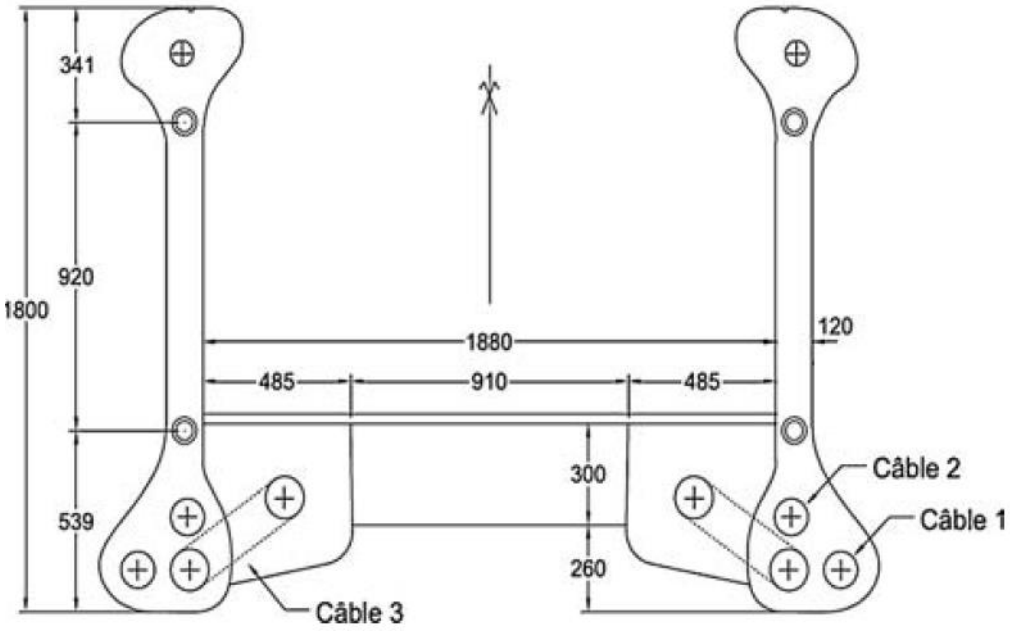

Figure 2.12 The cross-section dimensions of the Pont du Diable footbridge (Fehling et al., 2014).

Figure 2.13 View of Pont du Diable footbridge (Fehling et al., 2014).

The bridge is made by assembling 15 precast segments with long (4.6 m), resulting in a length of (69 m). Freyssinet prestressing system is used where eight tendons are utilised (Fehling et al., 2014). In each beam, there are three cables in the bottom bulb and one in the upper bulb(Fehling et al., 2014). Moreover, mass dampers are installed in the mid-span. The material used is UHPC made from Ductal® with compressive strength ranging between (180 MPa-200 MPa). A view of the bridge is shown in Figure 2.13.

Sweden

From 1991 to 1997, an international project with corroboration with researchers from the material industry, The Swedish Cement and Concrete Institute, and universities was carried out to investigate the practice implementation of HPC in Sweden. Moreover, the goal also was to increase the knowledge about the material properties, construction, and production of HPC (Fagerlund, 2014). As a result of this project, broader knowledge and experience of HPC were obtained, and the results have been published in the form of reports, journals, and conferences. Moreover, a handbook called "*Concrete Handbook High-Performance Concrete (2000)*" was also published (Fagerlund, 2014). However, the implementation of HPC is still limited in Sweden, and the knowledge is still limited to research and academic area while there are a few numbers of HPC applications that can be mentioned, and they were constructed during the research project, while the HPC and UHPC have effectively used worldwide (Fehling et al., 2014). Many applications of Ultra high-performance fibre reinforced concrete (UHPFRC) applications can be found in the USA, France, Canada, Australia, and Germany. In contrast, this type of concrete has never been used in Sweden (K-M. Krona, Personal Communication, 03 mars 2022). In this chapter, two applications of HPC are highlighted, while no application of UHPC or UHPFRC has been founded in the bridge industry.

Lasarettsbacksbron, Umeå (1998)
This cycle-pedestrian bridge is claimed to be the first bridge built with HPC in Sweden, completed in 1998. It has two spans of a length of 22 m and 23 m and a width of 5 m. It is a pre-stressed bridge with an eccentrically placed beam where fife pre-stressing strands of the type VSL 12ϕ 16 are used, and concrete class used was K80.

Figure 2.14 Cycle and pedestrian bridge in Umeå.

Åbromotet, Mölndal (1998)
Another cycle-pedestrian bridge made from HPC is located in Mölndal. The bridge has a span length of (6 m), a width of (4 m), and the concrete class is K80. The actual compressive strength was measured at 28 days to 100 MPa. The main purpose of building this bridge from HPC was to investigate the advantages and disadvantages of HPC before being fully exploited in the construction industry. The mix design of HPC used in this bridge is shown in Table 2-5.

Table 2-5 Concrete mix design proportion used in Åbromotet (Claeson, 1999).

Betongsammansättning	**[kg/m^3]**
Cement Degerhamn Std. P	470
Sand Kilanda 0-8 mm	520
Sand Gråbo 0-8 mm	360
Grus Kållered 8-11 mm	270
Grus Kållered 11-16 mm	600
Silika	15
Vatten	157
Glenium 51	3.5
Micro Air	0.2

The experience gained from investigating this bridge can be summarised as following (Claeson, 1999).

- HPC requires a longer mixing time than normal concrete.
- Higher pump pressure was required to pump the HPC concrete than normal concrete.
- Difficulties with obtaining a plain surface of the concrete due to concrete's tendency to flow out horizontally. However, this was solved by working the surface several times with a Concrete Vibratory Screed machine.

- Concrete workers perceived the high-strength concrete as straightforward and flexible to work with, the consistency was judged to be better than normal concrete, and it felt compliant.
- HPC is considered "pre-vibrated"; thus, considerably less vibration time is required.

All in all, HPC was considered as an accessible material to work with, and the difficulties and challenges that occurred were considered to be solved once this material started being used more frequently in the building industry(Claeson, 1999).

2.1.3 Production and Suppliers in Sweden

Since the implementation of HPC/UHPC is very limited in the Swedish industry, the availability of HPC/UHPC materials is also limited in the Swedish concrete market. Many global material suppliers such as (HOLCIM, Bouygues, EIFFAGE) are not active in Sweden. This is simply due to the poor implementation and investment in this material in the Swedish industry. However, after contacting with concrete suppliers in Sweden regarding the production of HPC/UHPC, it has been observed that they do not work with UHPC and do not produce this type of concrete. In contrast, HPC can be produced used with some challenges in production when producing concrete with compressive strength close to 100 MPa. According to (O. Esping, Personal Communication, 09 mars 2022), there are no obstacles when producing concrete with compressive strength of 60 MPa, while specific strength requirements on the aggregate are applied when producing concrete class (C70/85) and (C80/95). This agrees with another concrete supplier (Betongindustri), where (J.Carlswärd, Personal Communication, 08 mars 2022) highlighted that they delivered concrete (C80/95) and they can also produce concrete with a bit higher strength close to 100 MPa. However, it is worth mentioning that the aggregate in Sweden can fulfil the requirement for producing concrete with compressive strength of (120 MPa) (Claeson, 1999). More details about the requirement on aggregate will be discussed further (See **Aggregates**).

In general, it can be said that the status of HPC/UHPC in the Swedish concrete market is low due to the low investment and unpopularity of using this material in construction. Another reason is also considering the high initial cost of HPC and the difficulties of the production of UHPC with locally available materials such as aggregate.

2.1.4 Guidelines and standards

Several technical guidelines and design specifications and standards cover the application of high-performance concrete (HPC), Ultra high-performance concrete (UHPC). Different countries, e.g. France, Germany, the USA, Australia, Canada, and Japan, provide these standards.

Eurocode 2 is applicable for compressive strength class up to C90/105, while a modification of design stress-strain relationships for a concrete class higher than C90/105 is applied (Schmidt et al., 2017). In Sweden, a handbook is called "*High-performance concrete structures: design handbook,* published in 2000 by "Svensk byggtjänst" in Stockholm. This handbook came from the national project that started in Sweden between 1991-1997 and aimed to develop more efficient structures, better production methods and more durable materials (Elfgren et al., 1999).

The technical recommendations for structural design and material properties of UHPC were published for the first time years 2002 in France. The document was called the "AFGC-

SETRA recommendation" (Yoo & Yoon, 2016). In Germany, published in 2003, a state-of-the-art report on UHPFRC covers comprehensive design aspects and material properties. The German Committee published this guideline Structural Concrete (Deutscher Ausschuss für Stahlbeton – DAfStb) (Schmidt et al., 2017; Yoo & Yoon, 2016). In 2004 in Japan, another design recommendation for UHPFRC was based on Ductal and published by the Japan Society of Civil Engineers (JSCE) (Yoo & Yoon, 2016). The first French standard added to Eurocode 2 was published in 2016 and consists of two documents where (NF P18-470, 2016) considers the material and (NF P18-710, 2016) considers the design aspects. This is an officially approved standard called "National Addition to Eurocode2, Design of Concrete Structures: Specific Rules for Ultra-High Performance Fibre-Reinforced Concrete (UHPFRC), 2016)

2.2 Review of relevant materials properties used for HPC/UHPC

HPC/UHPC are made from material similar to conventional concrete but with requirements for specific properties of ingredients. The quality of material and proportioning are of deep concern with increased compressive strength (Aitcin, 1998). This sub-chapter reviews some relevant ingredients properties, starting from cement, which is the main ingredient, and supplementary cementitious materials, superplasticiser, and aggregates.

2.2.1 Cement

Since the HPC/UHPC has a considerable high compressive strength (up to more than 200 MPa), cement properties are considered a crucial issue regarding strength and rheology (Kumar et al., 2017). The strength development of concrete is achieved by presenting Calcium Silicates, where this component contributes 80% of the total mass of Portland cement (Aitcin, 1998). Hence, Portland cement must evolve as much Hydrated Calcium Silicate (C-S-H) as possible (Aitcin, 1998). The ability of Portland cement to develop (C-S-H) is related to the water/binder ratio, where decreasing of water/binder ratio enables Portland cement developing more (C-S-H), resulting in high strength of concrete (Aitcin, 1998). It is also important to mention that a significant decrease in the water/binder ratio can be critical considering the amount of water available to enable the hydration of cement. Hence, it is essential to achieve an appropriate water/binder ratio in which the rheology of young concrete is not impaired(Aitcin, 1998). From a rheology point of view, decreasing the amount of C3A in the Portland cement used for HPC/UHPC results in better rheology control and reduces the risk of cement-superplasticiser interaction problems(Kumar et al., 2017).

2.2.2 Supplementary Cementitious Materials (SCM)

Supplementary cementitious materials (SCM) (also known as Cement Replacement Materials (CRM)) are typically used in the production of HPC in order to substitute part of Portland cement resulting in reducing carbon footprint due to cement manufacturing. According to Aitcin (1998), HPC can be made using only Portland cement, but it is more environmentally efficient to use a combination of different SCM. In addition to the environmental aspect, using SCM enhances concrete properties in terms of strength, rheology, and durability (Ramezanianpour, 2014). Fly Ash, Slag, Silica Fume, and ground granulated blast furnace slag (GGBS) are commonly used as cement replacement materials in HPC/UHPC. Appropriate selection of SCM should be performed to avoid mitigation of properties of concrete(Meng, 2017). Different proportions of SCM used in the production of HPC/UHPC influence the mechanical properties such as strength as well as durability properties

2.2.2.1 Fly Ash

The proportion of Fly Ash added to concrete considerably influences concrete properties in terms of workability, pumpability and bleeding(Ramezanianpour, 2014). Fly Ash consists of small spherical particles that vary between 1μm and -150 μm. The small size of the particles provides cement paste with better workability and reduces the water needed compared to other cement paste without using Fly Ash (Ramezanianpour, 2014). Owens (1979) studied the effect of fly ash on the workability of concrete and found that particles greater than 45 μm have a significant influence on the workability. The results are presented in Figure 2.15, where the effect of fly ash particles on the amount of required water is shown.

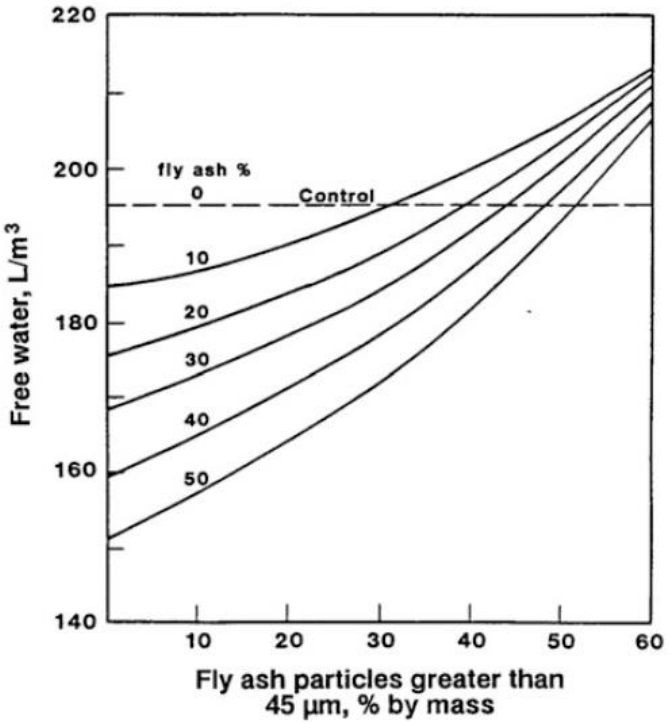

Figure 2.15 Influence of coarse-particulate content of FA on water requirement for equal workability in concrete (Bouaissi et al., 2018).

According to Figure 2.15, replacing 50% of fly ash particles greater than 45μm does not change the requirement of needed water.

2.2.2.2 Silica Fume

Silica fume particles are microscopic, where about 95% are less than 1μ, and they have a mean diameter of 0.2μ (Ramezanianpour, 2014), while the size of Portland cement particles ranges in general between 1μm-50μm (Bentz et al., 1999).

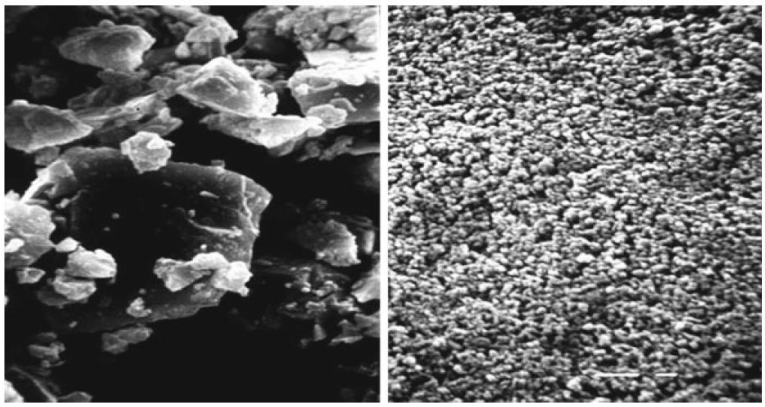

Figure 2.16 Photomicrograph of Portland cement grains (left) and silica fume particles (right) at the same magnification (Ramezanianpour, 2014).

According to Ramezanianpour (2014), concrete mixtures containing silica fume showed higher strength and better durability than Portland cement concrete. Ramezanianpour (2014) also states that presenting very fin silica fume particles in the concrete mixture results in slightly higher strength by increasing the adhesiveness of the concrete mixture. This results in a reduction in the workability of the mixture. Thus, water-reducing admixture is recommended to be used in concrete mixtures that contain silica fume.

On the other hand, silica fume provides fresh concrete with improved properties in significantly reducing segregation and bleeding (Duggal, 2008). Moreover, silica fume particles have a large specific surface area of 1500-2000cm2/g, reducing free water available in the concrete mixture for bleeding, resulting in a significant reduction of bleeding(Duggal, 2008). Since silica fume particles are very fine, they are able to block the pores in fresh concrete resulting in a significant reduction of bleeding (Duggal, 2008). However, due to the absence of bleeding, there is a need for adequate moist curing in order to protect concrete from early shrinkage, especially when concrete is placed in a hot environment. The curing should be initiated earlier than the conventional concrete (Ramezanianpour, 2014).

2.2.2.3 Ground granulated blast furnace slag(GGBS)

GGBS is a by-product of iron and consists of spherical glassy pellets of different sizes. It is observed that the particles' size has different effects on concrete properties (Ramezanianpour, 2014). Particles less than 10 μm have a role in developing early strength concrete. While particles with a diameter of 10 μm-45 μm contribute to developing strength after 28 days, articles larger than 45 μm have a minor or no effect on concrete (Ramezanianpour, 2014). However, since the reaction between slag and water is slow, presenting GGBS in concrete would lower the strength in young concrete, especially at the age of 1-6 days (Ramezanianpour, 2014). On the other hand, a strength development shows similar to the behaviour of ordinary Portland cement has been observed at the age of 7- 28 days and a slightly higher strength development after 28 days (Ramezanianpour, 2014).

From a durability point of view, utilising a partial replacement of Portland cement with GGBS in a concrete mixture provides the mixture with better durability by reducing the risk of sulfate attack, alkali-Silica reactions, and chloride ingress(Divsholi et al., 2014). On the other hand, it is reported that GGBS increases the rate of carbonation in concrete in comparison to Portland cement concrete, especially with a higher amount of GGBS (Divsholi et al., 2014; Duggal, 2008; Ramezanianpour, 2014). This can be explained by the higher

content of micropores formed in young concrete resulting in increased permeability (Ramezanianpour, 2014). Studies show that 50 % replacement of Portland cement with GGBS gives 1.5 times higher carbonation depth (Ramezanianpour, 2014). To reduce the carbonation rate caused by the higher replacement of GGBS, water curing should be utilised (Ramezanianpour, 2014).

2.2.3 Superplasticisers

There are different types of superplasticisers, and they affect the mechanical properties of concrete differently. Thus, selecting superplasticiser type and dosage is crucial (Aitcin, 1998). It is also worth mentioning that thanks to superplasticiser, concrete industry could produce concrete with very high compressive strength up to (200 MPa) by reducing the W/b ratio to levels that have not been experienced before while keeping a high level of fluidity and workability (Aitcin, 1998).

According to Domone & Illston (2010), it is more efficient to add superplasticiser after (1-2) minutes of mixing the cement with mix water to obtain desirable workability. It is observed that adding superplasticiser simultaneously as mixing water makes a significant amount of superplasticiser react with C3A/Gypsum,ecreasing the workability of concrete mixture (Domone & Illston, 2010). On the other hand, it is also important to mention that the duration effect of superplasticiser is limited. Therefore, it is essential to overcome this issue in the case of cast in situ, where the time of transportation from mixing place to site can be longer than superplasticising action time(Aitcin, 1998; Domone & Illston, 2010). Some practical methods have been suggested by Domone & Illston (2010) in order to face this challenge, for example, using of “retarder” with the concrete mixture to delay the setting time of the mix or adding superplasticiser on-site just before pumping from the mixer truck

2.2.4 Aggregates

Obtaining concrete with high compressive strength needs special attention to the material properties used for making this concrete. However, aggregate used for HPC/UHPC should have a high quality where the size, shape, surface texture and cleanness of aggregate have an essential role in achieving high strength and workability (Kumar et al., 2017). In general, the aggregate classification is based on shape and size. Figure 2.17 illustrates the different particle shapes of aggregate.

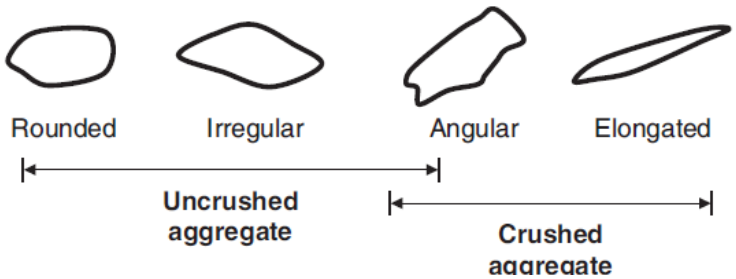

Figure 2.17 Different shaps of aggregate (Domone & Illston, 2010)

Aiticin (1998) reported that the flat and elongated aggregate shape reduces workability while the cubic and spherical shape provides better workability. In Europe, the principal aggregate size can be described by the ratio d/D where d is the smallest nominal size and D is the largest nominal particle size(Domone & Illston, 2010). The following categories can be identified:

- 0/4 is a fine aggregate (where 0 refers to particle size close to 0).
- 4/20 is coarse aggregate.
- 10/20 coarse aggregate with a minimum particle size of 10mm and a maximum of 20 mm.

Using a maximum number of larger particles size of aggregate results in (up to 20%) reduction of compressive strength (Domone & Illston, 2010). The "lower surface area can explain this with a weaker transition zone" of larger aggregate size, a critical issue in concrete mixture with low water to cement ratio(Domone & Illston, 2010).

Another critical factor is the strength of the aggregate itself, where experimental results point out that crushed stone gives 15-20 % higher compressive strength than gravel aggregate while using the same cementing material proportions (Domone & Illston, 2010).

In the case of HPC, there is a significant stress transfer between the hydrated cement paste and aggregate due to the higher bond behaviour of HPC, resulting in creating micro cracks on the microstructure of concrete. Thus, the aggregate strength is of deep concern in concrete with high compressive strength. The cement paste is the weakest connection in concrete in normal strength concrete, while the aggregate is the most robust connection (Fagerlund, 1998). As the compressive strength increases, the requirements on the strength of aggregate increase. In the case of HPC/UHPC, the high amount of cement and high density make the cement paste very strong. Thus this is no longer the weakest connection in concrete (The strength growth in HPC made with 8 types of aggregates is illustrated in Figure 2.17.

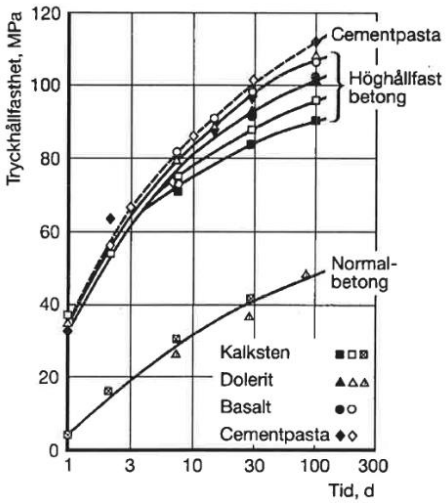

Figure 2.18 Strength growth in high-performance concrete made with I types of aggregate (Fagerlund, 1998).

It can be observed that the cement paste has a higher compressive strength than HPC, despite the aggregate used in HPC is very high (Fagerlund, 1998). The aggregate available in Sweden is suitable for achieving HPC with compressive strength of 90 MPa (Claeson, 1999). This is a challenge of producing HPC with compressive strength close to (100 MPa) according to J.Carlswärd (Personal Communication, 08 mars 2022).

Some types of aggregate are not suitable for HPC use, e.g. coarse, grained gneiss and coarse limestone, while other types have a more acceptable size, such as fine-grained rocks of eruptive origin and fine-grained limestones, are more suitable in the case of HPC (Fagerlund,

1998). Fine aggregate has higher strength than coarse aggregate of the same type. Thus, the recommended max value of aggregate particle size used in HPC should not exceed (10-12 mm)(Fagerlund, 1998).

2.3 Mixture proportions

The main objective of concrete mixture proportioning is to find a suitable combination of materials that is economical and, at the same time, able to achieve appropriate concrete properties that satisfy various application requirements. Recently, the concrete mix proportioning has become more complex due to the appearance of new components i.eg. Supplementary cementitious materials and additives affect concrete properties in terms of performance and durability. Moreover, emphasis was put on a growing number of sustainability issues that pushed concrete producers to work harder to find design methods that produce more environmentally efficient concrete at a low cost. However, there are different concrete proportioning methods used in different parts of the world, but according to Aitcin (1998), it is difficult to establish" a theoretical mix design method " that can be applied universally. Rather, a mix design method is said to be a starting point that needs to be modified in order to achieve desired concrete properties. However, in this chapter, two different mix recipes will be evaluated in terms of factors such as compressive strength and modulus of elasticity and workability.

2.3.1 Mixture design of HPC

Material and recipe

A Portland cement type I is used. The physical properties and chemical components are illustrated in Table 2-6.

Table 2-6 Mechanical, physical properties and chemical components of Portland cement type I (Jonbi et al., 2012a).

Coumpounds	Value %
SiO_2	19.0 -21.0
Al_2O_3	4.0 -6.0
Fe_2O_3	2.5 – 3.5
CaO	62.0 – 67.0
MgO	1.0 – 4.0
C_3S	55- 64
C_2S	9 - 20
C_3A	7- 11
C_4AF	9-11
Vicat Test	
Initial	≥ 45 min
Final	≤ 375min
Compressive Test (ASTM)	
3 day	≥ 1740 psi
7 day	≥ 2760 psi

The aggregates used in this recipe are silica sand as a fine aggregate with a specific gravity of 2.59 and coarse aggregate with a specific gravity of 2.60 (Jonbi et al., 2012a). Silica fume replaces the cement by 5-15% (ACI 211.4R-08, and is chosen according to (ASTM 1240-00)

with a bulk density of 0,6 kg/l. Sika Vistocrete-10 is used as a superplasticiser and complies with ASTM C 494-92 type F (Jonbi et al., 2012a). Two compressive strength classes of 60 MPa and 80 MPa are obtained, while a ready mix of 40 MPa is included in the table to compare. The mix proportion is shown in Table 2-7.

Table 2-7 Mix proportions (Jonbi et al., 2012a).

Mixture Proportions Kg/m^3	f'$_c$ 40 MPa	f'$_c$ 60 MPa	f'$_c$ 80 MPa
Cement	412	500	600
Fly ash	73	-	
Silica fume	-	75	120
Ratio water /binder	0.39	0.20	0.23
Water	189	115	165,5
Sand	634	641	603
Gravel	1038	1092	1119
Superplastizier			
Pozzolith 100 Ri ex BASF	1,44	-	-
Viscocrete 10 ex Sika	-	3,45	15

Test and results

The specimen size was 100 mm × 200 mm, demoulded after 24 hours of casting (ASTM C 39/C 39M-04a) standard was used to perform the compressive test at the age of 1, 3, 7, 28 and 56 days (Jonbi et al., 2012a).

The results of compressive strength obtained at different ages are shown in Figure 2.19

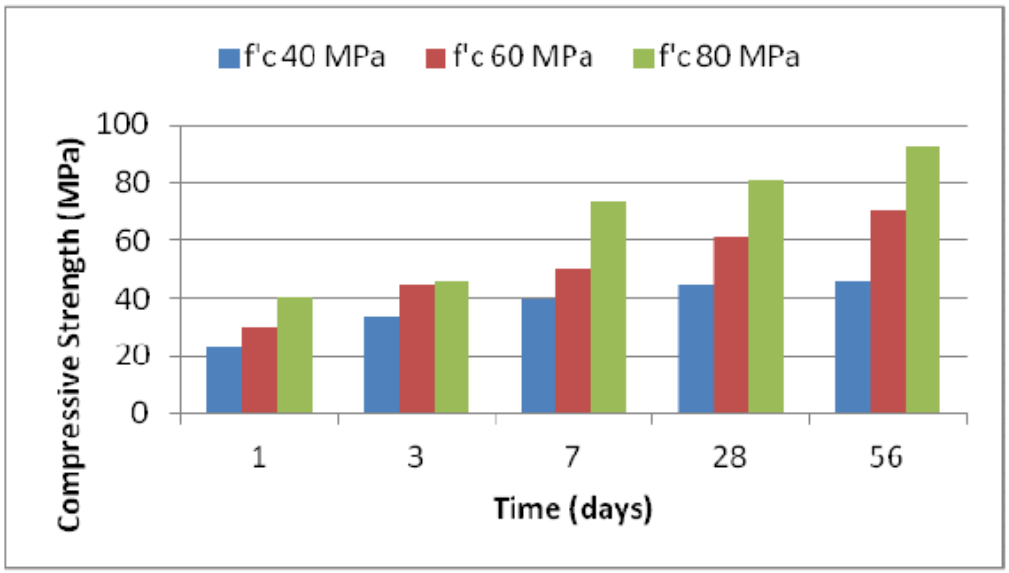

Figure 2.19 Result of Compressive Strength at different ages (Jonbi et al., 2012a)

As mentioned above, small size aggregate results in higher compressive strength. Using additives materials such as silica fume in the mixture provides higher concrete quality (Jonbi et al., 2012b). Furthermore, superplasticiser is crucial in mixing high-performance concrete to achieve high strength concrete with the desired workability and durability. The test results show that with the mix proportion described above, an 80 MPa compressive strength was gained at day 28, and the permeability test showed that for 80 MPa compressive strength, the permeability was 2,4 cm (Jonbi et al., 2012b). The aggregate size affects the cement

significantly, and the aggregate shape significantly influences the mixture mechanical properties and workability. Jonbi et al. (2012b) reported that the binder/cement ratio influences the mechanical properties and workability, making the high-performance concrete different from the normal concrete. The mechanical properties of the additives used in the high-performance concrete mixture mainly influence concrete behaviour, *"the strength of aggregate affects the strength of the concrete"* (Jonbi et al., 2012b).

2.3.2 Mixture design of optimised UHPFRC

Máca et al. (2013) performed research to formulate a UHPFRC optimised from a UHPC without steel fibre content. Three different UHPC mixtures have been evaluated in the beginning to select the best two performed mixtures. The best two mixture UHPC 2 and UHPC3) have been optimised by adding a straight steel fibre with different dosages to improve the tensile properties, and a new mixture of UHPRFC 2 and UHPRFC 3 have been achieved. After adding the different fibre dosages, the mixture with the best mechanical properties in terms of spread, compressive strength and flexural strength is chosen to be further evaluated with a new dosage of fibre.

Table 2-8 shows the mix proportions of the best two mixtures where a straight steel fibre content of 2% and 3% of the volume has been added to the respective mixture. The steel fibres have a length of 13 mm and a diameter of 0.15mm. The tensile strength of steel fibres is 2800 MPa due to the high strength of the cementitious matrix. The variation of coarse sand depends on the fibre content, where the fibres replaced up to 3% of the coarse sand (Máca et al., 2012)

Table 2-8 Proportions of UHPFRC with dieffernt fibre dosage (Máca et al., 2012).

Type of component	**UHPFRC 2-2**	**UHPFRC 2-3**	**UHPFRC 3-2**	**UHPFRC 3-3**
	Proportions by weight			
Cement CEM I 52,5R	1	1	1	1
Silica fume	0.25	0.25	0.25	0.25
Glass powder	0.25	0.25	0.25	0.25
Water	0.22	0.22	0.22	0.22
HRWR: Sika SVC 20 Gold	-	-	0.031	0.031
HRWR: Sika ViscoCrete 20He	-	-	0.019	0.019
HRWR: Sika ViscoCrete 30He	0.025	0.025	-	-
HRWR: Sika ViscoCrete 1035	0.025	0.025	-	-
Fine sand 0.1/0.6 mm	0.42	0.42	0.42	0.42
Fine sand 0.3/0.8 mm	0.8	0.7	0.8	0.7
Fibers	0.2	0.3	0.2	0.3
Spread [mm]	**153**	**140**	**240**	**160**

Different steel fibre content results in different workability and mechanical properties. Thus, the mixture with the highest mechanical properties and best workability is evaluated with a new steel fibre dosage of 0%. 1%. 2% and 3% (Máca et al., 2012). The final mixture design is shown in Table 2-9.

Table 2-9 Final mixture design of optimised UHPRFC (Máca et al., 2012).

Type of component	UHPFRC 3-1	UHPFRC 3-2	UHPFRC 3-3
	Proportions by weight		
Cement CEM I 52,5R	1	1	1
Silica fume	0.25	0.25	0.25
Glass powder	0.25	0.25	0.25
Water	0.22	0.22	0.22
HRWR: Sika SVC 20 Gold	0.031	0.031	0.031
HRWR: Sika ViscoCrete 20He	0.019	0.019	0.019
Fine sand 0.1/0.6 mm	0.42	0.42	0.42
Fine sand 0.3/0.8 mm	0.9	0.8	0.7
Fibres	0.1	0.2	0.3

Tests and results

Compressive Strength and Modulus of Elasticity
To perform a compressive strength test, a cylinder with a height of 200 mm and a diameter of 100mm has been tested, complying with CSN-EN 1015-11. The applied load has an average speed of 36 MPa/min(Máca et al., 2012). Figure 2.20 shows the compressive strength test results and modulus of elasticity.

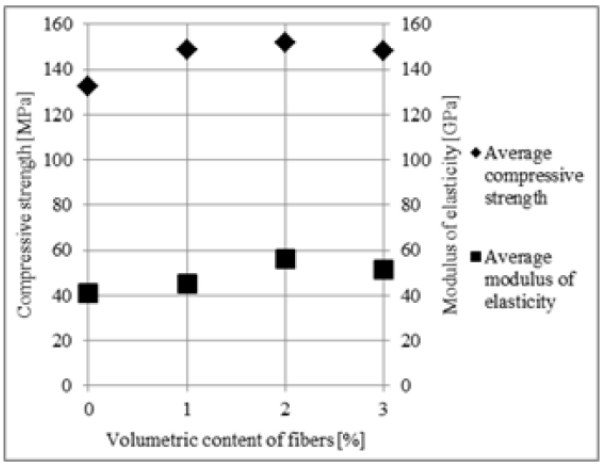

Figure 2.20 Results of the compressive strength and modulus of elasticity for different steel fibre content (Máca et al., 2012).

According to Figure 2.20, the highest compressive strength is obtained at fibre content of 2%, where the compressive strength reaches a value of 151 MPa (Máca et al., 2012). On the other hand, it can also be noticed that increasing fibre content by more than 2% results in decreasing the compressive strength, see Figure 2.20. Máca et al. (2012) explain this behaviour by increasing fibre and air content, thus decreasing the compressive strength. Máca et al. (2012) show that the modulus of elasticity is similar to compressive strength. The highest value of modulus of elasticity 56.9 GPa was obtained at 2% fibre content, and this value decreased with increasing fibre content.

Flexural strength
Máca et al. (2012) performed a three-point bending test on prisms of 40 ×40×160 mm3 to determine the flexural strength of UHPRFC concerning fibre content 0%, 1%, 2% and 3% volumetric content of fibres have been studied. A load rate of 1.5mm/min was applied, and the deflection was measured. The test complied with CSN-EN 1015-11 (n.d.), and the results are presented in Figure 2.21.

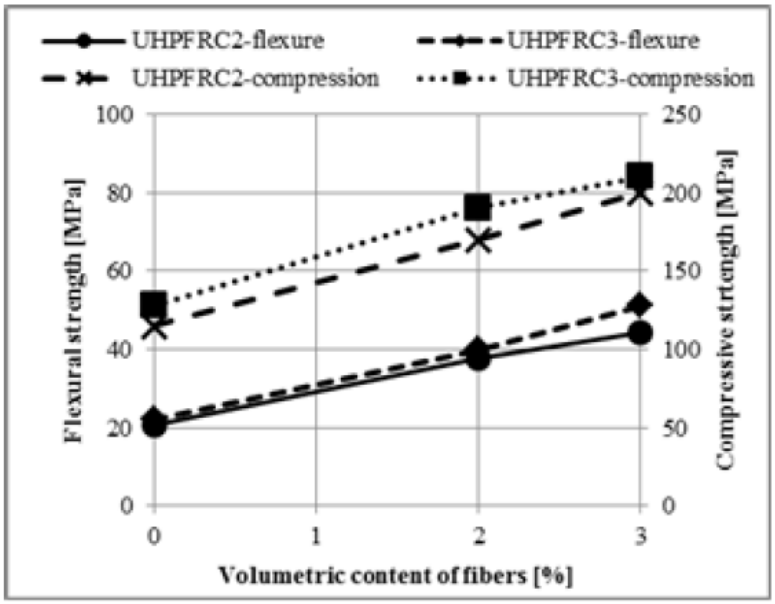

Figure 2.21 Mechanical properties of two different mixtures concerning different fibre content (Máca et al., 2012).

It can be noticed that the UHPFRC3 provides a higher flexural strength compared to UHPFRC 2. Moreover, the flexural strength increases with increased fibre content, where the maximum flexural strength is achieved at 3% fibre content(Máca et al., 2012).

2.4 Mechanical properties

In this chapter, the mechanical properties of HPC/UHPC are reviewed in a general manner because it is out of the project limitations to describe each precise detail because there are several kinds of UHPC concrete for many applications and conditions (P.-C. Aïtcin, 1998). The main focus is on the mechanical properties that distinguish this kind of concrete from normal concrete, such as compressive strength, tensile strength, elastic modulus, fracture energy, and creep/ shrinkage behaviour.

The old name of high-performance concrete is high strength concrete, which gives a clear idea about one of the essential properties: the high compressive strength, but Aïtcin (1998) said that the mechanical properties of high-performance concrete could not be concluded just in its compressive strength. Ultra-high-performance concrete has been developed in the last decade. Ultra-high-performance concrete does not present a high-compressive strength but also provides ultra-high durability (Ghafari et al., 2016).

2.4.1 Compressive Strength

The high compressive strength is achieved primarily by reducing the water/cement ratio, but it is affected by many factors such as cement type, additives and curing situations (Soliman, 2011). The compressive strength of high-performance concrete could be raised by choosing an aggregate with a strength more robust than the strength of the hydrated cement paste. An ultra-high compressive strength with 130 MPa can be achieved using a water/cement ratio of 0,2 (Aïtcin, 1998).
Table 2-10 below shows maximum compressive strength as a cement/water ratio function.

Table 2-10 Compressive strength as a function of w/c (Aïtcin, 1998).

Water / cement	Maximum compressive strength (MPa)
0,40-0,35	50-70
0,35-0,30	75-100
0,30-0,25	100-125
0,25-0,2	>125

Aïtcin (1998) mentioned that other components need to be considered regarding high-performance concrete's compressive strength, such as the early compressive strength and the effect of high temperature at initial age on compressive strength.

2.4.1.1 Early compressive strength of high-performance concrete

The used amount of superplasticiser has a remarkable effect on curing high-performance concrete, which has been used to decrease the water/cement ratio to a stage considering the needed compressive strength. Using a higher dose of superplasticiser may cause a problem for the wanted workability. Aïtcin (1998) emphasise that it is feasible to get a high early strength up to 30 MPa in 24 hours while using a water/cement ratio of 0,3 in an ambient temperature of 20C. Since the high dosage of superplasticiser results in delaying the hydration of high-performance concrete, it is better to prepare high-performance concrete using a higher cement/binder ratio than a lower cement/water ratio. Using cement type III, a particular type to get higher early strength (Helghts, 2016), and a binder ratio of 0,22 in high-performance concrete could give a compressive strength up to 75 MPa in 24 hours (Aïtcin, 1998). Pozzolanic materials also have a significant effect on early-age strength. Any type of pozzolans additions contributes to the development of compressive strength. Using fly ash in the mixture gives higher early-age strength. In contrast, other pozzolanic materials, such as slag, significantly improve the early-age strength compared to its remarkable contribution to the strength later (Soliman, 2011). In general, pozzolanic material could higher/lower early-age compressive strength based on which type of additives is used.

2.4.1.2 Effect of early temperature of high-performance concrete on compressive strength

The temperature influences the compressive strength of high-performance concrete in a significant matter, Jurowska & Jurowski (2020) have mentioned that a high curing temperature of concrete gives a higher early compressive strength, but it results in reduced compressive strength after a long-term more than 28 days. Some concrete was curing at 40C has shown after 3 days a compressive strength 18% higher than concrete was curing at 12C, but this high temperature gives a lower compressive strength after a long time. This high temperature increases the porosity of the structure due to the uneven distribution of cement products, and it harms concrete durability (Jurowska & Jurowski, 2020).

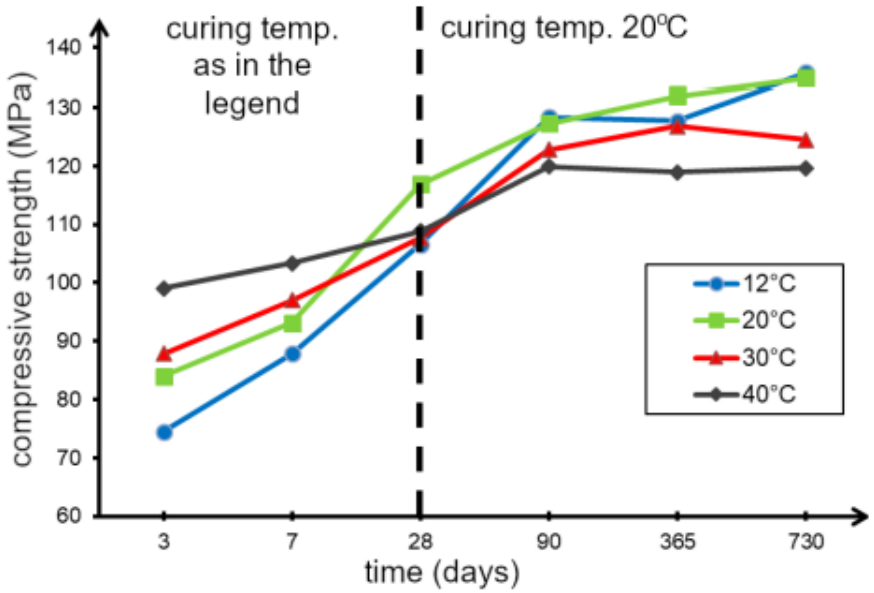

Figure 2.22 compressive strength of concrete cured at 12C, 20C, 30C and 40C (Jurowska & Jurowski, 2020).

Figure 2.22, Jurowska & Jurowski (2020) highlighted that the gained compressive strength after two years for temperatures 12 C and 20 C is the same with deference where the concrete made at 20 C gets its strength quicker, so that leads to making this concrete most favourable.

2.4.2 UHPC Compressive strength

The compressive strength of ultra-high-performance concrete has been developed compared with conventional/high-performance concrete regarding failure resistance such as bending, compression, and tension. The structure durability constructed with ultra-high-performance concrete has been improved. With a 0,2 water/binder ratio and some replacement material such as silica fume and superplasticiser, a 180 MPa compressive strength has been reached (Park et al., 2008). The early age compressive strength of ultra-high-performance concrete is substantially affected by the curing conditions like temperature. Soliman & Nehdi (2011) said that during the first 24 hours, the high curing temperature results in high compressive strength.

2.4.3 Modulus of Elasticity

The concrete modulus of elasticity is critical from a design point of view for the deformation estimation (Aïtcin, 1998). It is the main component in the evaluation of the deformation of a

structure as well as, and the modulus of elasticity is essential for designing a structure element exposed to flexure (Takafumi, 1995). The modulus of elasticity can be defined as the ratio between normal stress to normal strain where the factor of the stress-strain curve is not constant because the concrete is a material with a nonlinear stress-strain curve (Henrique et al., 2016). As long as the concrete consists of a mixture of cement, water, coarse and additives depending on the type of needed concrete with required compressive strength, that results in a different modulus of elasticity for different concrete mix proportions (Henrique et al., 2016). Figure 2.23 shows a concrete stress-strain curve derived from the compression test for concrete specimens with the main ingredients.

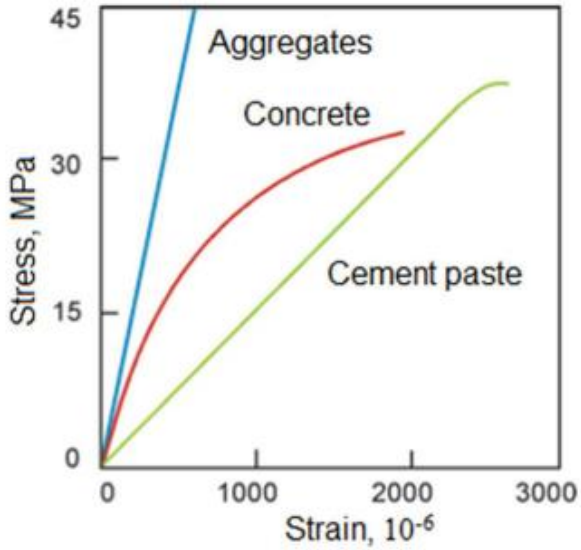

Figure 2.23 standard behaviour of the stress-strain curve for concrete (Henrique et al., 2016).

The concrete modulus of elasticity can be sorted out by the dynamic modulus, which is a way where the tangent to the origin of the stress-strain curve can be used, or by the static modulus where the ratio can be determined by the secant line of the stress-strain curve (Gutierrez & Fernandez, 1995). Figure 2.24 below shows how the elastic modulus of concrete can be obtained by stress-strain curve. Henrique et al. (2016) mentioned that the dynamic elastic modulus for high-performance concrete is 20% higher than the static elastic modulus.

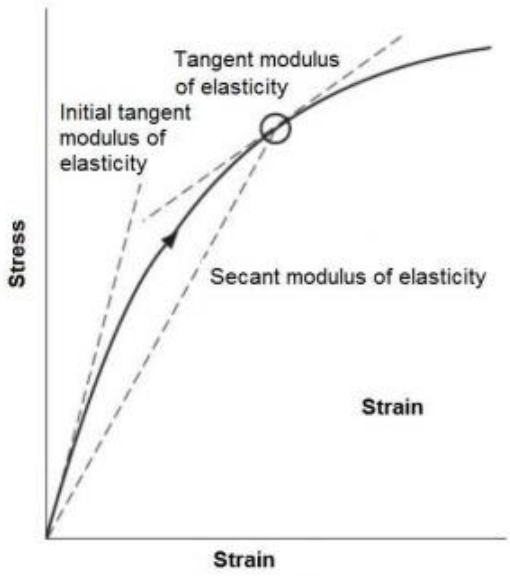

Figure 2.24 Different ways to obtain the modulus of elasticity from the stress-strain curve (Henrique et al., 2016).

The change in elastic modulus of concrete concerning its compressive strength at an early age can be affected by several components such as mixture design of concrete, properties of aggregates, and curing conditions (Soliman, 2011). (Gutierrez & Fernandez, 1995) said that the modulus of elasticity depends mainly on its porosity which is a function of the cement/water ratio. Henrique et al. (2016) illustrated in Figure 2.25 below how different factors can affect the concrete modulus of elasticity. Gutierrez & Fernandez (1995) emphasised that the aggregates have a different effect on the modulus of elasticity because the concrete mixture contains several aggregates.

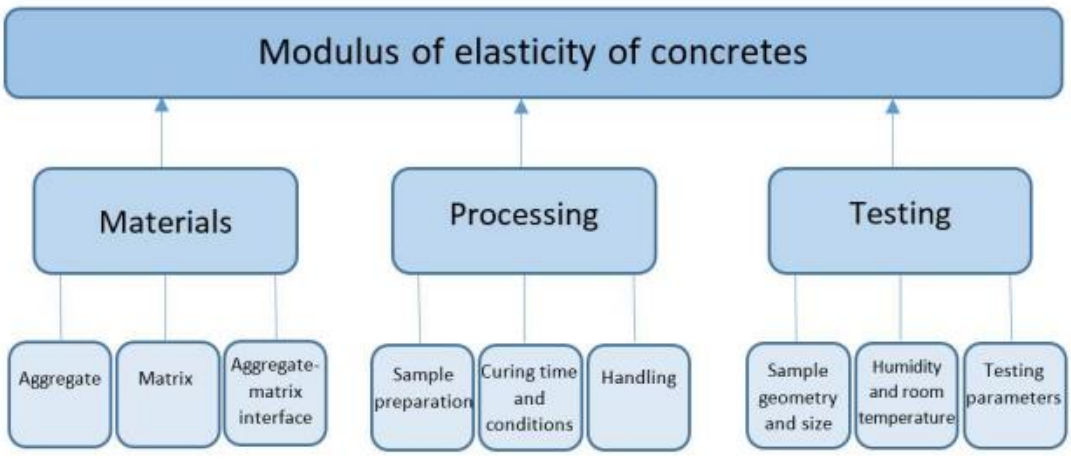

Figure 2.25 Parameters affecting the modulus of elasticity of concrete (Henrique et al., 2016).

The improved mechanical properties of ultra-high-performance concrete have increased flexural resistance and shear strength, and improved durability (Alsalman et al., 2017). The modulus of elasticity is an essential component in design because this component is linked to the shortening of the concrete parameters under compressive strength due to creep/shrinkage. The modulus of elasticity is essential when the deflection of a member is to be considered to

confirm that the member's serviceability requirements are fulfilled, as well as the rate of increase modulus of elasticity affects the speed of construction process remarkably when it is a kind of structure with in-situ cast (Fládr et al., 2019).UHPC is known for its low water/cement ratio and high supplementary cementitious material like fly ash. The usage of fly ash in ultra-high-performance concrete has significantly enhanced the modulus of elasticity. Fládr et al. (2019) emphasised that replacing 20-30% fly ash instead of cement is the best possible way to reach the highest modulus of elasticity of concrete. The value which could be reached is 60 GPa which is 70% higher than elastic modulus of conventional concrete (Ouyang et al., 2020). Ulta-high-performance concrete contains in its mixture basalt as a coarse aggregate. This aggregate rises the elastic modulus of elasticity due to its high elastic modulus, as Ouyang et al. (2020) said.

2.4.4 Flexural Strength

In order to investigate the flexural strength, a comparison between HPC and UHPC is carried out. According to Shanmuga Priya (2017), replacing nature sand with manufactured sand with 10% silica fume as a replacement material provides a higher flexural strength to HPC. Concrete has a brittle behaviour concerning resisting the tensile stress/strain without cracking. Thus, improvement of flexural strength requires a combination with steel reinforcement or optimisation of concrete mixture by adding fibres of different types and dosages (Abbas et al., 2015).

However, it has been shown in (chapter 2.3.2) that increasing steel fibre content results in a higher flexural capacity. However, Abbas et al. (2015) studied the influence of different types of fibres in terms of (length, tensile strength, and shape of fibres) on the flexural capacity of UHPFRC. They compared the results with control specimens without the addition of fibres. They observed that adding 1% of steel fibres with a length of 16 mm resulted in 37 % increase in the peak load compared to specimens without fibres (Abbas et al., 2015). Moreover, Abbas et al. (2015) have stated that the absence of fibres in the concrete lead to " a sudden drop in load-carrying capacity after reaching the peak load", in which brittle behaviour is dominated. The results are presented in Table 2-11.

Table 2-11 Flexural properties of UHPC with different steel fibre dosages (Abbas et al., 2015).

Mixture	Steel fiber		First crack load (kN)	Cracking deflection (mm)	Peak load (kN)	Peak deflection (mm)	Toughness (kN-mm)	
	Length (mm)	Dosage (%)					Cracking	Failure
1	–	–	20.07	0.45	20.45	0.47	9.03	5
2	8	1	28.68	0.81	32.52	1.35	23.23	52
3		3	45.87	0.95	54.32	1.65	43.60	108
4		6	76.32	1.10	88.24	2.08	83.95	181
5	12	1	26.76	0.68	29.87	1.08	18.20	58
6		3	40.43	0.81	49.12	1.40	32.75	120
7		6	64.34	0.94	77.54	1.80	60.50	201
8	16	1	24.76	0.61	27.97	0.95	15.10	63
9		3	35.38	0.75	43.26	1.26	26.53	130
10		6	53.76	0.88	66.13	1.63	47.30	221

1 mm = 0.04 in; 1 kN = 0.224 kip; 1 kN-mm = 0.009 kip-in.

Abbas et al. (2015) further show the influence of the length of fibres and dosage on the peak load-carrying capacity. The results are presented in Figure 2.26. It can be noticed that short fibres with a higher dosage increase peak load compared to longer fibres with the same dosage (Abbas et al., 2015). That can be explained by shorter fibres having an ability to control the formation of microcracks. In this case, the creation of macrocracks is delayed, resulting in a higher peak load (Abbas et al., 2015). However, the selection of fibres is crucial when they are used in design mixture because fibres content, shape and strength increase the

flexural strength and decrease the workability (Abbas et al., 2015; Aitcin, 1998; Máca et al., 2012; Shanmuga Priya, 2017a).

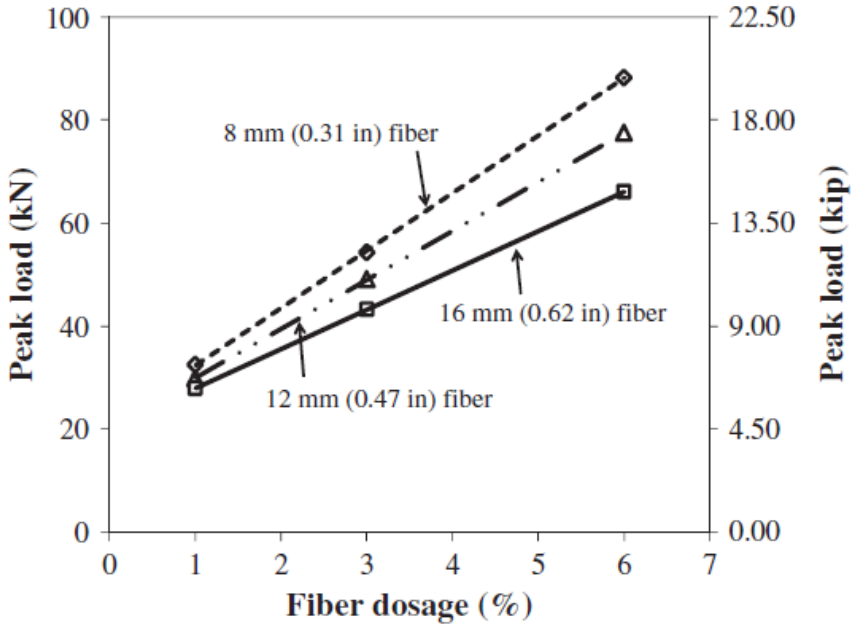

Figure 2.26 Peak load at different dosages and lengths of steel fibre (Shanmuga Priya, 2017a).

2.4.5 Fracture Energy

The increased usage of high-performance concrete in regular structures pushed the researcher towards knowing the suitable applications of high-performance concrete in the construction field, where the fracture behaviour of a structure built by high-performance concrete is essential due to its high brittleness. Two factors are important for fracture mechanics, fracture energy and the critical stress intensity factor (Petersson, 1980). Einsfeld & Velasco (2006) the fracture energy GF as "the amount of energy necessary to create a crack of the unit surface area projected in a plane parallel to the crack direction". While the critical stress intensity factor is "a measure of the magnitude of the stress concentration which exists in front of the crack tip when the crack starts to propagate" as Petersson (1980) described.
The formula can determine the fracture energy:

$$G_F = \frac{W}{b(d - a_0)}$$

Where b is the thickness of the beam, d is the height of the beam, a0 is the notch depth of the beam, and W is the total energy dissipated during the test (Einsfeld & Velasco, 2006).
Petersson (1980) mentioned that there is a relation between the fracture energy and the critical stress intensity factor where if one of these is known, then the formula can calculate the other one:

$$K_C = \sqrt{G_F . E}$$

K_C The critical stress intensity factor.
E Young's modulus.
G_F The fracture energy.

The fracture energy can be affected by some items such as water/cement ratio, type of additives and properties of each component of the concrete mixture. Since normal strength concrete and HPC/UHPC have different mixing, resulting in different fracture energy behaviour. Furthermore, high-performance concrete may include some additives that raise the heat of hydration and increase the thermal stress, which results in the behaviour of cracking and energy absorption (Beygi et al., 2013).

In general, Beygi et al. (2013) asserted that the fracture energy of high-performance concrete could increase with decreasing the water/cement ratio. The primary reason is that when the water/cement ratio decreases, cement paste's porosity becomes less and higher. In normal strength concrete, the water/cement ratio has a substantial effect on the quality of the interfacial transition zone. When the porosity in this zone increase, the microcracks appear and extend with porosity increasing. For normal strength concrete with water/cement ratio between 0,33-0,63, the highest fracture energy occurs for water/cement ratio 0,33 where the porosity is lowest (Beygi et al., 2013). The variation of fracture energy concerning water/cement ratio has been considered in many studies. Beygi et al. (2013) showed that the fracture energy varied between 201 and 128 for a 0,33-0,55 water/cement ratio, and another study showed fracture energy of 205-135 for 0,28-0,75 water/cement ratio. In high-performance concrete, the quality of cement pastes and the interfacial transition zone has been improved, giving higher strength. A decrease in water/cement ratio to 0,4 results in the highest value of fracture energy (Beygi et al., 2013). Figure 2.27 below shows how the fracture energy varies with regard to water/cement ratio.

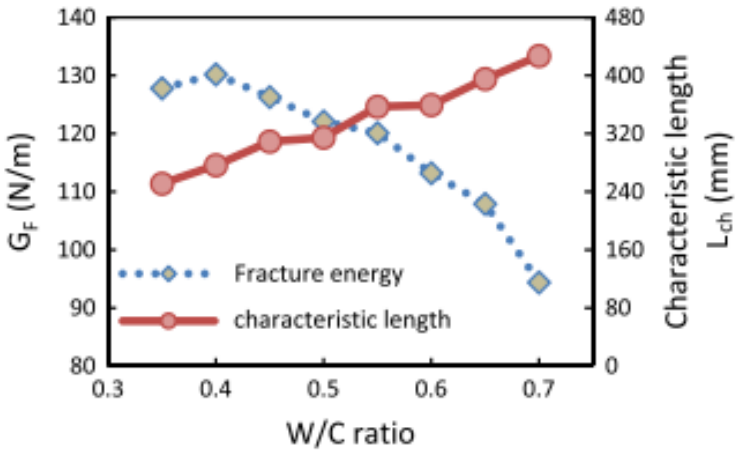

Figure 2.27 Variation of the fracture energy in regard to water/cement (Beygi et al., 2013).

Many of concrete mechanical properties depend on compressive strength. According to CEB-FIP (1990), the fracture energy can be determined as a function of the compressive strength in the form of power function. For high-performance concrete, an increase of strength up to 120 MPa increases the value of fracture energy up to 190 N/m, and for high-strength concrete with a 109 MPa compressive strength gives a 137 N/m fracture energy (Beygi et al., 2013). A high-performance concrete includes fly ash and silica fume in its mixture with a compressive strength of 45 MPa, giving a 108 N/m fracture energy, as shown in the figure below.

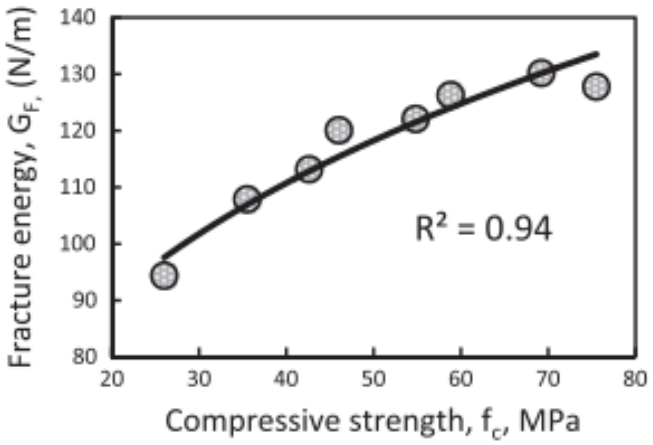

Figure 2.28 Fracture energy versus compressive strength (Beygi et al., 2013).

The main difference between conventional concrete and high-performance concrete is using chemical additives in the mixture. One of these additives is silica fume, the usage of silica fume has been increased recently, where the first use was in 1970 as a cementitious material in the concrete mixture (Zhang & Li, 2015). The use of silica fume has been applied in two different manners: as a cement replacement to reduce the cement content for an economic reason and as additive material to improve concrete properties. By adding silica fume, the compressive strength and durability have been improved. Furthermore, the addition of silica fume reduces the porosity of the transition zone to become stronger (Zhang & Li, 2015). The fracture properties are fundamental to the structure safety built by high-performance concrete. The fracture properties of high-performance concrete, such as fracture toughness, fracture energy and effective crack length have been improved by increasing the silica fume in a small amount, said Zhang & Li, (2015).

Another additive to HPC mixture is fly ash. It replaces Portland cement up to 30 % (Zhang et al., 2012). The mixture of high-performance concrete, including fly ash, has great betterment on the fracture energy, fracture toughness, and effective crack length. High-performing concrete containing fly ash has a better ability to resist crack propagation (Zhang et al., 2012).

For UHPC, which includes some cementitious replacement material in its mixtures such as fly ash and silica fume, as mentioned before, these additives affect mostl§y the magnitude of fracture energy and ultra-high-performance concrete has a significantly high strength which leads to a decrease in the fracture energy (Voit & Kirnbauer, 2014).

2.4.6 Shrinkage behaviour

For any type of concrete to get the highest strength and lowest permeability, water curing is essential to ensure hydration. For HPC, early curing is better than late, and for normal strength concrete, late curing is better than completely no curing (Aïtcin, 1998). The shrinkage of concrete is straightforward in its expression, as Aïtcin (1998) said, “a decrease in the apparent volume of the concrete.” However, it is not very easy when it is needed to be understood. Some concrete with a low cement/binder ratio is identified as UHPC and normal strength concrete, which is more prone to crack at an early age (Hammer, 2007). These cracks vary in shape and size depending on the concrete ingredient; ambient conditions

include temperature and moisture (Elzokra et al., 2020). The shrinkage properties can be affected by the surrounding environment, type of aggregate, water/cement ratio and the additives material. Some replacement material, such as fly ash, can improve the resistance of concrete regarding shrinkage and cracks propagation (Elzokra et al., 2020). It is possible to avoid the shrinkage phenomenon and the consequences that could be caused by the shrinkage behaviour, said Aïtcin (1998).
There are some kinds of concrete shrinkage as Aïtcin (1998) mentioned when describing the concrete shrinkage as it is an association of many elementary shrinkage:

- Early drying shrinkage (plastic shrinkage) grows at the surface of the fresh concrete.
- Autogenous shrinkage, it develops when cement hydrates.

Early drying shrinkage:

Plastic shrinkage is referred to the shrinkage of fresh concrete, which is subjected to drying. It occurs when the loss of the mixture's water is more than the rate of bleeding at the surface. In other words, it is defined as the volume change occurring during the early age of concrete when the concrete is still in its liquid state (Wu et al., 2017). The plastic shrinkage leads to initial cracking at the structure's surface, and it may continue to extend to reach the mid of the structure with time. The cracks that grow because of the plastic shrinkage increase with decreasing the water/cement ratio. That is why high-performancor high-strength concrete is more sensitive than usual concrete because high-performance concrete has a lower cement ratio (Petersson, 1980).
There is a remarkable difference between ultra-high-performance concrete and conventional concrete, especially in the hydration process and microstructure propagation, UHPC has improved mechanical properties and is more durable due to its low water/cement ratio, but on the other hand, this reduction in the water/cement ratio could lead to a rapid autogenous shrinkage at an early age (Liu & Wei, 2021). The large early shrinkage of concrete results in micro-cracks that can minimise the structure's service lifetime.

Autogenous shrinkage
Wu et al. (2017) have defined autogenous shrinkage as "a macroscopic volume reduction of cementitious material *when cement hydrates after initial setting".* When the water/cement ratio is low, then the internal moisture is limited to hydrate cement particles completely. Therefore, autogenous shrinkage needs to be considered in early age cracking of high-performance concrete Wu et al., (2017). Autogenous shrinkage is influenced by several factors such as relative humidity, ambient temperature, and water/cement ratio. Additives material to the mixture in high-performance concrete, such as fly ash and silica fume, can increase the autogenous shrinkage when the hydration reaction accelerates the water consumption at an early age Wu et al., (2017). At early days after concrete casting, the reaction between the cement and moisture will continue, leading to a chemical shrinkage, as Engström (2007) mentioned, which occurs between concrete and the surroundings. Figure 2.29 below illustrates the reaction that causes autogenous and chemical shrinkage. C is the cement, W is water, H_Y is hydration products, and V is the voids generated by hydration (Holt, 2001).

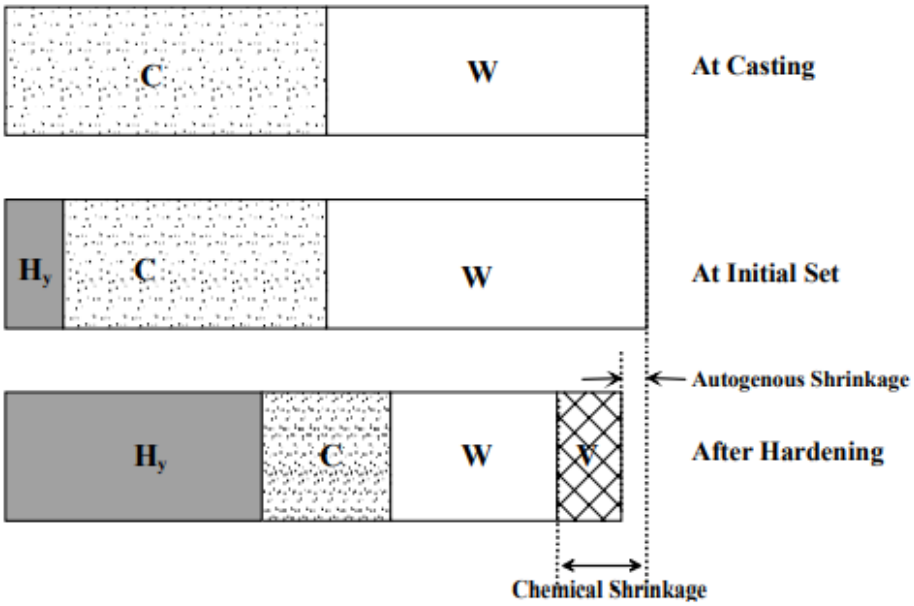

Figure 2.29 Reactions cause autogenous and chemical shrinkage (Holt, 2001).

It is noticed that autogenous shrinkage influences the concrete at different levels (Engström, 2007). The serious influence of autogenous shrinkage is related to the low water/cement ratio, such as high/ultra-high-performance concrete and a high amount of cementitious material (Holt, 2001). It was noted that autogenous shrinkage influences the concrete on different levels as Engström (2007), while the serious influence of autogenous shrinkage is related to the low water/cement ratio, such as HPC/UHPC and high amount of cementitious material (Holt, 2001). The autogenous shrinkage of ultra-high-performance concrete could be reduced by some applications, as Liu & Wei (2021)mentioned. An appropriate curing condition and using fly ash and silica fume can effectively reduce the autogenous shrinkage of ultra-high-performance concrete. Another component that could be used is coral aggregate (Liu & Wei, 2021), which is a replacement material that can be used instead of quartz sand and has a good result regarding the autogenous shrinkage and the compressive strength as well.

2.4.7 Creep

HPC has been used recently in building different applications such as high-rise buildings and bridges where the expected life span of these structures exceeds 100 years (le Roy et al., 2017). Creep of concrete is a substantial factor in designing and analysing concrete structures, especially for long-term serviceability and durability. Creep is one of the main factors that influence the behaviour of the high-performance concrete because it affects the early-age cracking, where the early-age cracking is higher in high-performance concrete than normal strength concrete due to its low water/binder ratio (Gu et al., 2019). HPC has been widespread due to its high strength, good workability, and high durability. HPC contains some additives, such as fly ash, which show promising creep resistance results. Zhao et al., (2015) showed that HPC mixture containing a 25% fly ash with good quality reduces the creep 30 % compared to a mixture without fly ash like normal concrete. fly ash is temperature-dependent and reacts actively with high temperatures, and this reaction affects the quantity and microstructures of the hydration products, which affects the concrete creep (Zhao et al., 2015).

2.5 Durability Properties

As mentioned before, the story began with optimizing the strength of normal strength concrete to be stronger. However, HPC has more beneficial properties than its high strength. For instance, durability and abrasion resistance (Aïtcin, 2003). The durability of concrete is a significant challenge, especially when it comes to corrosion caused by carbonation, which reduces the service life of the structure. The carbonation is faster in the industrial and seaside areas, Sohail et al. (2021) reported that the carbon dioxide concentration, the relative humidity 40 %-80 % and the temperature 20-50 C are the reasons for rapid carbonation. HPC/UHPC are expected to be the solution to the durability challenge to gain a more durable concrete structure (Sohail et al., 2021).

The replacement material used in HPC/UHPC, such as fly ash, results in higher strength and better flowability. UHPC can improve the structure's lifespan by decelerating harmful agents such as chloride ingress. Sohail et al (2021) said that the chloride permeability in ultra-high-performance concrete is 34 times less than high-performance concrete and 220 times less than normal concrete. In contrast, the oxygen diffusivity in ultra-high-performance concrete is 10 and 100 times less than HPC and normal concrete, respectively.

2.5.1 Carbonation

The amount of cement and cement/water ratio used in the concrete mixture has a good role in the carbonation resistance. Increased cement and lower water/cement ratio result in low permeability and better strength (Zhang & Li, 2013). The replacement material used in high/ultra-high-performance concrete like fly ash and silica fume has significantly improved the carbonation resistance. The figure below illustrates the carbonation process how it starts at the concrete cover of the structure and penetrates inside. Carbonation can be reduced by decreasing the water/cement ratio to prevent carbon dioxide flow in the capillary pores and reducing carbonation speed (Luping, 2021).

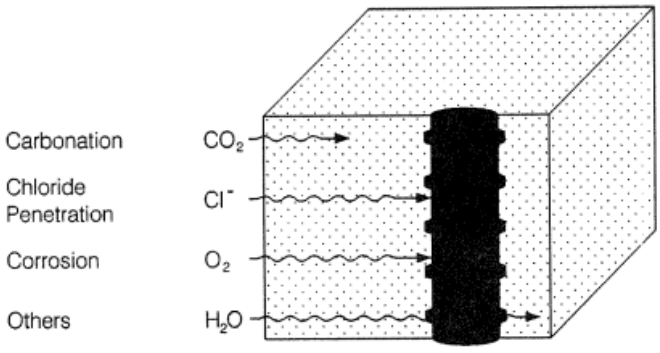

Figure 2.30 Deterioration of concrete structures (Luping, 2021).

2.5.2 Chloride penetration

The chloride ingress has a vital role in the durability of concrete structures. Any concrete structure is prone to different environmental factors affecting structural behaviour and life span. Chloride penetration is one of these environmental factors caused by several factors such as concrete structures exposed to a marine environment, roads where de-icing salts are used, etc. The chloride ingress reaches the structure's reinforcement and leads to corrosion of

the steel reinforcement, which causes durability problems (Luping et al., 2011). Some conditions need to be fulfilled for corrosion, electrical conductivity, moisture existence, electrical conductivity, and a pH level of less than 9 (Pernicová, 2014). HPC/UHPC has a high electrical resistance, which means the risk for corrosion is low. The absorption of the high/ultra-high-performance concrete is between one-half and one-third compared to normal concrete, decreasing chloride transportation (Sohail et al., 2021).

2.5.3 Freeze/thaw

Any structure is prone to some external factors from the surrounding environment, and one of these factors is the freeze/thaw cycle. In other words, it is a continuous cooling and warming process of water in the structure. When it is freezing weather, the water freeze until it becomes ice, then it expands and leads to weak the surrounding concrete structure, and when it melts, the expansion of the concrete structure will not go back to its old shape (Lu et al., 2021). The concrete mixture significantly influences the freeze-thaw resistance, and Lu et al (2021) said that the freeze-thaw resistance can be improved by lowering the water/binder ratio, which means a small pore size. As long as HPC/UHPC have a low water/binder ratio, high amount of cement, fine particles, minor porosity and good workability, high strength, and is more durable compared to normal concrete, that results in the freeze-thaw resistance of high/ultra-high-performance concrete is better compared to normal concrete (Lu et al., 2021).

3 Case study

3.1 Aim

The main aim of the case studies is to calculate the bending moment and shear capacities of the cross-section obtained by using HPC and UHPC, respectively, instead of normal strength concrete. The bending moment calculation will consider the middle of the span. In contrast, shear capacity will consider the section where the maximum shear force occurs, which is close to the support.

Moreover, a new design for the cross-section will be made using HPC and UHPC, where the aim is to design a cross-section that can carry the applied loads and fulfil the requirement in service limit state (SLS). Hence, crack width and deflection will be controlled for the case of HPC/UHPC and compared with the cross-section where normal strength concrete was used. The reduction of cross-section height and changing of reinforcement amount will be compared with the normal strength concrete cross-section to see the gains of using HPC and UHPC.

Only the bridge's superstructure will be considered in the calculation, where no calculation for the bridge legs or wings is included. The applied loads on the structure are retrieved from the case study provided by AFRY. In other words, there was no need to calculate the loads acting on the bridge or make any load combination.

As mentioned before, no life cycle cost (LCC) or life cycle analyses (LCA) will be considered, and the focus will be only on the design stage. Furthermore, no laboratory experiment or testing was conducted. Rather, the calculations were based on fictitious case studies where the mechanical properties of HPC and UHPC were picked up from EN-1992-1-1 and the French Standard (NF P18-710).

3.2 General description of case studies

To achieve the objective of this master thesis, three case studies are carried out. The input data are provided by AFRY and consider an exciting rigid-frame bridge. A general description of each case study is given below.

3.2.1 Case1

This case aims to calculate the bending moment capacity of a cross-section chosen in the middle of the span. The concrete used in this case is normal strength concrete (NC) of class C35/45, the same concrete class used in the case study provided by AFRY. The results are then compared with other case studies where HPC and UHPC will be used. For calculation, see Appendix A

3.2.2 Case 2

HPC of class C90/105 is used in this case study because this concrete can be produced in Sweden from locally available materials. In this case, there is no need to import materials such as aggregate from other countries to produce concrete up to C90/105. This case study consists of two scenarios.

Senario1: the cross-section has the same height as case 1 and the same reinforcement amount. The only parameter that is changed is material class. The bending moment capacity is calculated and compared with the bending moment capacity obtained from Case 1. The objective is to see how much the bending moment capacity can be increased by using HPC with characteristic compressive strength of 90 MPa.

Scenario 2: the cross-section is optimised by reducing the thickness and calculating the required reinforcement amount. The calculation considers both ULS and SLS, where bending moment capacity and shear design are calculated in ULS, while crack width and deflection are calculated in SLS. The results of this scenario are compared with Case 1.

For calculation, see Appendix B

3.2.3 Case 3

UHPC of class C 200/215 is used in this case study. Moreover, this is the maximum value of UHPC considered in the French standard. The mechanical properties of C200/215 are considerably higher than the other lower classes. The highest class is chosen to investigate the maximum gaining of utilizing UHPC. However, this case study consists of two scenarios:

Senario1: the cross-section has the same height as case 1 and the same reinforcement amount. The only parameter that is changed is material class, where concrete of 200MPa characteristic compressive strength is used. The bending moment capacity is calculated and compared with the bending moment capacity obtained from Case 1. The objective is to see how much the bending moment capacity can be increased using UHPC.

Scenario 2: the cross-section is optimised by reducing the thickness and calculating the appropriate reinforcement amount using a concrete with very high compressive strength (200 MPa) and reducing the cross-section height. The calculations consider both ULS and SLS, where the bending moment capacity and the shear reinforcement are checked in ULS, while crack width and deflection are checked in SLS. The results of this scenario are compared with Case 1. For calculation, see Appendix C

3.3 Geometry and dimensions.

A railway bridge is built at Holmängen in Vänersborg. The bridge is a single-track railway. The bridge is designed as a frame bridge with a width of 7.2 m and free opening between the frame legs is 6.0 m. The cross-sectional height of the bridge varies in the longitudinal direction. The dimension varies from 565 mm at the bridge end to 600 mm in the middle of the bridge, as seen in Figure 3.1, while the cross-sectional height is constant in the transverse direction. The effect of the reduced cross-sectional height is considered during calculations in ULS and SLS.

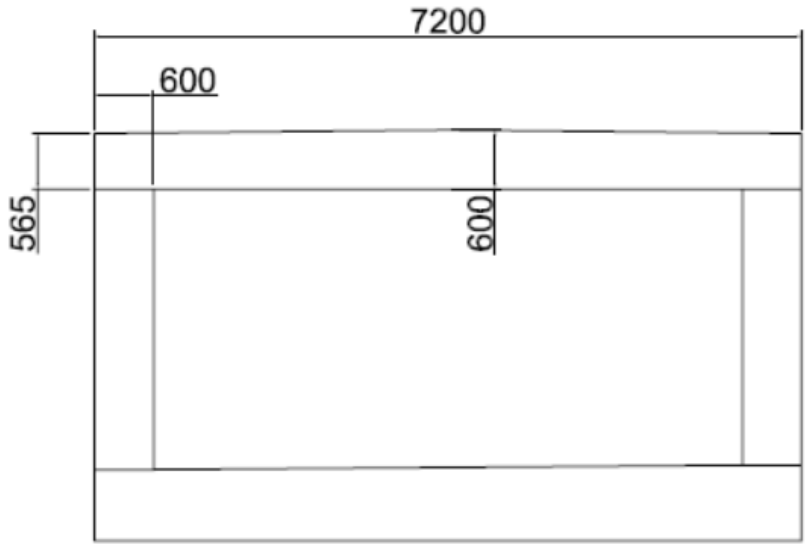

Figure 3.1 The cross-sectional height along the bridge.

3.4 Loads

The loads taken into account are the permanent loads from concrete, ballast, railing, and earth pressure. The variable load is the traffic load applied on the bridge with the load model (LM71) according to SS-EN 1991-2 Ch 6.3.2, see Figure 3.2 below.

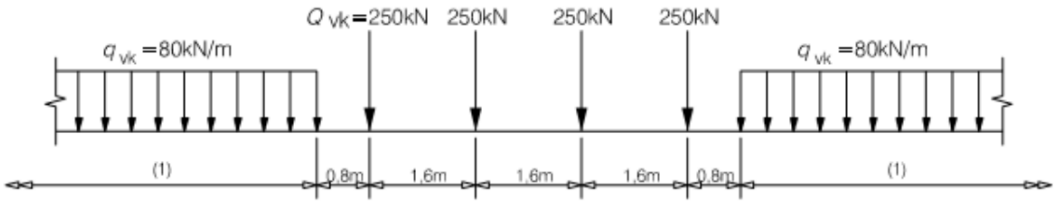

Figure 3.2 load model LM71.

3.5 Standards and requirements

The design and calculations are conducted according to some standards and requirement documents which are prescribed below:

- Design of concrete structures(Concrete bridges), SS-EN 1992-2:2005.
- Design of concrete structures(general rules), SS-EN 1992-1-1:2005.
- Krav Brobyggande (KRAV), TDOK 2016:0204, Version 3, 2019.
- Bärande konstruktioner part 1, 2013.
- Concrete – Application of EN 206-1 in Sweden, SS 137003:2008.
- National addition to Eurocode 2, NF P 18-710, 2016.
- The Swedish Transport Administration's regulations, TRVFS 2011:12.

3.6 Method

The methods for the three case studies differ from each other regarding some block factors and formulas used just for UHPC. The difference between each case study is described below.

3.6.1 Case 1 (NC)

As mentioned before, this case is unchanged. This case's main idea is to find out the moment capacity of a cross-section in mid span to compare results between different cases. Normal strength concrete has been used in this case with 35MPa compressive strength.

3.6.1.1 Construction classes

Bridge service life is set to be 120 years (L100), and for the bridge deck and the frame leg, a safety class 3 is chosen. Recommended exposure classes, concrete cover and crack width are selected with reference to (VVFS 2004:31, VVFS 2004:43, and SS-EN 1992-1-1:2005).

Table 3.1 Construction classes of the bridge.

Construction part	Exposure class	Service life	Concrete cover (mm)	$W_{K,}$ (mm)	Max w/c
Bridge deck top	XD1/XF4	L100	40	0,3	0,5
Bridge deck bottom	XC4/XF4	L100	40	0,3	0,45
Frame leg-air side	XD1/XF4	L100	40	0,3	0,45
Frame leg-soil side	XD1/XF4	L100	40	0,3	0,5

3.6.1.2 Material

The used concrete, in this case, is C35/45, which is the same concrete used in the original (real) project, and with a reinforcement type K500C with a 500 MPa strength. The partial factors of this case and other characteristics/design values are shown in the table below:

Table 3.2 Characteristics/design value of C35/45 according to SS-EN 1992-1-1:2005.

Type	strength parameters	partial coefficients
C35/45	f_{ck} = 35 MPa f_{ctm} = 3,2 MPa f_{ctk} = 2,2 MPa E_{cm} = 34 GPa	$\gamma_{c,uls}$ = 1,5 $\gamma_{c,als}$ = 1,2 $\gamma_{c,sls}$ = 1,0
K500C-T	f_{yk} = 500 MPa E_s = 200 GPa	$\gamma_{s,uls}$ = 1,15 $\gamma_{s,als}$ = 1,0 $\gamma_{s,sls}$ = 1,0

3.6.2 Case 2 (HPC)

In this case, where HPC is used, two scenarios are conducted. The first one has the exact dimensions and different strengths, and the second one with reduced high of the cross-section. It was supposed to calculate a new concrete cover according to TRVFS 2011:12, Ch. 21 due to changes in dimensions and a new crack width control was carried out.

3.6.2.1 Construction classes

The service life of the structure is L100 (120 years), and the safety class is chosen to 3, both are unchanged and selected according to (VVFS 2004:31 and VVFS 2004:43).

According to SS-EN 1992-1-1:2005, new exposure classes should be considered regarding HPC, which has different properties.

Table 3.3 Exposure classes of HPC.

Construction part	Exposure class	Service life	Concrete cover [mm]	W_k [mm]	Max w/c
Bridge deck top	XD1/XF4	L100	30	0,3	0,3
Bridge deck bottom	XC4/XF3	L100	30	0,2	0,3

According to SS-EN 1992-1-1:2005, ch. 4.4.1.1, the concrete cover is calculated with the formula:

$$c_{nom} = c_{min} + \Delta c_{dev} \tag{3.1a}$$

Where:

$$c_{min} = \max\left(c_{min.b}, c_{min.dur} + \Delta c_{dur.\gamma} - \Delta c_{dur.st} - \Delta c_{dur.add}, 10mm\right) \tag{3.1b}$$

And is $\Delta c_{.dev} := 10\text{mm}$ chosen according to SS-EN 1992-1-1:2005, ch.4.4.1.3

3.6.2.2 Material

Material properties of HPC (C90/105) are taken from table 3.1 in SS-EN 1992-1-1,2005.

Table 3.4 Material properties of HPC (C90/105).

Type	Strenght parameters	Partial factors
C90/105	f_{ck}=90 MPa f_{ctm}=5 MPa f_{ctk}=3.5 MPa E_{cm}=44 GPa	$\gamma_{.c} := 1.5$
K500C-T	f_{yk}= 500 MPa E_s=200 GPa	$\gamma_{.s} := 1.15$

The ultimate compressive strain of $\varepsilon_{cu} = 0.028$ (C90/105) is taken from Table 3.1 in SS-EN 1992-1-1,2005. Creep coefficient (φ_{ef} = 1.87) is selected according to SS-EN 1992-1-1, 2005. Figure 3.1.

3.6.3 Case 3 (UHPC)

In this case, UHPC with 200 MPa compressive strength is used instead of normal concrete. It was supposed to implement a new standard, the national addition to Eurocode 2, NF P 18-710, 2016 (approved French national standard), to perform the relative controls and required calculations.

3.6.3.1 Construction classes

The service life of the structure and safety class is unchanged compared to HPC and are chosen according to (VVFS 2004:31 and VVFS 2004:43). The recommended values regarding the exposure class are XD3/XF4 in conformity with NF P 18-710, 2016.
A new concrete cover has been calculated according to TRVFS 2011:12, Ch. 21, which considers this kind of material that includes steel fibres in its mixture.

$$c_{nom} = c_{min} + \Delta c_{dev} \tag{3.1}$$

$$c_{min} = \max\left(c_{min.b}, c_{min.dur} + \Delta c_{dur.\gamma} - \Delta c_{dur.st} - \Delta c_{dur.add}, \Delta c_{min.p}, 10mm\right) \tag{3.2}$$

$$c_{min.p} = \max\left(1.5L_f, 1.5.\, D_{sup}, \emptyset_{s.bot}\right) \tag{3.3}$$

Where:
L_f is the length of the longest fibres, NF, P18-710 (2016), Table T.1, Annex T.
D_{sub} is the nominal upper dimension of the largest aggregate Ch. 5.4.3 of standard NF P18-470.

3.6.3.2 Material

Values of UHPFRC C200 are taken from NF P18-710 (2016), Table T.1, Annex T, and it is shown in the table below:

Table 3.5 Material properties of UHPFRC C200, NF P18-710 (2016), Table T.1.

f_{ck}=200 MPa	Characteristic compressive strength
f_{cm}=230 MPa	Mean compressive strength
$f_{ctk,el}$=10 MPa	Characteristic tensile strength
$f_{tcm,el}$= 12MPa	Mean tensile strength
f_{ctk}=10 MPa	Characteristic post-cracking strength
f_{ctm}=12 MPa	Mean post-cracking strength
E_{cm}= 65 GPa	Modulus of elasticity

Design compressive strength of UHPFRC C200 is calculated with formula in NF P18-710 (2016):

$$f_{cd} = \frac{\alpha_{cc} \cdot f_{ck}}{\gamma_c} \tag{3.4}$$

Where $\alpha_{.cc} := 0.85$ is coefficient which takes account of long-term effects.

Maximum design elastic shortening strain at ULS is calculated according to NF P18-710 (2016), Ch. 3.1.7 and Figure 3.3 with following formula:

$$\varepsilon_{c0d} = \frac{f_{cd}}{E_{cm}} \tag{3.5}$$

And the maximum design shortening strain can be calculated according to NF P18-710 (2016), Ch. 3.1.7:

$$\varepsilon_{cud} = \left(a + 14.\frac{f_{ctfm}}{K_{global} \cdot f_{cm}}\right).\varepsilon_{c0d} \tag{3.6}$$

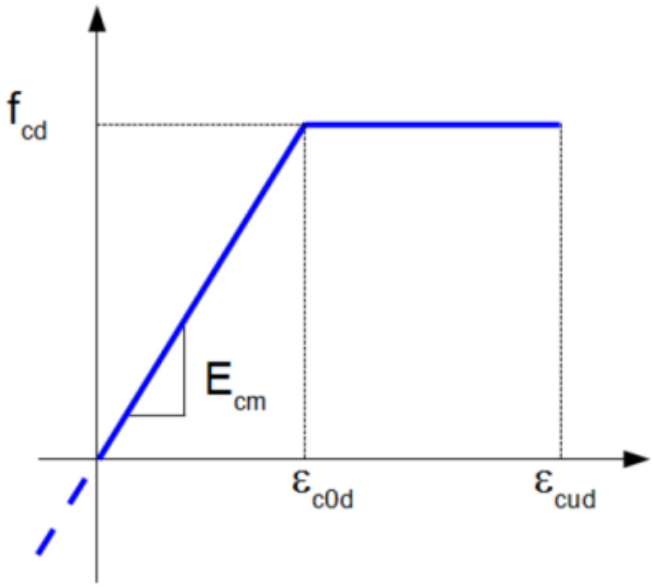

Figure 3.3 stress-strain relation of UHPFRC in compression for designs at ULS, NF P18-710 (2016).

K_{global} is a factor used in strain calculation and it is defined in NF P18-710 (2016) as following:
"K_{global} deals with the global effects corresponding to resistant mechanisms which require the fibres to act over wider areas and where a localized fault will not have significant consequences".

When calculating the tensile strength, the tensile class must be defined according to NF P18-710 (2016), ch.7.3.1.

- Class T1 if, $f_{ctf}/K < f_{ct,el}$ both for the mean curve and the characteristic curve.
- Class T2 if, $f_{ctf} / K \geq f_{ct,el}$ for the mean curve and $f_{ctf} / K < f_{ct,el}$ for the characteristic curve.
- Class T3 if, $f_{ctf} / K \geq f_{ct,el}$ both for the mean curve and the characteristic curve.

Tensile strength divers depending on the member if it is thick or thin. In other words, slenderness control is required here. Member is considered thick if $h > 3L_f$, where h is the member's height, and L_f is the length of the longest fibres contributing to ensuring non-brittleness.
At ULS, the design value of the tensile limit of elasticity can be expressed as follow:

$$f_{ctd.el} = \frac{f_{ctk.el}}{\gamma_{cf}} \tag{3.7}$$

elastic tensile strain can be calculated by:

$$\varepsilon_{u.el} = \frac{f_{ctd.el}}{E_{cm}} \tag{3.8}$$

Where the design value of post-cracking strength:

$$f_{ctdf} = \frac{f_{ctfk}}{\gamma_{cf}.K_{global}} \tag{3.9}$$

Characteristic length relates the crack width to an equivalent deformation where h is the height of the section in accord with NF P18-710 (2016), ch.3.1.7.3.2.

$$L_c = \frac{2.h}{3} \tag{3.10}$$

Tensile strain limit beyond which the participation of the fibres is no longer considered at the ultimate limit state NF P18-710 (2016), ch.3.1.7.3.2.

$$\varepsilon_{u.lim} = \frac{L_f}{4.L_c} \tag{3.11}$$

Maximum limit of elasticity at SLS can be expressed as:

$$\varepsilon_{el} = \frac{f_{ctd,el,sls}}{E_{cm}} \tag{3.12}$$

and design value of post-cracking strength at SLS:

$$f_{ctfd,SLS} = \frac{f_{ctfk}}{K_{global}} \tag{3.13}$$

Calculation of compressive zone:

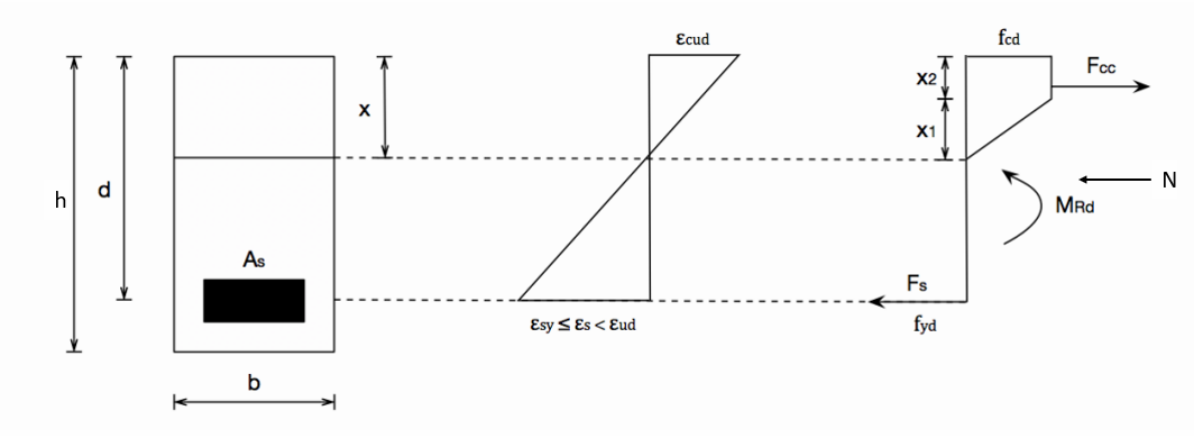

Figure 3.4 Stress-strain relation with section forces for the cross-section.

Figure 3.4 shows the stress-strain behaviour, and it is used to calculate the compressive zone and the following calculation.

From the Figure 3.4, F_{cc} is the compressive force of UHPFRC, and it can be calculated as follow:

$$F_c = f_{cd}\left(\frac{\left(\frac{\varepsilon_{cod}}{2}\right)+(\varepsilon_{cud}-\varepsilon_{cod})}{\varepsilon_{cud}}\right).x_{bot}.b \tag{3.14}$$

where x_{bot} is the compressive depth at the bottom side, x_1 the height from the natural layer up to the strain and x_2 the height between the ε_{c0d} and ε_{cud} and it can be calculated as follow:

$$x_1 = \frac{\varepsilon_{c0d}}{\varepsilon_{cud}} . x \tag{3.16}$$

$$x_2 = x - x_1 \tag{3.17}$$

x_c is the lever arm to the neutral axis and it can be estimated as:

$$x_c = \frac{\left(\frac{x_1 . 2}{3}\right) . \frac{x_1}{2} + \left(x_1 + \frac{x_2}{2}\right) . x_2}{\frac{x_1}{2} + x_2} \tag{3.18}$$

A condition of reinforcement strain should be fulfilled:

$$\varepsilon_{sy} \leq \varepsilon_s \leq \varepsilon_{ud} \tag{3.19}$$

Shear reinforcement

Shear force must always be checked against the shear capacity or shear stress capacity of the section. Moreover, according to NF P18-710 (2016), the design shear force at ULS must be smaller than the resisting shear force. The shear force depends on the support conditions of the beam and the location of the load on the member. The first axle force is located at a distance d from the support, while the shear reinforcement is designed for the shear force at the support because the shear force is maximum.

Strain at the maximum limit of elasticity can be calculated with:

$$\varepsilon_{el} = \frac{f_{ctd.el.SLS}}{E_{cm}} \tag{3.20}$$

According to NF P18-710 (2016), design resisting shear force from UHPC can be estimated from:

$$V_{Rd.c} = \frac{0.18}{(\gamma_{cf} . \gamma_E)} . K . f_{ck}{}^{\frac{1}{2}} . b . h \tag{3.21}$$

$$K = 1 + 3 . \frac{\sigma_{cp}}{f_{ck}} \tag{3.22}$$

$$\sigma_{cp} = \frac{N_{Ed}}{h . b} \tag{3.23}$$

Chapter 6.2.1.3 in NF P18-710 (2016) shows how the contribution from shear force reinforcement can be calculated:

$$V_{Rd,s} = 0$$

Because it is assumed that there is no shear reinforcement.

The contribution from the fibres $V_{Rd,f}$ can be calculated according to Chapter 6.2.1.3 in NF P18-710 (2016) as:

$$V_{Rd,f} = A_{fv} . \sigma_{Rd.f} . \cot\theta \tag{3.24}$$

For a rectangular cross-section:

$$A_{fv} = b.z \tag{3.25}$$

$$z = 0.9.d \tag{3.26}$$

When using UHPFRC with tensile class, the post-cracking strength means value can be calculated according to NF-P-18-710:

$$\sigma_{Rd,f} = \frac{1}{K_{global} \cdot \gamma_{cf}} . \frac{1}{\varepsilon - \varepsilon_{el}} . \int_{\varepsilon_{el}}^{\varepsilon} \sigma_f(\varepsilon) d\varepsilon \tag{3.27}$$

$$\int_{\varepsilon_{el}}^{\varepsilon} \sigma_f(\varepsilon) d\varepsilon = f_{ctfd} . \left(\frac{\varepsilon_{u.lim} - \varepsilon_{el}}{\varepsilon_{u.lim}}\right) + \left(f_{ctd.el.SLS} - f_{ctfd}\right) . \left(\frac{\varepsilon_{u.lim} - \varepsilon_{el}}{2.\varepsilon_{u.lim}}\right) \tag{3.28}$$

$$\sigma_{Rd,f} = \frac{1}{K_{global} \cdot \gamma_{cf}} . \frac{1}{\frac{\varepsilon - \varepsilon_{el}}{\%}} . \left(f_{ctfd} . \left(\frac{\varepsilon_{u.lim} - \varepsilon_{el}}{\varepsilon_{u.lim}}\right) + \left(f_{ctd.el.SLS} - f_{ctfd}\right) . \left(\frac{\varepsilon_{u.lim} - \varepsilon_{el}}{2.\varepsilon_{u.lim}}\right) \right) \tag{3.29}$$

Total shear resistance became:

$$V_{Rd} = V_{Rd,c} + V_{Rd,s} + V_{Rd,f} \tag{3.30}$$

When no shear reinforcement is assumed, $V_{Rd,max}$ can be calculated according to NF P18-710 (2016), Chapter 6.2.1.5:

$$V_{Rd,max} = 2{,}3 . b . z . f_{ck}^{\frac{2}{3}} . \tan\theta \tag{3.31}$$

The design of shear force resistance is the minimum value of:

$$V_{Rd} = \min\left(V_{Rd,max}, V_{Rd}\right) \tag{3.32}$$

Crack control

Control of crack is performed according to Chapter 7.3.1 in NF P18-710 (2016), where the max crack width is shown in Table 3.3.
In conformity with NF P18-710 (2016) Ch 7.3.4. it is not essential to check the crack width as long as the member is UHPFRC with tensile behaviour class T3, but a crack control is performed to be on the safe side.

The cracking moment is calculated to be compared with the bending moment:

$$M_{cr} = \frac{I_I \cdot \left(f_{ctd.el.SLS} - \frac{N_{Ed.F}}{A_I}\right)}{h - x_I} \tag{3.33}$$

Deflection Control

The deformation requirement will be checked according to SS-EN 1990, and the deflection control due to traffic load is obtained from the characteristic load combination. The deflection is obtained from the cross-section properties on stage I of UHPC.
Since the deflection is linear between the cross-section I (conventional concrete) and cross-section II (HPC), the deflection of the HPC section will be calculated by liner interpolation, where the deflection of cross-section I will be obtained from the case study given from AFRY.
The maximum allowed vertical deflection due to characteristic traffic load according to SS-EN 1990 (A2.4.4.3.2), and it can be checked by:

$$\delta_{max.1} = \frac{L_s}{600} \tag{3.34}$$

The studied bridge is a frame bridge and can be assumed as a continuous bridge with a minimum of 3 spans, and the comfort level is assumed to be (Good). The design value of the train speed for this bridge is 160km/h.

4 Results

This chapter presents the results obtained from the calculation made in Appendix A, B and C. Since case 1 refers to the exciting bridge provided by AFRY and considers the bridge built with normal strength concrete (NC) C35/45. Then this case is assumed to be the reference case where the results of case 2 (HPC) and case 3 (UHPC) are to be compared with case 1. For a description of each case, see (3.2)

4.1 Bending moment capacity

Two different scenarios were considered when calculating the bending moment capacity. The results of each are presented in this sup-chapter.

4.1.1 Scenario 1

The results of scenario one are shown in Table 4.1. According to Figure 4.1, HPC provides the cross-section with a 7% higher bending moment capacity while UHPC provides the cross-section with 10% for the bottom edge. In the top edge, it can be seen that only 4% higher bending moment capacity is obtained by using HPC, while 41 % higher capacity is obtained by using UHPC. It can also be seen in Table 4.1 that case 3 gives the lowest utilization ratio of ductility, where only 7% is utilized. The amount of the reinforcement and cross-section height is identical for all cases.

Table 4.1 Bending moment capacity and utilization ratio for different cases.

	Case1	**Case2**	**Case3**	
h [mm]	600	600	600	Height of cross section
As.bot [mm2]	2094.4			Reinforcement area bottom
As.top [mm2]	1340			Reinforcement area top
M.Rd.bot [kN.m]	449.68	482.23	501	Moment capacity bottom
M.Rd.top [kN.m]	231	241	393.86	Moment capacity top
Utilization M.Rd.bot	81%	76%	72%	Utilization ratio bottom
Utilization M.Rd.top	18%	17%	10%	Utilization ratio top
η.x/d	30%	16%	7%	Ductility

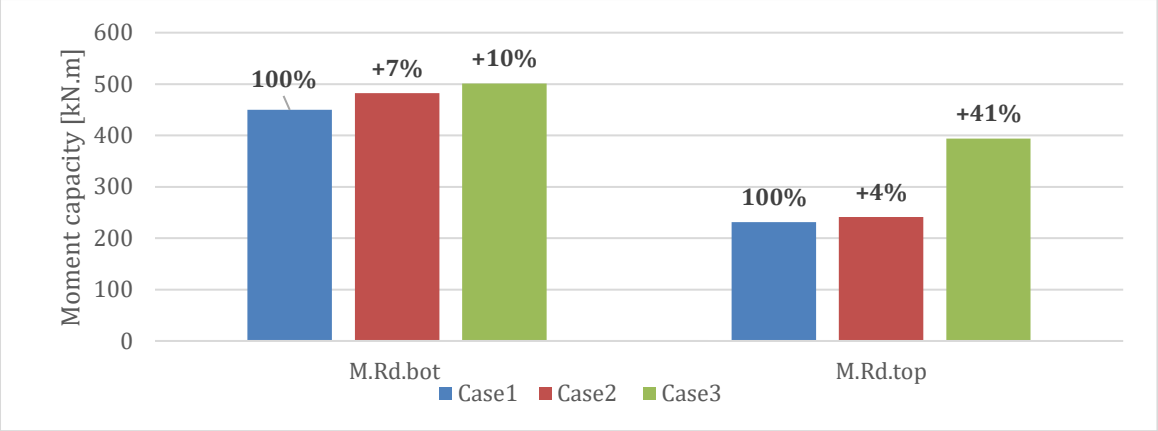

Figure 4.1 Changing of moment capacity for the bottom and top edge.

4.1.2 Scenario 2

The cross-section height is optimized, and the results of the bending moment capacity are presented in Table 4.2. In this scenario, the cross-section height of case 2 is reduced by 25 % of the original height. In case1, the height was 600 mm in the middle of the span, and it was reduced to 450mm in case 2. In case 4, the cross-section reduction was made in 40% of the case1 where cross-section was after the reduction 365 mm, see Table 4.2 and.

The exact amount of reinforcement was used in case 1 and case 2, while the amount was increased in case 3 only on the bottom edge. This increase considered 52% of the amount used in cases 1 and 2; see Table 4.2 and Figure 4.2 Cross-section height.

To verify the cross-section in case1 and case 2, checks in ULS and SLS were made. The results of ULS checks are shown in Table 4.2. It can be noticed that case 2 gives a lower bending moment capacity than case 1, but it still fulfils the requirement of ULS, where 98 % of cross-section capacity was utilized. On the other hand, the bending moment capacity is lower than case 1 but has the same utilization ratio. So, the result shows the amount of reinforcement needed to achieve the same utilization ratio in case 1 with reduced cross-section height and using UHPC. According to Figure 4.3 and Table 4.2, the amount of reinforcement In the bottom edge should be increased by 52% to achieve the same utilization ratio for bending moment while the cross-section is reduced by 40%.

Table 4.2 Bending moment capacity and utilization ratio for different cases.

	Case1	**Case2**	**Case3**	
h [mm]	600	450	365	Height of cross section
As.bot [mm2]	2094.4		3200	Reinforcement area bottom
As.top [mm2]	1340			Reinforcement area top
M.Rd.bot [kNm]	449.68	359	427.6	Moment capacity bottom
M.Rd.top [kNm]	231	174	226	Moment capacity top
Utilization M.Rd.bot	81%	98%	81%	Utilization ratio bottom
Utilization M.Rd.top	18%	17%	9%	Utilization ratio top
η.x/d	30%	8%	20%	Ductility

It is presented in Table 4.2, case 2 provides the best ductile cross-section compared to case1 and case 3 where only 8% of the maximum allowed ductility is utilized.

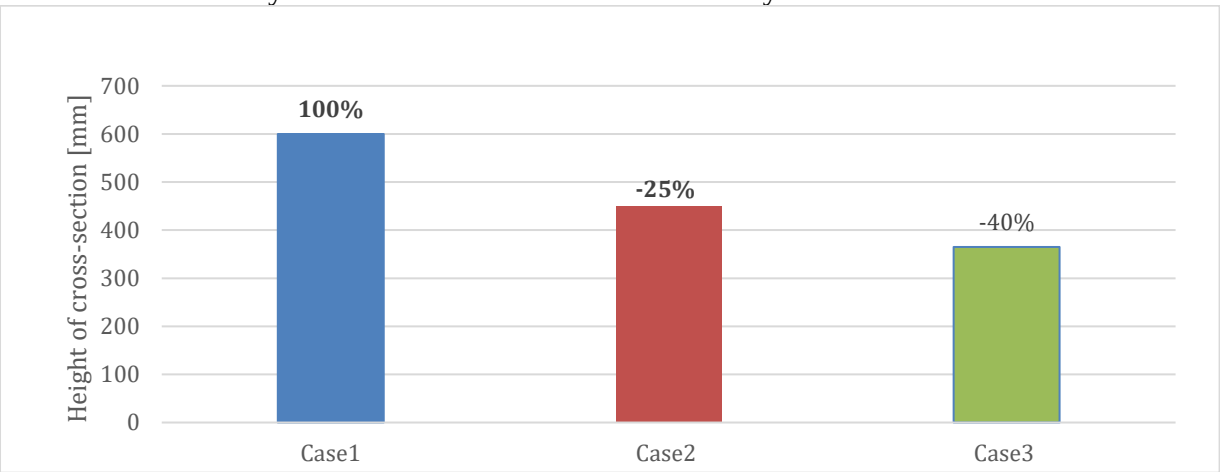

Figure 4.2 Cross-section height for different cases.

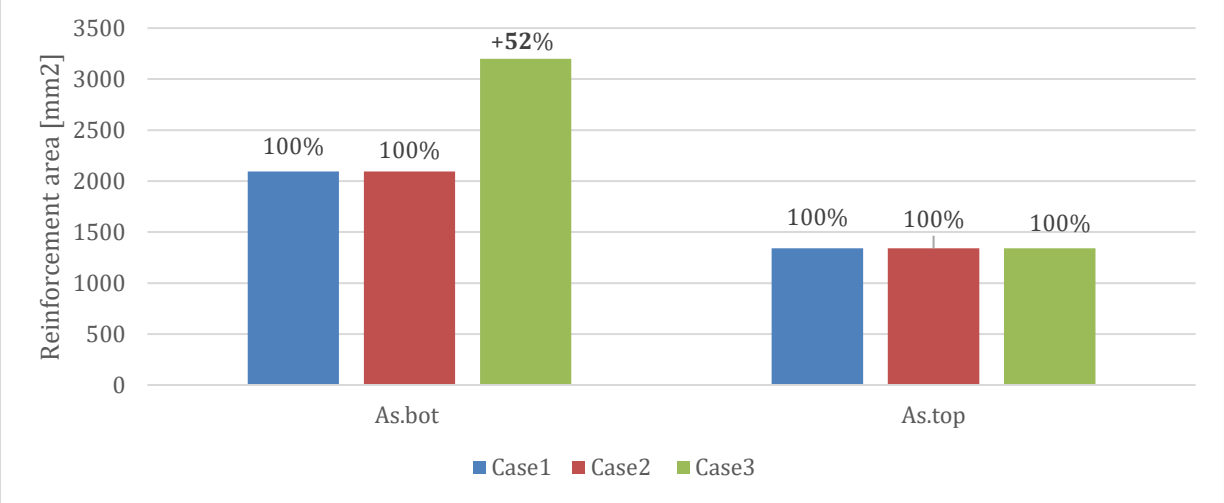

Figure 4.3 Reinforcement amount for different cases.

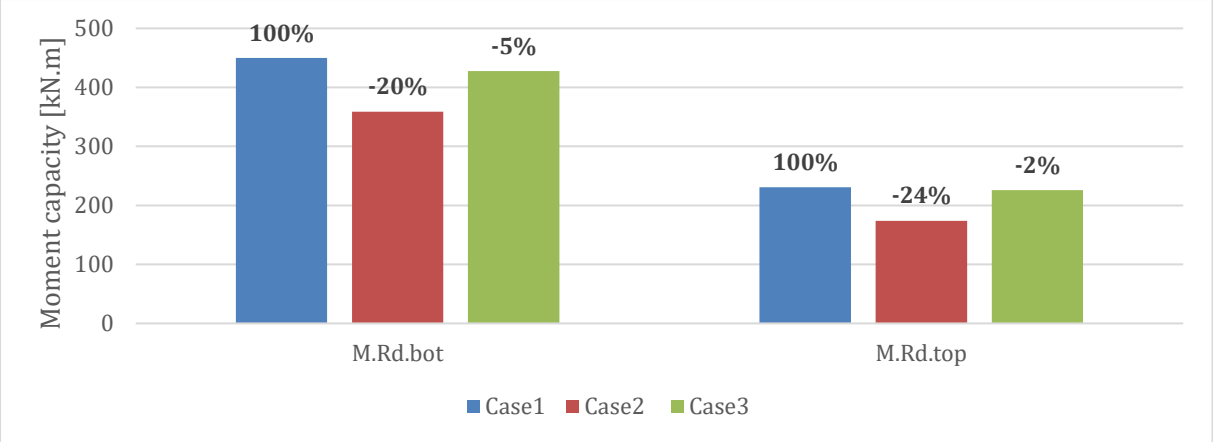

Figure 4.4 Changing of moment capacity for the bottom and top edge.

It can be noticed in Figure 4.4Figure 4.4 that case2 gives the lowest reduction in capacity compared to case 1 by reducing the cross-section height by 25 %. On the other hand, only 5 % and 2% of bending moment capacity for the bottom and top edges respectively reduced. It is also worth mentioning that the amount of reinforcement for case 3 has to be increased to fulfil the failure mode and make the cross-section normal reinforced.

4.2 Shear reinforcement

Two scenarios were considered in calculation of shear reinforcement. The results of calculation are reported in this chapter.

4.2.1 Scenario 1

Without shear reinforcement

It can be seen in

Table 4.3 that HPC provides a higher shear resistance of the cross-section. An increase of 36% can be noticed in case 2 compared to case 1, but the shear capacity of case 2 is still insufficient to resist shear loading, and shear reinforcement is required. On the other hand, case 3 shows the best resistance of shear, where the shear capacity obtained from case 3 is 5425.4 [kN], which is equal to 1645% higher than case 1. In this case, no shear reinforcement is needed; see

Table 4.3 and Figure 4.5.

*Table 4.3 Shear resistance **without** Shear reinforcement.*

	Case 1	Case 2	Case 3
h [mm]	579		
V,Ed [kN]	555.9		554.5
V.Rd.c [kN]	310.9	423	5425.4
ηV.c	1.79	1.31	0.1

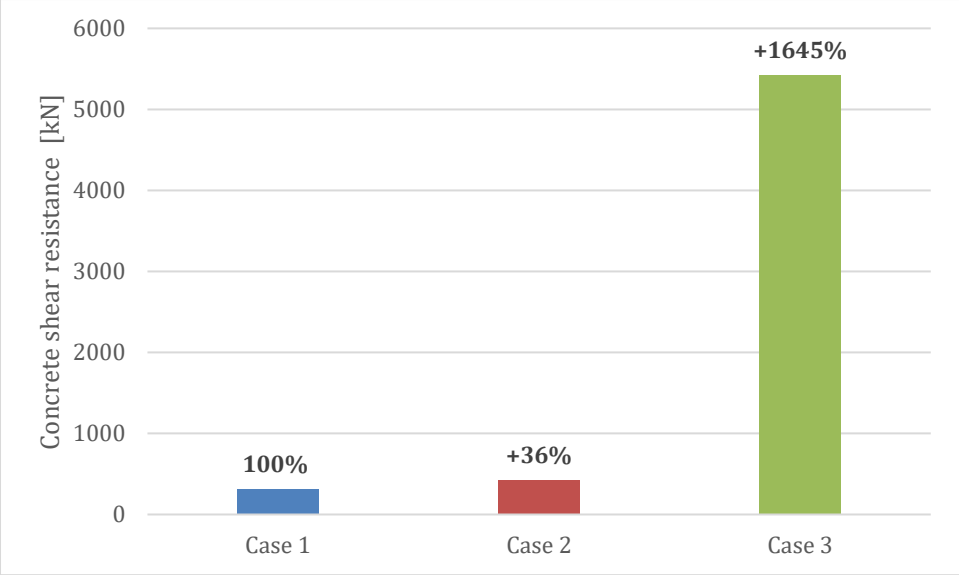

Figure 4.5 Changing of shear resistance for different cases.

Shear reinforcement is provided

The same shear reinforcement amount is used in case 2 to compare the difference in shear capacity between the two cases. Table 4.4 shows that 4 % increase is obtained while no shear reinforcement was provided in case 3.

*Table 4.4 Shear resistance **with** Shear reinforcement.*

	Case 1	Case 2	Case 3
V,Ed [kN]	555.9		554.5
V.Rd.s [kN]	937.18	975	No shear reinforce-ment needed
A.sw.req [mm^2]	1118	1118	
ηV.s	59%	57%	

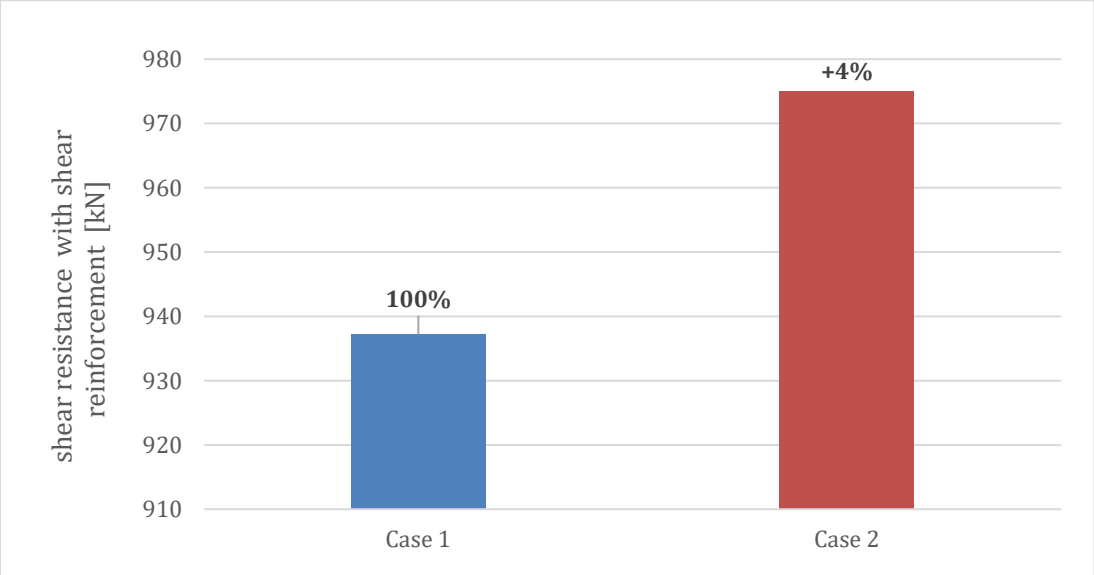

Figure 4.6 Shear resistance with shear reinforcement for case 1 and case 2.

4.2.2 Scenario 2

The results of shear resistance without shear reinforcement for different cases where the cross-sections were optimised are presented in Table 4.5. The shear control is made at 1.2m from the support, where the maximum shear force occurs.

According to Table 4.5, case 2 has a 20 % higher capacity than case 1. Although the cross-section height in case 2 is reduced by 25 % compared to case 1, it still needs shear reinforcement. On the other hand, case 3 shows superior shear capacity than case 1 and 2, where 962% higher capacity was obtained from case 3. Thus, no shear reinforcement is needed in case 3; see Table 4.5 and Figure 4.7.

Table 4.5 Shear resistance without Shear reinforcement for different cases.

	Case 1	Case 2	Case 3
h [mm]	579	450	365
V,Ed [kN]	555.9	542.83	533.346
V.Rd.c [kN]	310.9	374	3302
ηV.c	1.79	1.45	0.16

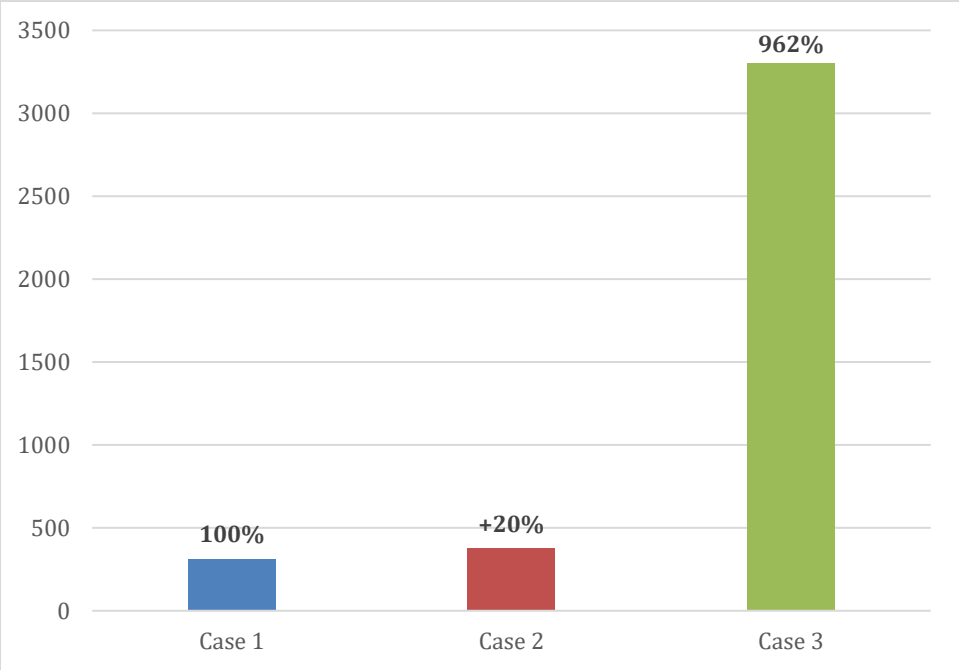

Figure 4.7 Shear resistance without Shear reinforcement.

Shear resistance <u>with</u> shear reinforcement

According to Table 4.6, the required shear reinforcement for case 2 needs to be increased by 23% in order to resist the shear force, while the utilization ratio in case 2 is still higher than in case 1. Case 3 shear reinforcement is not needed.

Table 4.6 Shear resistance with shear reinforcement.

	Case 1	Case 2	Case 3
V,Ed [kN]	555.9	542	533.346
h [mm]	579	450	365
V.Rd.s [kN]	937.18	602	No shear reinforcement needed
A.sw.req [mm2]	1118	1378	
ηV.s	58%	90%	

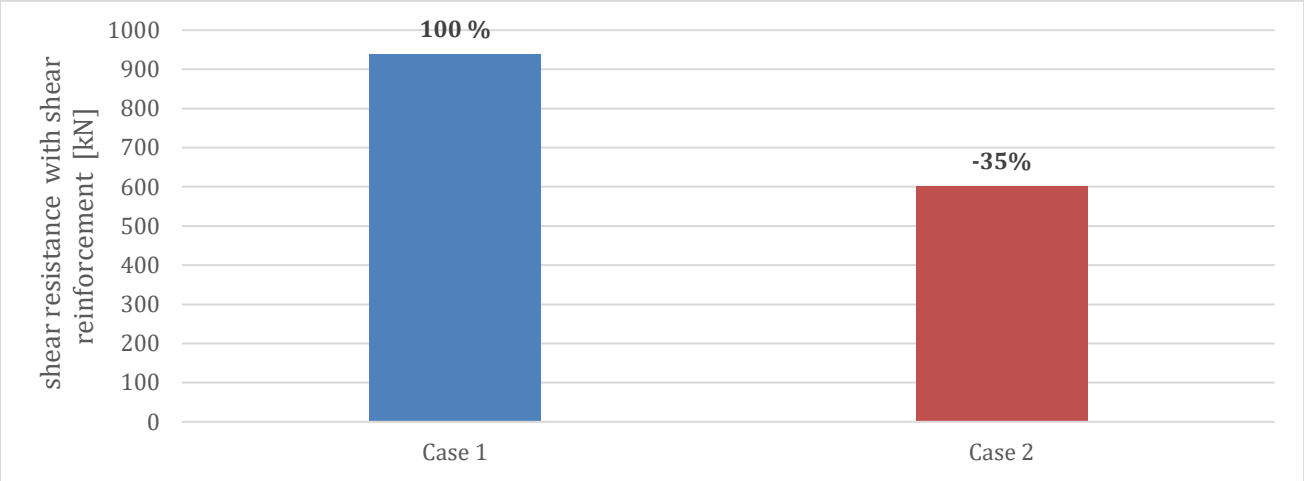

Figure 4.8 Shear resistance with shear reinforcement of two cases.

4.3 Cracking

Crack control is carried out only for scenario 2, where the cross-section is optimised. The results are presented in the following chapter.

4.3.1 Scenario 2

Crack width for case 2 is increased by 10.4% compared to case 1, where the cross-section in case 2 is reduced by 25%. However, the crack width in case 2 is under the maximum allowed limit, where the utilization ratio is 72%, see Table 4.7. In contrast, no crack occurs in case 3.

Table 4.7 Crack width for different cases.

	Case1	Case2	Case 3	
h [mm]	600	450	No crack occurs	Height of cross section
W.k [mm]	0.144	0.159		Crack width
W.k. max[mm]	0.2			Max allowed crack width
$\eta_{crack.width}$	72%	80%		Utilization ratio

4.4 Deflection

Deflection control is carried out only for scenario 2, where the cross-section is optimised. The results are presented in the following chapter.

4.4.1 Scenario 2

Table 4.8 shows deflection results for each case in mid-span. It can be seen that the deflection in case 2 is lowest compared with other cases, where the cross-section height is reduced.

Table 4.8 deflection results for different cases in mid-span.

	Case1	Case2	Case3
H [mm]	600	450	365
deflection [mm]	1.72	0.622	1.368
Max allowed deflection	10.59		
η-deflection	16.24%	5.87%	12.92%

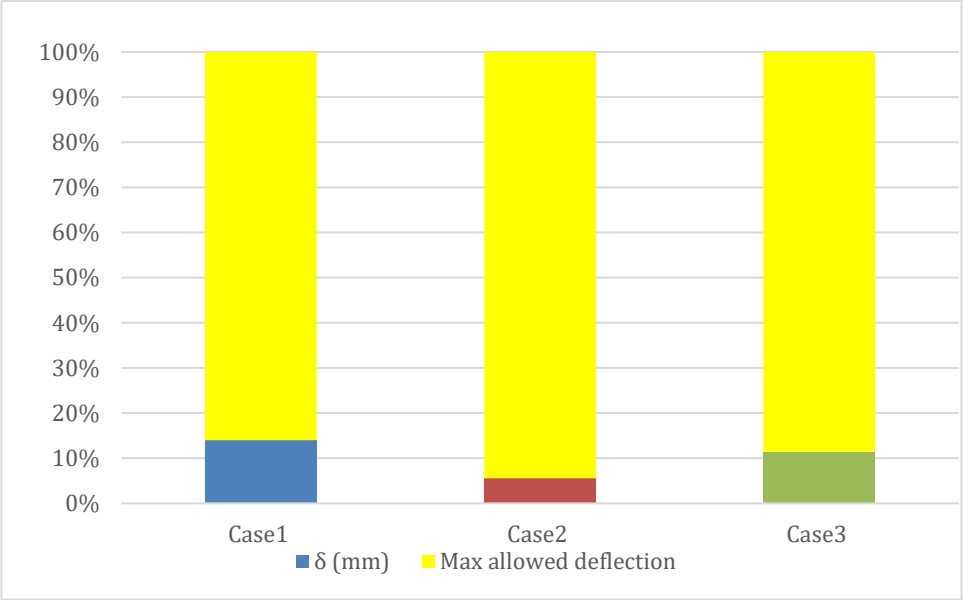

Figure 4.9 Deflection in the middle of span for different cases.

4.5 Total amount of concrete

By comparing the total amount of concrete on the total width and one longitudinal meter, it has been noticed that the superstructure self-weight in case 2 is 25% lighter than in case1. In contrast, a 40.69% reduction in self-weight can be achieved in case 3, see Table 4.9 and Figure 4.10.

Table 4.9 Amount of concrete for each case in total width and longitudinal meter.

	Case1	Case2	Case3
Total concrete amount [kg/m]	11258.72	8444.037	6677.826
Percentage difference [%]	100%	-25.00%	-40.69%

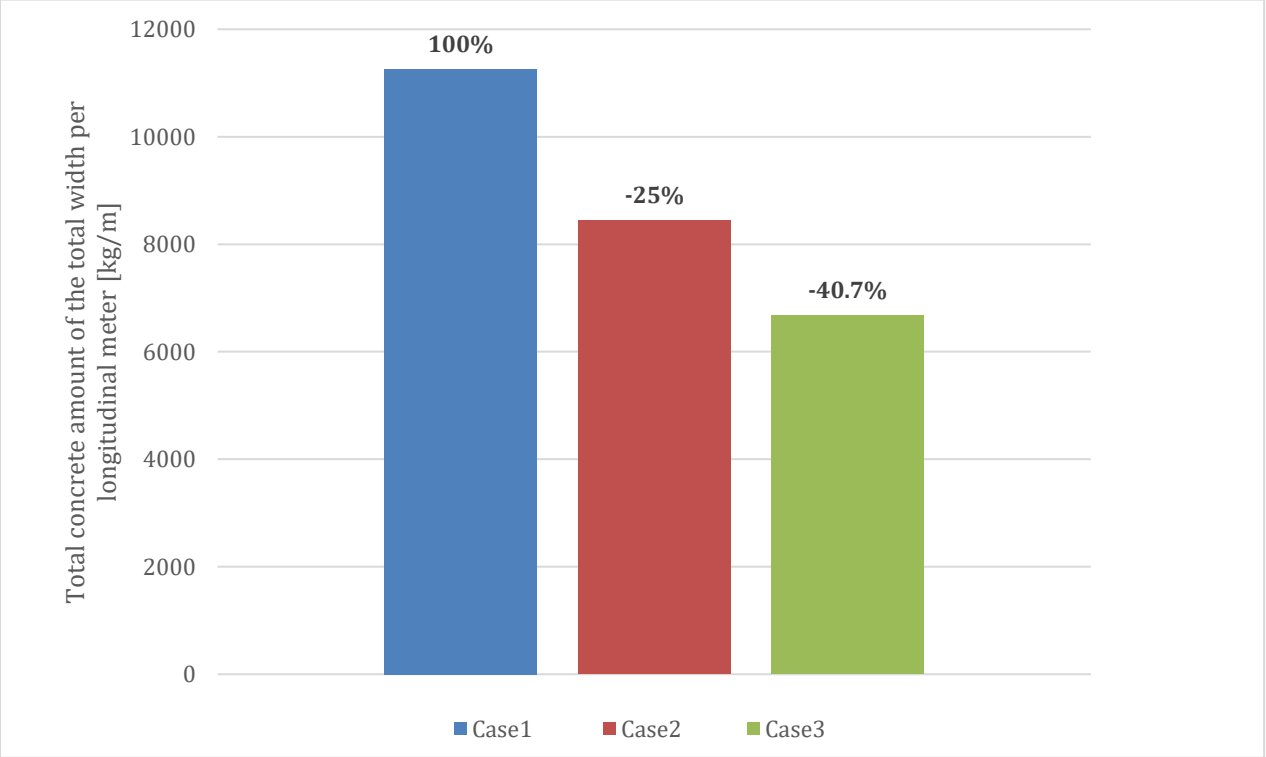

Figure 4.10 Amount of concrete for each case.

5 Analysis and Discussions

The results obtained from the case studies and presented in chapter 1 are discussed here.

For case2 scenario 1, when the high-performance concrete of class C90/105 is used, a slightly higher bending moment capacity is observed when taking a cross-section in the middle of the bridge. Considering the strength aspect, there are no significant gains from using concrete with high compressive strength with normal reinforcing. This was not unexpected because using concrete with high compressive strength could be more beneficial if the concrete was pre or post-tensioned. In the case of pre or post-tensioned elements, the compressive strength of concrete is to be utilized differently. Considering the moment resistance, it can be seen clearly from the calculations that the structure is over reinforced, and the required reinforcement amount is less than what is used. That can be motivated by other aspects that need this amount of reinforcement, such as fatigue, which are not considered in this thesis. Moreover, it is noticed that the top edge in case 3 gives a relative higher capacity compared to the bottom edge, where the increase of capacity is calculated to be 41% higher than in case 1. This can be explained by the high compressive strength provided by UHPC, which is utilized in the top part of the cross-section.

In scenario 2, where HPC is used, the bending moment capacity decreased by 20 % compared to case 1. On the other hand, the cross-section is reduced by 25%, but it still fulfils the requirement. In case3, the cross-section is reduced by 40 % compared to the case1, and the bending capacity is reduced only by 5% on the bottom edge compared with case1. In comparison, the bending reinforcement amount on the lower edge is increased by 52% to obtain a ductile failure mode. The utilization ratio of ductility decreases by 10 % in case3 compared to case 1, which means the cross-section is more ductile and almost has half cross-section height.

Regarding the shear capacity of concrete in case2, it is observed that the cross-section in case 2 scenario 1 (same height as case1) could not carry the shear forces without providing shear reinforcement. At the same time, case3 shows significantly higher shear capacity, calculated to 1645%. This can be explained by the fact that concrete in case 3 includes fibres content up to 2% of total content, contributing to higher shear capacity. Another reason can be the high compressive strength of UHPC (200 MPa) which is much bigger than the strength in the conventional concrete C35/45. Consequently, no shear reinforcement is required in case 3. In case 2, when the same amount of shear reinforcement in case 1 is used, the shear capacity is increased by only 4%. This means that HPC of class C90/105 provides a minor gain in both bending moment and shear capacity, while a significant gain of shear capacity is observed in the case of UHPC. Consequently, it is worth using UHPC if slender structure elements are desired but not lose sight of the fact that a higher amount of bending reinforcement is needed while no shear reinforcement is needed.

Furthermore, in case2 scenario 2 (reduced cross-section height), cracks still occur, where the utilization ratio of crack width is 10% bigger than case1. However, it still fulfils the maximum allowed crack width requirement. The bigger crack width in case2 is due to the reduction of cross-section, which results in a lower moment of inertia, meaning a lower cracking moment. In case 3, no cracks occur, even though the cross-section height is reduced to 40 %. This can be explained by the superior tensile strength of UHPC, which is 12 MPa resulting in a higher cracking moment. According to NF P18 -710 (2016), no crack control is

needed if the cross-section is classified as thick and has class 3, which is agreed with the cross-section in case 3. The contribution of fibres also has a considerable effect on crack resistance.

In contrast, the decisive factor in case 3 is the deflection, where case 3 shows the highest deflection compared to the other cases. This is expected due to the relatively high reduction of cross-section height and, consequently, loss of a moment of inertia that results in higher deflection. However, deflection is not a critical design case in the design of concrete structures. However, only 12.92 % of the maximum allowed deflection is utilized even though the cross-section height is reduced to 40 % compared to the case1.

The amount of concrete used in the different case studies differs considerably. Thus, it is worth mentioning that the self-weight of the superstructure is reduced to 25% in case 2 and 40.69 % in case 3. This is valuable for such a bridge being constructed to be launched. The launching process might be more manageable in terms of launching equipment choices when dealing with a lighter and stiffer structure.

According to the literature review, there is only one approved standard in Europe for UHPC, *"French Standard NF P18 -710 (2016),"* and the calculations of case 3 (UHPC) are based on this standard. When calculating the design value of compressive strength for UHPC, it is observed that "α_{cc} Coefficient, which takes account of long-term effects on compressive strength and adverse effects resulting from the way the load is applied" (NF P18 -710 (2016)) has a different value compared with the value applied for normal strength concrete. According to EN 1992-1-1, α_{cc} has a value between 0.8 and 1. The recommended value in Sweden is 1 for normal strength concrete, while in France is 0.80 for the same concrete. The recommended value for α_{cc} for UHPC is 0.85 in French Standard while no recommended α_{cc} can be found for UHPC in Sweden. Consequently, the recommended value in French Standard is applied. This results in 15 % decrease in the compressive strength design value of UHPC, while this decrease might be unnecessary if α_{cc} for UHPC in Sweden is found.

Another consideration is observed regarding the minimum and surface reinforcement. According to the French standard NF P18 -710 (2016), there is no need for a minimum quantity of steel reinforcement for cracking control because UHPC is assumed to be sufficiently ductile in tension. This does not match with the requirement of (Krav Brobyggande) (TDOK 2016:0204), in which more quantity of minimum reinforcement is required when applying (TDOK 2016:0204). Consequently, some modification of (TDOK 2016:0204) is suggested in the implementation of UHPC in Sweden.

Durability can be described as the ability to last long without notable deterioration. As well as durable materials can help the environment by reducing waste, fewer reparations and saving in material consumption to achieve the goal of sustainability. HPC/ UHPC is expected to solve the durability challenge to gain a more durable concrete structure. The stronger strength caused by HPC/ UHPC gives the structure a longer lifespan. A water/binder ratio less than 0.30, as in HPC/UHPC, is usually more durable than normal concrete. It is not only because it is less porous but also because its capillary and pore networks are somewhat disconnected from the development of self-desiccation, as mentioned in the literature study. In HPC/UHPC, the penetration of aggressive agents in a kind of carbonation and so forth is quite difficult and only superficial, which improves the structure's performance.

6 Conclusion and future work

This master thesis has assessed the probability of implementation of HPC and UHPC in bridge construction in the design stage. The main aim is to investigate the benefits of using these materials instead of the conventional concrete used today. Moreover, giving a deeper understanding of HPC and UHPC in terms of mechanical properties, availability in the Swedish market and possibilities and challenges of production. This was performed by a comprehensive literature study covering the previously mentioned aspects and highlighting several internationally and locally applications. Furthermore, two case studies are carried out in order to highlight the differences in design between conventional concrete and HPC/UHPC.

In terms of HPC's bending and shear capacity, there is no remarkable gain from using concrete with compressive strength of 90 MPa with a normal reinforcing. On the other hand, as mentioned in Ch 2.5, HPC shows superior performance in terms of carbonation and corrosion resistance. This aspect has been discussed only in the literature study. In contrast, a superior achievement concerning bending and shear capacity is observed using UHPC. UHPC shows ductile behaviour and saving in shear reinforcement. This results in longer service life and better performance. No shear reinforcement is required in the case of UHPC, and no cracks occur.
Nonetheless, there is a need for a higher amount of cement in the production of UHPC and a higher amount of steel reinforcement when decreasing the cross-section by 40 %. However, it cannot be concluded if the UHPC gives higher carbon dioxide emissions only by looking at the design stage. Consequently, there is a need to investigate and consider the whole service life of the structure in order to be able to judge if the HPC/UHPC is more advantageous to use instead of conventional concrete.

Future work

To develop the main subjects and reach a more accurate result, the following proposals are suggested for future work.

Possible development of the case study might be by designing a bridge using pre or post tensioned HPC/UHPC. In this case, it might be possible to utilize the compressive strength of concrete to achieve a slenderer structure with a longer span. Moreover, it might be useful to make fatigue check to make a fairer comparison between the case of conventional concrete and HPC/UHPC. Moreover, a finite element model can be implemented to optimize the cross-section optimally and get accurate results of the moment and normal forces. LCC and LCCA can be carried out to evaluate if HPC/UHPC is environmentally friendly and beneficial economically. A dynamic study can be conducted in order to evaluate the dynamic response of the bridge by using concrete with high compressive strength and slender elements. It is also useful to study other type of the bridge and other parts where large normal force is acting.

7 References

Abbas, S., Soliman, A. M., & Nehdi, M. L. (2015). Exploring mechanical and durability properties of ultra-high performance concrete incorporating various steel fiber lengths and dosages. *Construction and Building Materials*, *75*, 429–441. https://doi.org/10.1016/j.conbuildmat.2014.11.017

Aïtcin, P. C. (2003). The durability characteristics of high performance concrete: A review. *Cement and Concrete Composites*, *25*(4-5 SPEC), 409–420. https://doi.org/10.1016/S0958-9465(02)00081-1

Aitcin, P.-C. (1998). *High-performance concrete*.

Al-Emrani, M., Engström, B., Johansson, M., & Johansson, P. (2013). *Bärande konstruktioner Del 1* (Vol. 2013, Issue 1).

Bentz, D. P., Garboczi, E. J., Haecker, C. J., & Jensen, O. M. (1999). Effects of cement particle size distribution on performance properties of Portland cement-based materials. In *Cement and Concrete Research* (Vol. 29).

Beygi, M. H. A., Kazemi, M. T., Nikbin, I. M., & Amiri, J. V. (2013). The effect of water to cement ratio on fracture parameters and brittleness of self-compacting concrete. *Materials and Design*, *50*, 267–276. https://doi.org/10.1016/j.matdes.2013.02.018

Bouaissi, A., Li, L. Y., Moga, L. M., Sandu, I. G., Abdullah, M. M. A. B., & Sandu, A. V. (2018). A review on fly ash as a raw cementitious material for geopolymer concrete. *Revista de Chimie*, *69*(7), 1661–1667. https://doi.org/10.37358/rc.18.7.6390

Byggtjänst, S. (2000). Betonghandbok, Högpresterande betong-Material och utförande.

CEB-FIP Model Code 1990-Final Draft, Comite Euro-International du Beton. (1990).

Claeson, C. (1999). *Praktisk tillämpning av högpresterande betong*.

Divsholi, B. S., Lim, T. Y. D., & Teng, S. (2014). Durability Properties and Microstructure of Ground Granulated Blast Furnace Slag Cement Concrete. *International Journal of Concrete Structures and Materials*, *8*(2), 157–164. https://doi.org/10.1007/s40069-013-0063-y

Domone, P., & Illston, john. (2010). *Construction Materials Fourth edition* (4th ed.). Taylor & Francis Group.

Duggal, S. K. (2008). Building Materials. *In new age international (p) limited.*

Duggal, S. K. (2017). *Building materials*. Routledge.

Eide, M. B., & Hisdal, J.-M. (2012). *Ultra High Performance Fibre Reinforced Concrete (UHPFRC)– State of the art*. www.coinweb.no

Einsfeld, R. A., & Velasco, M. S. L. (2006). Fracture parameters for high-performance concrete. *Cement and Concrete Research*, *36*(3), 576–583. https://doi.org/10.1016/j.cemconres.2005.09.004

Elfgren, L., Bernander, S., Emborg, M., Gabrielsson, h, Groth, P., Hedlund, H., & Westman, G. (1999). Design of high performance concrete structures- A swedish handbook. *5th International Symposium on the Utilization of High Strength/High Performance Concrete*, 20–24.

Elzokra, A., al Houri, A., Habib, A., Habib, M., & Malkawi, A. B. (2020). Shrinkage behavior of conventional and nonconventional concrete: A review. *Civil Engineering Journal (Iran)*, *6*(9), 1839–1851. https://doi.org/10.28991/cej-2020-03091586

Engström, B. (2007). *Restraint cracking of reinforced concrete structures*.

Fagerlund, G. (1998). *Inverkan av ballastens mineraliska sammansättning på brottegenskaper hos normalbetong*.

Fagerlund, G. (2014). *Projekt högpresterande betong, 1991-1997 lista över rapporter publicerade vid avd byggnadsmaterial, lth lunds tekniska högskola Avdelning byggnadmaterial*. www.byggnadsmaterial.lth.se

Fehling, E., Schmidt, M., Walraven, J. C. (Joost C., Leutbecher, T., & Fröhlich, S. (Researcher in structural engineering). (2014). *Ultra-high performance concrete UHPC : fundamentals, design, examples*. Ernst & Sohn.

Fládr, J., Bílý, P., & Trtík, T. (2019). Analysis of the influence of supplementary cementitious materials used in UHPC on modulus of elasticity. *IOP Conference Series: Materials Science and Engineering*, *522*(1). https://doi.org/10.1088/1757-899X/522/1/012010

Ghafari, E., Ghahari, S. A., Costa, H., Júlio, E., Portugal, A., & Durães, L. (2016). Effect of supplementary cementitious materials on autogenous shrinkage of ultra-high performance concrete. *Construction and Building Materials*, *127*, 43–48. https://doi.org/10.1016/j.conbuildmat.2016.09.123

Graybeal, B. A. (2009a). *Lightweight Concrete View project Dimensional Stability and Bond Performance of Grouted Connections View project*. https://www.researchgate.net/publication/266135146

Graybeal, B. A. (2009b). *Structural Behavior of a 2nd Generation Ultra-High Performance Concrete Pi-Girder*.

Gu, C., Wang, Y., Gao, F., Yang, Y., Ni, T., Liu, J., Lou, X., & Chen, J. (2019). Early age tensile creep of high performance concrete containing mineral admixtures: Experiments and modeling. *Construction and Building Materials*, *197*, 766–777. https://doi.org/10.1016/j.conbuildmat.2018.11.218

Gustafsson, J., Nilsson, T., Carlsson, F., Ab, B., & Persson, K. (2011). *Structural Mechanics ANALYS AV PLATTRAMBROAR MED KRÖKTA RAMBEN Master's Dissertation by FRIDA HULT*.

Gutierrez, P. A., & Fernandez, M. (1995). The modulus of elasticity of high performance concrete. In *Materials and Structures* (Vol. 28).

HAJAR, Z., Resplendino, J., SIMON, A., LECOINTRE, D., & PETITJEAN, J. (2004). *Ultra-High-Performance Concretes: First recommendations and examples of application*.

Henrique, A., Pereira, A., & Pereira, A. H. A. (2016). *Estimation of the static modulus of elasticity of concrete using the Impulse Excitation Technique*. https://doi.org/10.13140/RG.2.2.10454.45120

Holt, E. E. (2001). *Early age autogenous shrinkage of concrete 4 4 6*.

Jonbi, Hariandja, B., Imran, I., & Pane, I. (2012a). Development of mix proportion for high-performance concrete using locally available ingredients based on compressive strength and durability. *Applied Mechanics and Materials*, *174–177*, 1067–1071. https://doi.org/10.4028/www.scientific.net/AMM.174-177.1067

Jonbi, Hariandja, B., Imran, I., & Pane, I. (2012b). Development of mix proportion for high-performance concrete using locally available ingredients based on compressive strength and durability. *Applied Mechanics and Materials*, *174–177*, 1067–1071. https://doi.org/10.4028/www.scientific.net/AMM.174-177.1067

Jurowska, A., & Jurowski, K. (2020). The influence of ambient temperature on high performance concrete properties. *Materials*, *13*(20), 1–16. https://doi.org/10.3390/ma13204646

Kumar, A., Verma, B., & Nasrin, T. (2017). *HIGH PERFORMANCE CONCRETE & ITS APPLICATIONS IN CIVIL ENGG*.

le Roy, R., le Maou, F., & Torrenti, J. M. (2017). Long term basic creep behavior of high performance concrete: data and modelling. *Materials and Structures/Materiaux et Constructions*, 50(1). https://doi.org/10.1617/s11527-016-0948-8.

Lehne, J., & Preston, F. (2018). *Making Concrete Change: Innovation in*

Liu, Y., & Wei, Y. (2021). Effect of calcined bauxite powder or aggregate on the shrinkage properties of UHPC. *Cement and Concrete Composites*, *118*. https://doi.org/10.1016/j.cemconcomp.2021.103967

Lu, Z., Feng, Z. gang, Yao, D., Li, X., & Ji, H. (2021). Freeze-thaw resistance of Ultra-High performance concrete: Dependence on concrete composition. *Construction and Building Materials*, *293*. https://doi.org/10.1016/j.conbuildmat.2021.123523

Luping, T. (2021). *Deterioration of Concrete Structures*.

Luping, T., Nilsson, L.-O., & Muhammed Basheer, P. A. (2011). *Resistance of concRete to chloRide ingRess TesTing and Modelling*. www.sponpress.com

Martin, A. J. (2004, December). Concrete bridges in sustainable development. In *Proceedings of the Institution of Civil Engineers-Engineering Sustainability* (Vol. 157, No. 4, pp. 219-230). Thomas Telford Ltd.

Máca, P., Sovják, R., & Konvalinka, P. (2012). *Mixture Design and Testing of Ultra High Performance Fiber Reinforced Concrete Structural behaviour of FRP-reinforced concrete members View project Cement and concrete composites under high-velocity projectile impact View project*. https://www.researchgate.net/publication/263298131

Meng, W. (2017). *Design and performance of cost-effective ultra-high performance concrete for prefabricated elements*. https://scholarsmine.mst.edu/doctoral_dissertations/2582.

Meyer, C. (2005, August). Concrete as a green building material. In *Construction Materials Mindess Symposium*.

Ouyang, X., Shi, C., Wu, Z., Li, K., Shan, B., & Shi, J. (2020). Experimental investigation and prediction of elastic modulus of ultra-high performance concrete (UHPC) based on its composition. *Cement and Concrete Research, 138*. https://doi.org/10.1016/j.cemconres.2020.106241

Pernicová, R. (2014). *Chloride Transport in Ultra High Performance Concrete*.

Persson, B. (1992). *HÖGPRESTERANDE BETONGS HYDRATATION, STRUKTUR OCH HÅLLFASTHET*.

Petersson, P. (1980). *FRACTURE ENERGY OF CONCRETE; METHOD OF DETERMINATION* (Vol. 0).

Ramezanianpour, A. A. (2014). *Mineralogy Cement Replacement Materials*. http://www.springer.com/series/10171

Rouse, jon, Wipf, T. J., Phares, B., Fanous, F., & Berg, O. (2011). *Design, Construction, and Field Testing of an Ultra-High Performance Concrete Pi-Girder Bridge Final Report*. www.intrans.iastate.edu

Russell, Henry. G., & Graybeal, B. A. (2013). *Ultra-High Performance Concrete: A State-of-the-Art Report for the Bridge Community*.

Schmidt, M., Fehling, E., & Geisenhanslüke, C. (2004). *Ultra high performance concrete (UHPC) ; proceedings of the International Symposium on Ultra High Performance Concrete*.

Schmidt, M., & Fehling, E. (2005). Ultra-high-performance concrete: research, development and application in Europe. *ACI Spec. Publ*, *228*(4), 51-78.

Schmidt, M., Leutbecher, T., Piotrowski, S., & Wiens, U. (2017). *Symposium on Ultra-High Performance Fibre-Reinforced Concrete*.

Shafieifar, M., Farzad, M., & Azizinamini, A. (2017). Experimental and numerical study on mechanical properties of ultra high performance concrete. Construction and Building Materials, 156, 402-411. doi:10.1016/j.conbuildmat.2017.08.170

Shanmuga Priya, T. (2017a). *Experimental and numerical study on mechanical properties of Ultra High Performance Concrete (UHPC)*.

Shanmuga Priya, T. (2017b). Experimental investigation on high performance RC column with manufactured sand and silica fume. *IOP Conference Series: Materials Science and Engineering*, *263*(3). https://doi.org/10.1088/1757-899X/263/3/032021

Sofia Utsi. (2008). *Performance Based Concrete Mix-Design. Aggregate and micro mortar optimization applied on self-compacting concrete containing fly ash*. http://www.ltu.se

Sohail, M. G., Kahraman, R., al Nuaimi, N., Gencturk, B., & Alnahhal, W. (2021). Durability characteristics of high and ultra-high performance concretes. *Journal of Building Engineering*, *33*. https://doi.org/10.1016/j.jobe.2020.101669

Soliman, A. (2011). *Early-Age Shrinkage of Ultra High-Performance Concrete: Mitigation and Compensating Mechanisms*. http://ir.lib.uwo.ca/etd

Voit, K., & Kirnbauer, J. (2014). Tensile characteristics and fracture energy of fiber reinforced and non-reinforced ultra high performance concrete (UHPC). *International Journal of Fracture*, *188*(2), 147–157. https://doi.org/10.1007/s10704-014-9951-7

Wayne, A. (2007). A Whole new cast. *ASPIRE*.

Wu, L., Farzadnia, N., Shi, C., Zhang, Z., & Wang, H. (2017). Autogenous shrinkage of high performance concrete: A review. In *Construction and Building Materials* (Vol. 149, pp. 62–75). Elsevier Ltd. https://doi.org/10.1016/j.conbuildmat.2017.05.064

Yoo, D. Y., & Yoon, Y. S. (2016). A Review on Structural Behavior, Design, and Application of Ultra-High-Performance Fiber-Reinforced Concrete. *International Journal of Concrete Structures and Materials*, *10*(2), 125–142. https://doi.org/10.1007/s40069-016-0143-x

Zhang, P., & Li, & Q. (2015). *Australian Journal of Structural Engineering Fracture Properties of High Performance Concrete Containing Silica Fume*. https://doi.org/10.7158/13287982.2013.11465141

Zhang, P., & Li, Q. F. (2013). Combined effect of polypropylene fiber and silica fume on workability and carbonation resistance of concrete composite containing fly ash. *Proceedings of the Institution of Mechanical Engineers, Part L: Journal of Materials: Design and Applications*, *227*(3), 250–258. https://doi.org/10.1177/1464420712458198

Zhang, P., Li, Q., & Zhang, H. (2012). Fracture properties of high-performance concrete containing fly ash. *Proceedings of the Institution of Mechanical Engineers, Part L: Journal of Materials: Design and Applications*, *226*(2), 170–176. https://doi.org/10.1177/1464420711435759

Zhao, Q., Liu, X., & Jiang, J. (2015). Effect of curing temperature on creep behavior of fly ash concrete. *Construction and Building Materials*, *96*, 326–333. https://doi.org/10.1016/j.conbuildmat.2015.08.030

8 Appendix

Appendix A- Case study 1: Design the bridge with normal strength concrete

Appendix B- Case study 2: Design the bridge with HPC

Appendix C- Case study 3: Design the bridge with UHPC

Appendix A- Case 1:
Design the bridge with normal strength concrete

A.1 Geometry

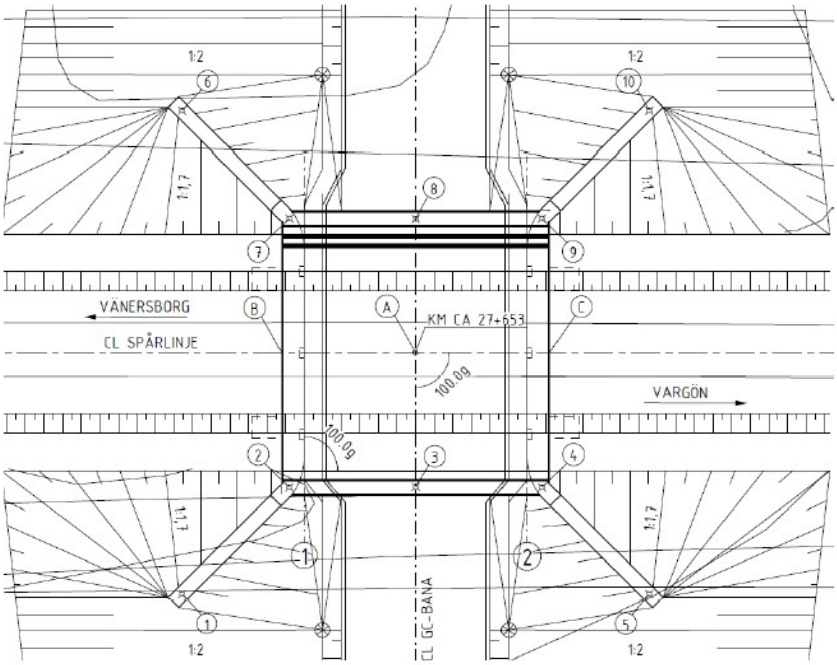

Figure Bridge plan

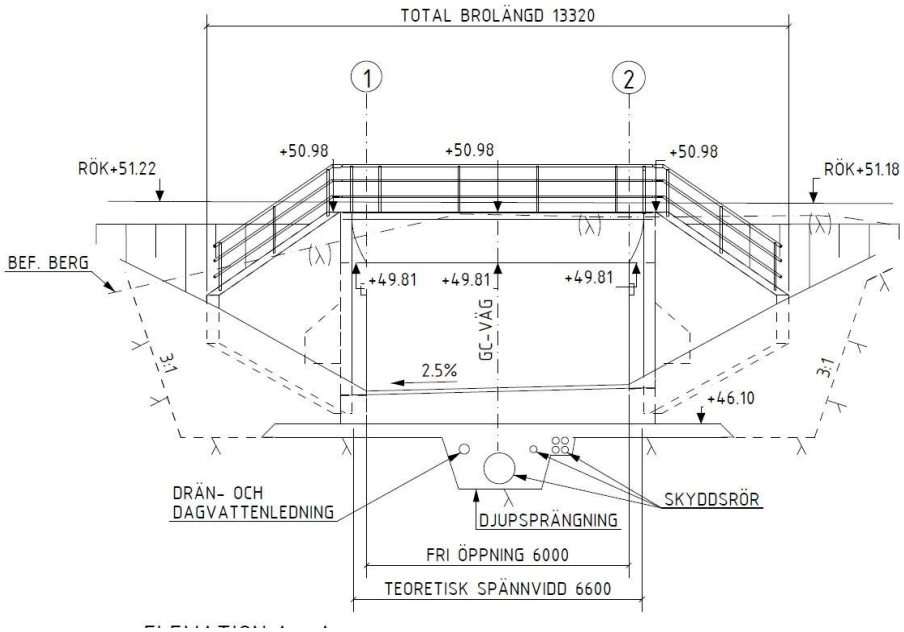

Figure. Elevation

A.2 Calculation conditions

Service life: L100 (120 years)

For the bridge deck and the frame leg a safety class 3 is chosen.

$\gamma_d := 1$

Exposure classes according to TDOK 2016:0203

Construction part	Exposure class	Service life	Concrete cover[mm]	W.k[mm]	Max w/c
Bridge deck, top	XD1/XF4	L100	40	0.30	0.50
Bridge deck, bottom	XC4/XF3	L100	40	0.20	0.45
Frame-leg air-side	XD1/XF4	L100	40	0.20	0.45
Frame-leg soil-side	XD1/XF4	L100	40	0.40	0.50

A.3 Material properties

A.3.1 Concrete:

C35/45

$f_{ck} := 35MPa$ $\gamma_{c.sls} := 1$

$f_{ctm} := 3.2MPa$ $\gamma_{c.uls} := 1.5$

$f_{ctk} := 2.2MPa$

$E_{cm} := 34GPa$

$\varepsilon_{cu} := 0.35\%$

$\varphi_{ef} := 1.87$

A.3.2 Steel K500C-T

$f_{yk} := 500MPa$ $\gamma_{s.uls} := 1.15$

$E_s := 200GPa$ $\gamma_{s.sls} := 1$

$\rho_s := 78.5 \frac{kN}{m^3}$

A.4 Control on ultimate limit state ULS

A.4.1 Calculation of moment resistance for bottom edge $M_{Rd,max\ (Bottom)}$

Input

$\alpha := 0.810$ $\beta := 0.416$ $h := 600mm$ $\gamma_s := 1.15$

$b := 1000mm$ $\gamma_c := 1.5$ $M_{Ed.max} := 366kN \cdot m$ $N_{Ed.max} := -28.4kN$ (compression)

$d_{bot} := 522mm$ $d'_{bot} := 78mm$ $A_{s.bot} := 2094.4mm^2$

$f_{cd} := \frac{f_{ck}}{\gamma_c} = 23.333 \cdot MPa$ $f_{yd} := \frac{f_{yk}}{\gamma_s} = 434.783 \cdot MPa$ $\varepsilon_{sy} := \frac{f_{yd}}{E_s} = 2.174 \times 10^{-3}$

Calculation of compressive zone

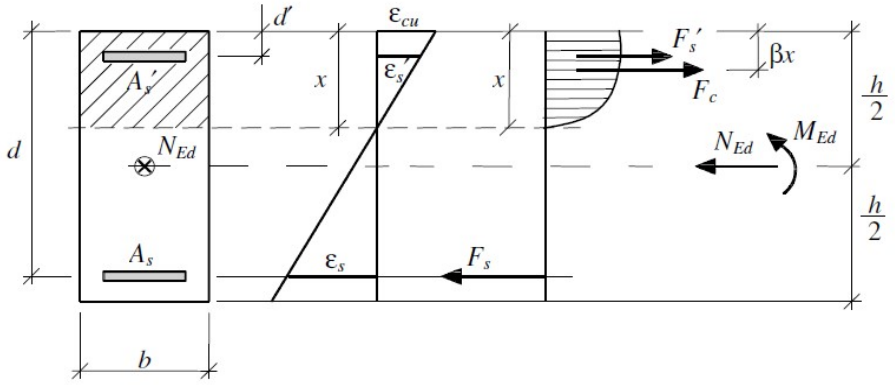

Figure Stress - strain distribution

Horizontal equilibrium

$\alpha \cdot f_{cd} \cdot b \cdot x := f_{yd} \cdot A_{s.bot} + N_{Ed.max}$

Assume $x := 50mm$

Assume yielding $\varepsilon_{s.bot} > \varepsilon_{sy}$

$x_{bot} := root\left(f_{yd} \cdot A_{s.bot} + N_{Ed.max} - \alpha \cdot f_{cd} \cdot b \cdot x, x\right)$

$x_{bot} = 46.678 \cdot mm$

$f_{yd} \cdot A_{s.bot} + N_{Ed.max} - \alpha \cdot f_{cd} \cdot b \cdot x_{bot} = 0\,N$ Horizontal equilibrium fulfilled

$\varepsilon_{s.bot} := if\left(x_{bot} > 0, \frac{d_{bot} - x_{bot}}{x_{bot}} \cdot \varepsilon_{cu}, \varepsilon_{sy}\right) = 3.6 \times 10^{-2}$

$Kontroll_{\varepsilon.s.bot} := if\left(\varepsilon_{s.bot} > \varepsilon_{sy}, "OK", "NOT\ OK"\right)$ $Kontroll_{\varepsilon.s.bot} = "OK"$

Required reinforcement

$\sigma_{s.bot} := \begin{cases} E_s \cdot \varepsilon_{s.bot} & if\ \varepsilon_{s.bot} \le \varepsilon_{sy} \\ f_{yd} & if\ \varepsilon_{s.bot} \ge \varepsilon_{sy} \end{cases} = 435 \cdot MPa$

$A_{sd.bot} := \frac{\alpha \cdot f_{cd} \cdot b \cdot x_{bot} + N_{Ed.max}}{\sigma_{s.bot}}$

$A_{sd.bot} = 1964 \cdot mm^2$

$M_{Rd.max} := \alpha \cdot f_{cd} \cdot b \cdot x_{bot} \cdot \left(d_{bot} - \beta \cdot x_{bot}\right) - N_{Ed.max} \cdot \left(d_{bot} - \frac{h}{2}\right)$

$M_{Rd.max} = 449.687 \cdot kN \cdot m$

Check moment capacity

$\eta_{bot} := \frac{M_{Ed.max}}{M_{Rd.max}} = 81.39 \cdot \%$ $\quad M_{Ed.max} = 366\ m \cdot kN$

$Kontroll_{\eta.bot} := if\left(\eta_{bot} < 100\%, "OK", "NOT\ \ OK"\right)$

$Kontroll_{\eta.bot} = "OK"$

Ductility

$xd_{bot} := \frac{x_{bot}}{d_{bot}} = 0.089$

A.4.2 Calculation of moment resistance for top edge MRd, top

$M_{Ed.min} := 42.1kN \cdot m$ (Konstructionsberäkningar Bro 100-2990-1, Appendix 4.1.B)

$N_{Ed.min} := -260.5kN$ (Konstructionsberäkningar Bro 100-2990-1, Appendix 4.1.B)

$A_{s.top} := 1340.4mm^2$ (Konstructionsberäkningar Bro 100-2990-1, Appendix 4.1.B)

$d_{top} := 536mm$ (Konstructionsberäkningar Bro 100-2990-1, Appendix 4.1.B)

$d'_{top} := 64mm$ (Konstructionsberäkningar Bro 100-2990-1, Appendix 4.1.B)

Horizontal equilibrium

$\alpha \cdot f_{cd} \cdot b \cdot x := f_{yd} \cdot A_{s.top} + N_{Ed.min}$

Assume $x := 60mm$

$x_{top} := root\left(f_{yd} \cdot A_{s.top} + N_{Ed.min} - \alpha \cdot f_{cd} \cdot b \cdot x, x\right)$

$x_{top} = 17.052 \cdot mm$

$f_{yd} \cdot A_{s.top} + N_{Ed.min} - \alpha \cdot f_{cd} \cdot b \cdot x_{top} = 0\ N$ Horizontal equilibrium fulfilled

Assume yielding $\varepsilon_{s.top} > \varepsilon_{sy}$

$$\varepsilon_{s.top} := \text{if}\left(x_{top} > 0, \frac{d_{top} - x_{top}}{x_{top}} \cdot \varepsilon_{cu}, \varepsilon_{sy}\right)$$

$$\text{Kontroll}_{\varepsilon.s.top} := \text{if}\left(\varepsilon_{s.top} > \varepsilon_{sy}, \text{"OK"}, \text{"NOT OK"}\right)$$

$\text{Kontroll}_{\varepsilon.s.top} = \text{"OK"}$

Required reinforcement

$$\sigma_{s.top} := \begin{cases} E_s \cdot \varepsilon_{s.top} & \text{if } \varepsilon_{s.top} \le \varepsilon_{sy} \\ f_{yd} & \text{if } \varepsilon_{s.top} \ge \varepsilon_{sy} \end{cases} = 435 \cdot MPa$$

$$A_{sd.top} := \frac{\alpha \cdot f_{cd} \cdot b \cdot x_{top} - N_{Ed.min}}{\sigma_{s.top}}$$

$A_{sd.top} = 1340.400 \cdot mm^2$

$$M_{Rd.min} := \alpha \cdot f_{cd} \cdot b \cdot x_{top} \cdot \left(d_{top} - \beta \cdot x_{top}\right) - N_{Ed.min} \cdot \left(d_{top} - \frac{h}{2}\right)$$

$M_{Rd.min} = 231.935 \cdot kN \cdot m$

Check moment capacity

$$\eta_{top} := \frac{M_{Ed.min}}{M_{Rd.min}} = 18 \cdot \%$$

OK

Ductility

$$xd_{top} := \frac{x_{top}}{d_{top}} = 0.03181$$

A.5 Amount of concrete

$b_{tot} := 7670mm$

$$\rho_c := 25 \frac{kN}{m^3}$$

$$m_c := h \cdot b_{tot} \cdot \left(\rho_c - 1 \frac{kN}{m^3}\right) \cdot \frac{1}{9.81N} \cdot kg$$

$m_c = 11258.716 \frac{kg}{m}$

A.6 Summary of case 1

Bottom

$$\eta_{bot} := \frac{M_{Ed.max}}{M_{Rd.max}} = 81 \cdot \%$$ Moment capacity

Top

$$\eta_{top} := \frac{M_{Ed.min}}{M_{Rd.min}} = 18.15 \cdot \%$$ Moment capacity

Ductility

According to SS-EN 1992-2:2005 section 5.6.3 , $\frac{x}{d}$ should not be larger than 0.3

$$xd_{max} := 0.3$$

$$\eta_{xd} := \frac{\max(xd_{top}, xd_{bot})}{xd_{max}} = 30 \cdot \%$$

Amount of concrete

$$m_c = 11258.716 \frac{kg}{m}$$

Appendix B- Case 2:
Design the bridge with HPC C90/105

B.1 Geometry

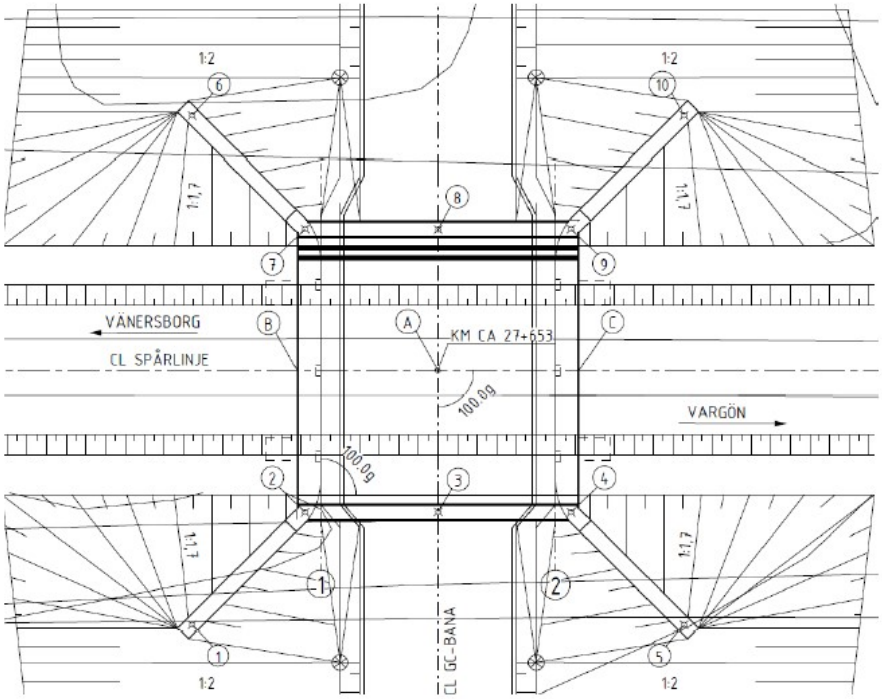

Figure Bridge plan

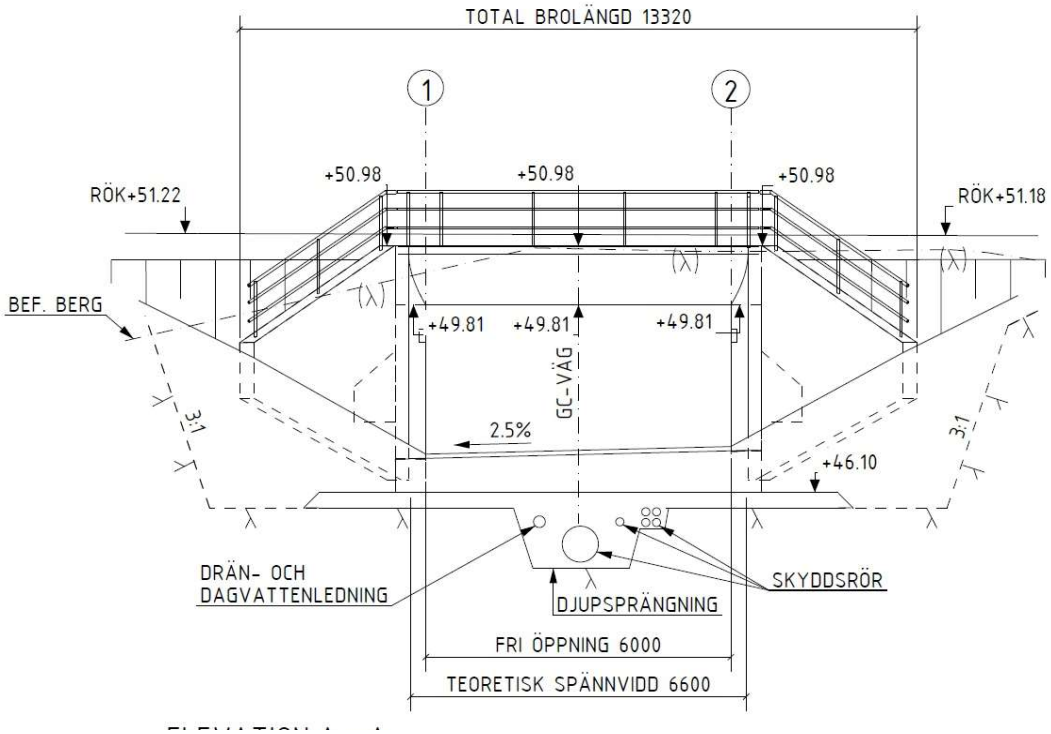

Figure. Elevation

The bridge type is concrete frame bridge made from high performance concrete C90/105

Dimensions

Free span	6000mm
Theoretical span	6600mm
Bridge width	7210mm
Thickness is varying between	565mm-600mm

$h := 600mm$

$b_{tot} := 7670mm$ total width of the bridge

B.2 Calculation conditions

Service life: L100 (120 years)
For the bridge deck a safety class 3 is chosen. (VVFS 2004:31 and VVFS 2004:43).

Exposure classes according TDOK 2016:0203

Construction part	Exposure class	Service life	Concrete cover[mm]	W.k[mm]	Max w/c
Bridge deck, top	XD1/XF4	L100	30	0.3	0.3
Bridge deck, botton	XC4/XF3	L100	30	0.2	0.35

B.3 Concrete cover

Concrete cover is calculated according to TRVFS 2011:12, Ch. 21 Table a:

B.3.1 Bottom

Longitudinal reinforcement diameter

$\phi_{s.bot} := 20mm$

Stirrups diameter

$\phi_{stirup} := 12mm$

$\Delta c_{dev} := 10mm$ SS-EN 1992-1-1:2005, ch.4.4.1.3

$\Delta c_{dur.st} := 0mm$ SS-EN 1992-1-1:2005, ch. 4.4.1.2.

$\Delta c_{dur.add} := 0mm$ SS-EN 1992-1-1:2005, ch. 4.4.1.2.

$\Delta c_{dur.\gamma} := 0mm$ SS-EN 1992-1-1:2005, ch. 4.4.1.2.

$c_{min.b} := \phi_{s.bot}$ SS-EN 1992-1-1:2005, ch. 4.4.1.2. table 4.2.

$c_{min.dur} := 20mm$ TRAV2011-12, table a

$c_{min} := \max\left(c_{min.b}, c_{min.dur} + \Delta c_{dur.\gamma} - \Delta c_{dur.st} - \Delta c_{dur.add}, 10mm\right) = 20 \cdot mm$

$c_{nom} := c_{min} + \Delta c_{dev}$ SS-EN 1992-1-1:2005, ch. 4.4.1.1. Eq (4.1)

Concrete cover bottom

$c_{nom} = 30 \cdot mm$

$d'_{bot} := c_{nom} + \frac{1}{2} \cdot \phi_{s.bot} + \phi_{stirup} = 52 \cdot mm$

$d_{bot} := h - d'_{bot} = 0.548\,m$

B.3.2 Top

$\phi_{s.top} := 16mm$

$c_{min.b} := \phi_{s.top}$ SS-EN 1992-1-1:2005, ch. 4.4.1.2. table 4.2.

$c_{min.dur} := 20mm$ TRAV2011-12, table a

$c_{min} := \max\left(c_{min.b}, c_{min.dur} + \Delta c_{dur.\gamma} - \Delta c_{dur.st} - \Delta c_{dur.add}, 10mm\right)$

$c_{nom} := c_{min} + \Delta c_{dev}$

$c_{nom} = 30 \cdot mm$

$d'_{top} := c_{nom} + \frac{1}{2} \cdot \phi_{s.top} + \phi_{stirup} = 50 \cdot mm$

$d_{top} := h - d'_{top} = 550 \cdot mm$

B.4 Material properties

B.4.1 Concrete:

Values are taken from table 3.1, SS-EN 1992-1-1,2005

C90/105

$f_{ck} := 90MPa$ Characteristic compressive strength. SS-EN 1992-1-1,2005 Table 3.1

$f_{ctm} := 5MPa$ Mean compressive strength. SS-EN 1992-1-1,2005 Table 3.1

$f_{ctk} := 3.5MPa$ Characteristic tensile strength. SS-EN 1992-1-1,2005, Table 3.1

$E_{cm} := 44GPa$ Modulus of elasticity. SS-EN 1992-1-1,2005, Table 3.1

$\varepsilon_{cu} := 0.0026$ Ultimate compressive strain. SS-EN 1992-1-1,2005, Table 3.1

$\varphi_{ef} := 1.87$ Creep coefficient, SS-EN 1992-1-1, 2005.figure 3.1, page 27.

$\alpha := 0.550$

$\beta := 0.350$ Tryckblocksfaktorer, SS-EN 1992-1-1,2005.

B.4.2 Steel K500C-T

$f_{yk} := 500MPa$ Characteristic value for the yield strength of the reinforcement.

$E_s := 200GPa$ Steel modulus of elasticity. SS-EN 1992-1-1,2005.

$\rho_s := 78.5 \frac{kN}{m^3}$ Density of steel. SS-EN 1991-1-1:2002,Table A.4.

$\varepsilon_{uk} := 7.5\%$ Characteristic ultimate strain of reinforcement. SS-EN 1992-1-1:2005, Annex C Table C.1.

B.4.3 Strength

Concrete

$\gamma_c := 1.5$ Partial factor for compressed concrete in ULS. SS-EN 1992-1-1:2005, Ch. 2.4.2.4 Table 2.1N

$f_{cd} := \frac{f_{ck}}{\gamma_c} = 60 \cdot MPa$

Steel

$\gamma_s := 1.15$ Reinforcement partial factor in ULS,SS-EN 1992-1-1, Table 2.1.

$f_{yd} := \frac{f_{yk}}{\gamma_s} = 434.783 \cdot MPa$

$\varepsilon_{sy} := \frac{f_{yd}}{E_s} = 0.00217$

$\alpha_{ef} := \frac{E_s}{E_{cm}} = 4.545$ Ratio between steel modulus of elasticity and concrete modulus of elasticity

$\varepsilon_{ud} := 0.9 \cdot \varepsilon_{uk} = 0.0675$ Design ultimate strain of reinforcement.

B.5 Scenario 1:

B.5.1 Calculation of moment resistance for bottom edge MRd,max (Bottom)

Cross section at x=3600mm

Input

The moment and its normal force are picked up from provided calculation from AFRY case study.

$M_{Ed.max} := 366kN \cdot m$ (Konstructionsberäkningar Bro 100-2990-1, Appendix 4.1.B)

$N_{Ed.max} := -28.4kN$ (Konstructionsberäkningar Bro 100-2990-1, Appendix 4.1.B)

$A_{s.bot} := 2094.4mm^2$ (Konstructionsberäkningar Bro 100-2990-1, Appendix 4.1.B)

$b := 1000mm$ $h := 600mm$ $d_{bot} = 548 \cdot mm$ $d'_{bot} = 52 \cdot mm$

Calculation of compressive zone

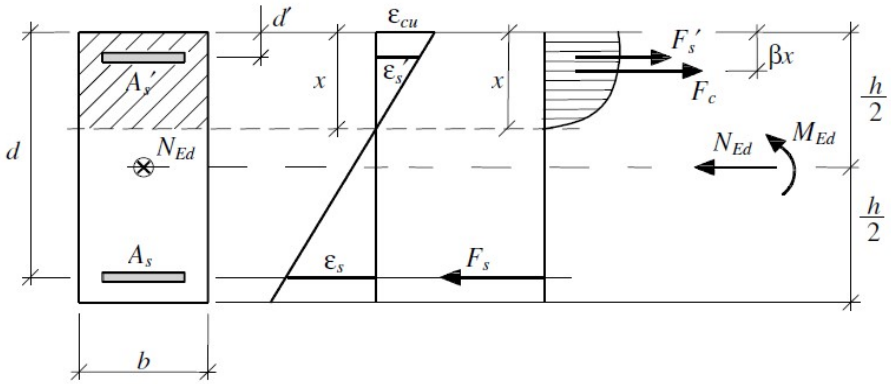

Figure stress - strain distribution

Horizontal equilibrium

$\alpha \cdot f_{cd} \cdot b \cdot x := f_{yd} \cdot A_{s.bot} + N_{Ed.max}$

Assume $x := 60mm$

$x_{bot} := root\left(f_{yd} \cdot A_{s.bot} + N_{Ed.max} - \alpha \cdot f_{cd} \cdot b \cdot x, x\right)$

$x_{bot} = 26.734 \cdot mm$

$f_{yd} \cdot A_{s.bot} + N_{Ed.max} - \alpha \cdot f_{cd} \cdot b \cdot x_{bot} = 0\,N$ Horizontal equilibrium fulfilled

Assume yielding $\varepsilon_{s.bot} > \varepsilon_{sy}$

$$\varepsilon_{s.bot} := \text{if}\left(x_{bot} > 0, \frac{d_{bot} - x_{bot}}{x_{bot}} \cdot \varepsilon_{cu}, \varepsilon_{sy}\right) = 5 \cdot \%$$

Elongation in the reinforcement

$$\text{Kontroll}_{\varepsilon.s.bot} := \text{if}\left(\varepsilon_{s.bot} > \varepsilon_{sy}, \text{"OK"}, \text{"NOT OK"}\right)$$

$$\text{Kontroll}_{\varepsilon.s.bot} = \text{"OK"}$$

Required reinforcement

$$\sigma_{s.bot} := \begin{cases} E_s \cdot \varepsilon_{s.bot} & \text{if } \varepsilon_{s.bot} \le \varepsilon_{sy} \\ f_{yd} & \text{if } \varepsilon_{s.bot} \ge \varepsilon_{sy} \end{cases} = 435 \cdot \text{MPa}$$

$$A_{sd.bot} := \frac{\alpha \cdot f_{cd} \cdot b \cdot x_{bot} + N_{Ed.max}}{\sigma_{s.bot}}$$

$$A_{sd.bot} = 1964 \cdot \text{mm}^2$$

$$M_{Rd.max} := \alpha \cdot f_{cd} \cdot b \cdot x_{bot} \cdot \left(d_{bot} - \beta \cdot x_{bot}\right) - N_{Ed.max} \cdot \left(d_{bot} - \frac{h}{2}\right)$$

Moment capacity

$$M_{Rd.max} = 482.239 \cdot \text{kN} \cdot \text{m}$$

Check moment capacity

$$\eta_{bot} := \frac{M_{Ed.max}}{M_{Rd.max}} = 75.896 \cdot \%$$

$$\text{Kontroll}_{\eta.bot} := \text{if}\left(\eta_{bot} < 100\%, \text{"OK"}, \text{"NOT OK"}\right)$$

$$\text{Kontroll}_{\eta.bot} = \text{"OK"}$$

Ductility

$$xd_{bot} := \frac{x_{bot}}{d_{bot}} = 0.049$$

B.5.2 Calculation of moment resistance for top edge MRd, top

Input

$M_{Ed.min} := 42.1kN \cdot m$ (Konstructionsberäkningar Bro 100-2990-1, Appendix 4.1.B)

$N_{Ed.min} := -260.5kN$ (Konstructionsberäkningar Bro 100-2990-1, Appendix 4.1.B)

$A_{s.top} := 1340.4mm^2$ (Konstructionsberäkningar Bro 100-2990-1, Appendix 4.1.B)

$d_{top} = 550 \cdot mm$ $d'_{top} = 50 \cdot mm$

Calculation of compressive zone

Horizontal equilibrium

$\alpha \cdot f_{cd} \cdot b \cdot x := f_{yd} \cdot A_{s.top} + N_{Ed.min}$

Assume $x := 60mm$

$x_{top} := root\left(f_{yd} \cdot A_{s.top} + N_{Ed.min} - \alpha \cdot f_{cd} \cdot b \cdot x, x\right)$

$x_{top} = 9.766 \cdot mm$

$f_{yd} \cdot A_{s.top} + N_{Ed.min} - \alpha \cdot f_{cd} \cdot b \cdot x_{top} = 0\,N$ Horizontal equilibrium fulfilled

Assume yielding $\varepsilon_{s.top} > \varepsilon_{sy}$

$$\varepsilon_{s.top} := if\left(x_{top} > 0, \frac{d_{top} - x_{top}}{x_{top}} \cdot \varepsilon_{cu}, \varepsilon_{sy}\right)$$

$Kontroll_{\varepsilon.s.top} := if\left(\varepsilon_{s.top} > \varepsilon_{sy}, "OK", "EJ\ OK"\right)$ $Kontroll_{\varepsilon.s.top} = "OK"$

Required reinforcement

$$\sigma_{s.top} := \begin{cases} E_s \cdot \varepsilon_{s.top} & \text{if } \varepsilon_{s.top} \le \varepsilon_{sy} \\ f_{yd} & \text{if } \varepsilon_{s.top} \ge \varepsilon_{sy} \end{cases} = 435 \cdot MPa$$

$$A_{sd.top} := \frac{\alpha \cdot f_{cd} \cdot b \cdot x_{top} - N_{Ed.min}}{\sigma_{s.top}}$$

$A_{sd.top} = 1340.400 \cdot mm^2$

Minimum reinforcement

Surface reinforcement TDOK 2016:0204, chapter D.1.4.1, and SS-EN 1992-1-1, chapter 9.3.1.

$$A_{s.min.a} := 4 \cdot \frac{f_{ctm}}{3} \cdot \frac{cm^2}{MPa} \qquad A_{s.min.a} = 666.667 \cdot mm^2$$

$$A_{s.min.b} := \begin{cases} (0.05\% \cdot h \cdot b) & \text{if } \frac{b_{tot}}{h} \le 5 \\ (0.08\% \cdot h \cdot b) & \text{otherwise} \end{cases} \qquad A_{s.min.b} = 480 \cdot mm^2$$

$$A_{s.min.c} := 5.6 \cdot cm^2 \qquad A_{s.min.c} = 560 \cdot mm^2$$

$$A_{s.min.1} := \max\left(A_{s.min.a}, A_{s.min.b}, A_{s.min.c}\right) \qquad A_{s.min.1} = 666.667 \cdot mm^2$$

$$A_{s.top} := \max\left(A_{sd.top}, A_{s.min.1}\right) \qquad A_{s.top} = 1340.400 \cdot mm^2$$

$$M_{Rd.min} := \alpha \cdot f_{cd} \cdot b \cdot x_{top} \cdot \left(d_{top} - \beta \cdot x_{top}\right) - N_{Ed.min} \cdot \left(d_{top} - \frac{h}{2}\right)$$

$M_{Rd.min} = 241.279 \cdot kN \cdot m$ Moment capacity of bottom side

Check moment capacity

$$\eta_{top} := \frac{M_{Ed.min}}{M_{Rd.min}} = 17.449 \cdot \%$$

Ductility

$$xd_{top} := \frac{x_{top}}{d_{top}} = 0.018$$

B.5.3 Shear reinforcement

Shear force must always be checked against the shear capacity or shear stress capacity of the section. But according to SS-EN 1992-1-1:2005, Ch. 6.2.1. Shear force have not to be checked at distance less than d from the support when a uniformly distributed load is applied on the member. The shear force depends on the support conditions of the beam and the location of the load on the member. The first axle force is located at a distance d from the support, while the shear reinforcement is designed for the shear force at the support because the shear force is maximum.

In this case the shear reinforcement is designed at x= 1200mm.

Input:

$V_{Ed} := 555.9kN$ (Konstructionsberäkningar Bro 100-2990-1, Appendix 4.1.B)

$N_{Ed} := -231kN$

$M_{Ed} := -237.5$

$L := 6000mm$ Free span length

$h := 579mm$ Height of HPC cross section

$b_w := 1m$

$c_{nom} = 30 \cdot mm$

$d'_{top} := c_{nom} + \frac{1}{2} \cdot \phi_{s.top} + \phi_{stirup} = 50 \cdot mm$

$d_{top} := h - d'_{top} = 529 \cdot mm$

$d := d_{top}$

$f_{ck} := 90MPa$

$f_{yk} := 500MPa$ $A_{sl} := 3272.5mm^2$

$\alpha_{cc} := 1.0$ $\gamma_a := 1.5$

$k_1 := 0.15$ Recommended values from SS-EN 1992-1-1:2005, ch.6.2.2

$k_2 := 0.18$

$\theta := 21.8deg$ $\alpha := 90deg$ $\phi_b := 12mm$ $cc_b := 300mm$ $n_{skar} := 1$

$f_{ywd} := f_{yk} \div 1.15 = 435 \cdot MPa$

B.5.3.1 Control shear without shear reinforcement

$\rho_1 := \min\left(\frac{A_{sl}}{b_w \cdot d}, 0.02\right) = 0.0062$ SS-EN 1992-1-1:2005, ch.6.2.2

$k := \min\left[\left(1 + \sqrt{200mm \div d}\right), 2.0\right] = 1.615$

$C_{Rd.c} := k_2 \div \gamma_c = 0.120$ SS-EN 1992-1-1:2005, ch.6.2.2.

$\sigma_{cp} := \min\left[-N_{Ed} \div \left(b_w \cdot h\right), \left(0.2 \cdot \alpha_{cc} \cdot f_{ck} \div \gamma_c\right)\right] = 0.399 \cdot MPa$ SS-EN 1992-1-1:2005, ch.6.2.2

$V_{Rd.c} := \left[C_{Rd.c} \cdot k \cdot \left(100 \cdot \rho_1 \cdot f_{ck} \div MPa\right)^{1 \div 3} \cdot MPa + k_1 \cdot \sigma_{cp}\right] \cdot b_w \cdot d = 423 \cdot kN$ SS-EN 1992-1-1:2005, ch.6.2.2. Eq. (6.2a).

$\nu_{min} := 0.035 \cdot k^{3 \div 2} \cdot \left(f_{ck} \div MPa\right)^{1 \div 2} = 0.681$ SS-EN1992-2-2005,Eq. (6.3N).

$V_{Rd.c.min} := \left(\nu_{min} \cdot MPa + k_1 \cdot \sigma_{cp}\right) \cdot b_w \cdot d = 392 \cdot kN$ SS-EN1992-2-2005,Eq. (6.2b).

$V_{Rd.c.max} := \max\left(V_{Rd.c}, V_{Rd.c.min}\right) = 423 \cdot kN$ Shear force.

Controll_Shear := if$\left(V_{Rd.c.max} \geq V_{Ed}, \text{"capacity sufficient"}, \text{"capacity unsufficient "}\right)$

Controll_Shear = "capacity unsufficient "

$V_{Ed} \leq 0.5 \cdot b_w \cdot d \cdot \upsilon \cdot f_{cd}$

$f_{cd} := \alpha_{cc} \cdot f_{ck} \div \gamma_c = 60 \cdot MPa$

$\upsilon := 0.6 \cdot \left[1 - \left(f_{ck} \div MPa\right) \div 250\right] = 0.384$ SS-EN1992-2-2005, Eq.(6.10.bN)

$V_{Rdc.max} := 0.5 \cdot b_w \cdot d \cdot \upsilon \cdot f_{cd} = 6094 \cdot kN$

Design shear reinforcement

$z := 0.9 \cdot d = 0.476\,m$ $\cot(\theta) = 2.5$ The angle should be fulfilled with regard to SS-EN 1992-1-1:2005, Ch. 6.2.3.

$0.9 \cdot d \cdot \cot(\theta) = 1.19\,m$

$A_{sw} := n_{skar} \frac{1m}{cc_b} \cdot \pi \cdot \frac{\phi_b^{\,2}}{4} = 377 \cdot mm^2$ Cross-sectional area of the shear reinforcement

Spacing of frames or stirrups.

$s_{b.erf} := 337mm$

$s_b := 200mm$

$s_{b.max} := 0.75 \cdot d \cdot (1 + \cot(\alpha)) = 397 \cdot mm$ $\geq s_{bv} := 200mm$

$cc_{b.max} := 1.5d = 793 \cdot mm$ $\geq cc_b = 300 \cdot mm$

$\alpha_{cw} := 1 + \frac{\sigma_{cp}}{f_{cd}} = 1.007$ For non-prestressed SS-EN1992-2-2005, Eq.(6.11.aN)

$f_{cd} := \alpha_{cc} \cdot f_{ck} \div \gamma_c = 60 \cdot MPa$

$$\upsilon_1 := \max\left(0.9 - \frac{f_{ck}}{200\,MPa}, 0.5\right) = 0.5$$

Strength reduction factor,SS-EN1992-2-2005, eq.6.6

Final shear resistance

$$V_{Rd.s} := \frac{A_{sw} \cdot z \cdot f_{ywd} \cdot \cot(\theta)}{s_b} = 975.534 \cdot kN$$

Max shear force:

$$V_{Rd.max} := \frac{\alpha_{cw} \cdot b_w \cdot z \cdot \upsilon_1 \cdot f_{cd}}{\cot(\theta) + \tan(\theta)} = 4958 \cdot kN \qquad \geq V_{Ed} = 555.9\,kN$$

$$A_{sw.erf} := \frac{1m}{s_{b.erf}} \cdot A_{sw} = 1119 \cdot mm^2$$

$$A_{sw.inlagd} := \frac{1m}{s_b} \cdot A_{sw} = 1885 \cdot mm^2$$

$$U := A_{sw.erf} \div A_{sw.inlagd} = 0.59$$

$$\rho_w := A_{sw} \div \left(s_b \cdot b_w \cdot \sin(\alpha)\right) = 0.188 \cdot \%$$

$$\rho_{w.min1} := \left(0.08 \cdot \sqrt{f_{ck} \div MPa}\right) \div \left(f_{yk} \div MPa\right) = 0.1518 \cdot \% \qquad \leq \quad \rho_w = 0.1885 \cdot \%$$

SS-EN1992-2-2005, Eq.(9.5N).

$$a_1 := z \cdot (\cot(\theta) - \cot(\alpha)) \div 2 = 595.167 \cdot mm$$

$$shear\_force\_check := if\left(s_b \leq s_{b.erf} \wedge s_{b.max} \geq s_b \wedge cc_{b.max} \geq cc_b \wedge V_{Rd.max} \geq V_{Ed}, "OK", "EJ\ OK"\right)$$

shear_force_check = "OK"

$$\eta V_s := \frac{V_{Ed}}{\min\left(V_{Rd.s}, V_{Rd.max}\right)} = 56.984 \cdot \%$$

B.6 Scenario 2

The cross section is optimized by reducing the thickness and making required controls in ULS and SLS. The amount of reinforcement is unchanged (same reinforcement amount used in provided bridge input).

Step 1:

New thickness is assumed to be 450mm, a new design value of the applied internal bending moment (M.Ed) is obtained due to reduction of the thickness where a new design moment of self-weight is considered.

B.6.1 ULS new moment for optimized cross section in HPC

cross-section at x=3.6m

Max design moment value of applied load, obtained from ULS load combination for conventional concrete's cross section (bottom)

$M_{Ed.con.max.uls} := 366kN \cdot m$ (Konstructionsberäkningar Bro 100-2990-1, Appendix 4.1.B)

Minimum design moment value of applied load, obtained from ULS load combination for conventional concrete's cross section (Top)

$M_{Ed.con.min.uls} := 42.1kN \cdot m$ (Konstructionsberäkningar Bro 100-2990-1, Appendix 4.1.B)

Moment due to self-weight of conventional concrete's cross section characteristic value

$M_{Ed.sw.conv} := 40.9kN \cdot m$

$h := 450mm$ Height of HPC cross section (assumed)

$h_{con} := 600mm$ Height of conventional concrete cross section (original height)

$\rho_c := 25 \frac{kN}{m^3}$ density of concrete

$G_{s.con} := \rho_c \cdot h_{con} = 15 \cdot \frac{kN}{m^2}$ Self-weight of conventional cross section

$G_{s.HPC} := h \cdot \rho_c = 11.25 \cdot \frac{kN}{m^2}$ Self-weight of HPC cross section

$M_{Ed.sw.hpc} := \frac{G_{s.HPC}}{G_{s.con}} \cdot M_{Ed.sw.conv}$ Moment due to self-weight of HPC cross section

$M_{Ed.sw.hpc} = 30.675 \cdot kN \cdot m$ Moment due to self-weight of HPC cross section

$M_{Ed.max} := M_{Ed.con.max.uls} - \left(1.35 M_{Ed.sw.conv}\right) + 1.35 M_{Ed.sw.hpc} = 352.196 \cdot kN \cdot m$

$M_{Ed.min} := M_{Ed.con.min.uls} - \left(1.35M_{Ed.sw.conv}\right) + 1.35M_{Ed.sw.hpc} = 28.296 \cdot kN \cdot m$

Step 2 (ULS)

C.6.2 Calculation of moment resistance for bottom edge density,max (Bottom)

Input

$b := 1000mm$ $h := 450mm$ $N_{Ed.max} := -28.4kN$ $M_{Ed.max} := 352.196kN \cdot m$ $A_{s.bot} := 2094.4mm^2$

$d'_{bot} := c_{nom} + \frac{1}{2} \cdot \phi_{s.bot} + \phi_{stirup} = 52 \cdot mm$ $d'_{bot} = 52 \cdot mm$

$d_{bot} := h - d'_{bot}$ $d_{bot} := 405mm$

Calculation of compressive zone

Horizontal equilibrium

$\alpha \cdot f_{cd} \cdot b \cdot x := f_{yd} \cdot A_{s.bot} + N_{Ed.max}$

Assume $x := 50mm$

$x_{bot} := root\left(f_{yd} \cdot A_{s.bot} + N_{Ed.max} - \alpha \cdot f_{cd} \cdot b \cdot x, x\right)$

$x_{bot} = 9.361 \cdot mm$

Assume yielding $\varepsilon_{s.bot} > \varepsilon_{sy}$

$\varepsilon_{s.bot} := if\left(x_{bot} > 0, \frac{d_{bot} - x_{bot}}{x_{bot}} \cdot \varepsilon_{cu}, \varepsilon_{sy}\right) = 1.1 \times 10^{-1}$ Elongation in the reinforcement

$Kontroll_{\varepsilon.s.bot} := if\left(\varepsilon_{s.bot} > \varepsilon_{sy}, "OK", "NOT OK"\right)$ $Kontroll_{\varepsilon.s.bot} = "OK"$

Required reinforcement

$\sigma_{s.bot} := \begin{cases} E_s \cdot \varepsilon_{s.bot} & if \ \varepsilon_{s.bot} \le \varepsilon_{sy} \\ f_{yd} & if \ \varepsilon_{s.bot} \ge \varepsilon_{sy} \end{cases} = 435 \cdot MPa$ Tensile stress in the reinforcement

$A_{sd.bot.req} := \frac{\alpha \cdot f_{cd} \cdot b \cdot x_{bot} + N_{Ed.max}}{\sigma_{s.bot}}$ Needed amount of the reinforcement at top

$A_{sd.bot.req} = 1964 \cdot mm^2$

Check minimum reinforcement

Surface reinforcement

TDOK 2016:0204, chapter D.1.4.1, and SS-EN 1992-1-1, chapter 9.3.1.

$A_{s.min.a} := 4 \cdot \frac{f_{ctm}}{3} \cdot \frac{cm^2}{MPa}$

$A_{s.min.a} = 666.667 \cdot mm^2$

$A_{s.min.b} := \begin{cases} (0.05\% \cdot h \cdot b) & \text{if } \frac{b_{tot}}{h} \le 5 \\ (0.08\% \cdot h \cdot b) & \text{otherwise} \end{cases}$

$A_{s.min.b} = 360 \cdot mm^2$

$A_{s.min.c} := 5.6 \cdot cm^2$

$A_{s.min.c} = 560 \cdot mm^2$

$A_{s.min.1} := \max(A_{s.min.a}, A_{s.min.b}, A_{s.min.c})$

$A_{s.min.1} = 666.667 \cdot mm^2$

Minimum tension reinforcement

$A_{s.min.d} := 0.26 \cdot \frac{f_{ctm}}{f_{yk}} \cdot d_{top} \cdot 1m$

$A_{s.min.d} = 1375.40 \cdot mm^2$

$A_{s.min.e} := 0.0013 \cdot d_{top} \cdot 1m$

$A_{s.min.e} = 687.7 \cdot mm^2$

$A_{s.min.2} := \max(A_{s.min.d}, A_{s.min.e})$

$A_{s.min.2} = 1375.400 \cdot mm^2$

$A_{sd.bot} := \max(A_{sd.bot.req}, A_{s.min.1}, A_{s.min.2})$

$A_{sd.bot} = 1963.760 \cdot mm^2$

$\eta_{bot} := \frac{A_{sd.bot}}{A_{s.bot}} = 94 \cdot \%$

$M_{Rd.max} := \alpha \cdot f_{cd} \cdot b \cdot x_{bot} \cdot \left(d_{bot} - \beta \cdot x_{bot}\right) - N_{Ed.max} \cdot \left(d_{bot} - \frac{h}{2}\right)$

$M_{Rd.max} = 359.516 \cdot kN \cdot m$

Moment capacity

Check moment capacity

$\eta_{bot} := \frac{M_{Ed.max}}{M_{Rd.max}} = 98 \cdot \%$

$Kontroll_{\eta.bot} := \text{if}(\eta_{bot} < 100\%, \text{"OK"}, \text{"NOT OK"})$

$Kontroll_{\eta.bot} = \text{"OK"}$

Ductility

$xd_{bot} := \frac{x_{bot}}{d_{bot}} = 0.023$

B.6.3 Calculation of moment resistance for top edge MRd, top

$M_{Ed.min} := 28.29kN \cdot m$ $N_{Ed.min} := -260.5kN$ $A_{s.top} := 1340.4mm^2$

$d'_{top} := c_{nom} + \frac{1}{2} \cdot \phi_{s.top} + \phi_{stirup}$ $d'_{top} = 50 \cdot mm$

$d_{top} := h - d'_{top}$ $d_{top} = 400 \cdot mm$

Horizontal equilibrium

$\alpha \cdot f_{cd} \cdot b \cdot x := f_{yd} \cdot A_{s.top} + N_{Ed.min}$

Assume $x := 60mm$

$x_{top} := root\left(f_{yd} \cdot A_{s.top} + N_{Ed.min} - \alpha \cdot f_{cd} \cdot b \cdot x, x\right)$

$x_{top} = 3.42 \cdot mm$

$f_{yd} \cdot A_{s.top} + N_{Ed.min} - \alpha \cdot f_{cd} \cdot b \cdot x_{top} = 0\,N$ Horizontal equilibrium fulfilled

Assume yielding $\varepsilon_{s.top} > \varepsilon_{sy}$

$\varepsilon_{s.top} := if\left(x_{top} > 0, \frac{d_{top} - x_{top}}{x_{top}} \cdot \varepsilon_{cu}, \varepsilon_{sy}\right)$

$Kontroll_{\varepsilon.s.top} := if\left(\varepsilon_{s.top} > \varepsilon_{sy}, "OK", "EJ\ OK"\right)$ $Kontroll_{\varepsilon.s.top} = "OK"$

Required reinforcement

$\sigma_{s.top} := \begin{cases} E_s \cdot \varepsilon_{s.top} & \text{if } \varepsilon_{s.top} \le \varepsilon_{sy} \\ f_{yd} & \text{if } \varepsilon_{s.top} \ge \varepsilon_{sy} \end{cases} = 435 \cdot MPa$ Tensile stress in the reinforcement

$A_{sd.top.req} := \frac{\alpha \cdot f_{cd} \cdot b \cdot x_{top} + N_{Ed.min}}{\sigma_{s.top}}$ Needed amount of the reinforcement at top edge

$A_{sd.top.req} = 142.1 \cdot mm^2$

Check minimum reinforcement

Surface reinforcement TDOK 2016:0204, chapter D.1.4.1, and SS-EN 1992-1-1, chapter 9.3.1.

$A_{s.min.a} := 4 \cdot \frac{f_{ctm}}{3} \cdot \frac{cm^2}{m \cdot MPa}$ $A_{s.min.a} = 666.667 \frac{1}{m} \cdot mm^2$

$A_{s.min.b} := \begin{cases} (0.05\% \cdot h) & \text{if } \frac{b_{tot}}{h} \le 5 \\ (0.08\% \cdot h) & \text{otherwise} \end{cases}$ $A_{s.min.b} = 360 \frac{1}{m} \cdot mm^2$

$A_{s.min.c} := \frac{5.6 \cdot cm^2}{m}$ $A_{s.min.c} = 560 \frac{1}{m} \cdot mm^2$

$A_{s.min.1} := \max(A_{s.min.a}, A_{s.min.b}, A_{s.min.c})$ $A_{s.min.1} = 666.667 \frac{1}{m} \cdot mm^2$

Minimum tension reinforcement

$A_{s.min.d} := 0.26 \cdot \frac{f_{ctm}}{f_{yk}} \cdot d_{top}$ $A_{s.min.d} = 1040.00 \frac{1}{m} \cdot mm^2$

$A_{s.min.e} := 0.0013 \cdot d_{top}$ $A_{s.min.e} = 520 \frac{1}{m} \cdot mm^2$

$A_{s.min.2} := \max(A_{s.min.d}, A_{s.min.e})$ $A_{s.min.2} = 1040.000 \frac{1}{m} \cdot mm^2$

$A_{sd.top} := \max\left(\frac{A_{sd.top.req}}{m}, A_{s.min.1}, A_{s.min.2}\right)$ $A_{sd.top} = 1040.000 \frac{1}{m} \cdot mm^2$

$M_{Rd.min} := \alpha \cdot f_{cd} \cdot b \cdot x_{top} \cdot (d_{top} - \beta \cdot x_{top}) - N_{Ed.min} \cdot \left(d_{top} - \frac{h}{2}\right)$

$M_{Rd.min} = 174.115 \cdot kN \cdot m$

Check moment capacity

$\eta_{top} := \frac{M_{Ed.min}}{M_{Rd.min}} = 16 \cdot \%$

$xd_{top} := \frac{x}{d}$ $\eta_{bot} := \frac{A_{sd.bot}}{A_{s.bot}} = 94 \cdot \%$

Ductility

$xd_{max} := 0.3$ According to SS-EN 1992-2:2005 section 5.6.3 , $\frac{x}{d}$ should not be larger than 0.3

$\eta_{xd} := \frac{\max(xd_{top}, xd_{bot})}{xd_{max}} = 8 \cdot \%$

B.6.4 Shear reinforcement

Shear force must always be checked against the shear capacity or shear stress capacity of the section. But according to SS-EN 1992-1-1:2005, Ch. 6.2.1. Shear force have not to be checked at distance less than d from the support when a uniformly distributed load is applied on the member. The shear force depends on the support conditions of the beam and the location of the load on the member. The first axle force is located at a distance d from the support, while the shear reinforcement is designed for the shear force at the support because the shear force is maximum.

In this case the shear reinforcement is designed at x= 1200mm.

ULS new Shear for optimized cross section in HPC

$V_{Ed.conv} := 555.9kN$ (Konstructionsberäkningar Bro 100-2990-1, Appendix 4.1.B)

$L := 6000mm$ Free span length

$h := 450mm$ Height of HPC cross section (optimized)

$\rho_c := 25\frac{kN}{m^3}$ density of concrete

$b := 1000mm$

$q_c := h \cdot \rho_c = 11.25 \cdot \frac{kN}{m^2}$ Load coming from HPC

$V_c := \frac{q_c \cdot L \cdot b}{2} = 33.75 \cdot kN$ Shear force from HPC

$h_1 := 579mm$ Height of conventional concrete cross section (original height)

$q_{c1} := h_1 \cdot \rho_c = 1.447 \times 10^4 Pa$ Load coming from conventional concrete

$V_{c.1} := \frac{q_{c1} \cdot L \cdot b}{2} = 43.425 \cdot kN$ Shear coming from conventional concrete

$V_{Ed.ULS.max} := \left[V_{Ed.conv} - \left(V_{c.1} \cdot 1.35\right)\right] + V_c \cdot 1.35 = 542.839 \cdot kN$ New shear force of HPC cross section

Input:

$V_{Ed} := 542.84kN$ $N_{Ed} := -231kN$ $f_{ck} := 90MPa$ $h := 450mm$

$f_{yk} := 500MPa$ $A_{sl} := 3272.5mm^2$ $b_w := 1m$ $d := 400mm$

$\alpha_{cc} := 1.0$ $\gamma_c := 1.5$

$k_1 := 0.15$ $k_2 := 0.18$ Recommended values from SS-EN 1992-1-1:2005, ch 6.2.2

$\theta := 21.8deg$ $\alpha := 90deg$ $\phi_b := 12mm$ $cc_b := 300mm$ $n_{skar} := 1$

$f_{ywd} := f_{yk} \div 1.15 = 435 \cdot MPa$

C.6.4.1 Control shear without shear reinforcement

$\rho_1 := \min\left(\frac{A_{sl}}{b_w \cdot d}, 0.02\right) = 0.0082$ SS-EN 1992-1-1:2005, ch.6.2.2

$k := \min\left[\left(1 + \sqrt{200mm \div d}\right), 2.0\right] = 1.707$

$C_{Rd.c} := k_2 \div \gamma_c = 0.120$ SS-EN 1992-1-1:2005, ch.6.2.2.

$\sigma_{cp} := \min\left[-N_{Ed} \div \left(b_w \cdot h\right), \left(0.2 \cdot \alpha_{cc} \cdot f_{ck} \div \gamma_c\right)\right] = 0.513 \cdot MPa$ SS-EN 1992-1-1:2005, ch.6.2.2

$V_{Rd.c} := \left[C_{Rd.c} \cdot k \cdot \left(100 \cdot \rho_1 \cdot f_{ck} \div MPa\right)^{1 \div 3} \cdot MPa + k_1 \cdot \sigma_{cp}\right] \cdot b_w \cdot d = 374 \cdot kN$ SS-EN 1992-1-1:2005, ch.6.2.2. Eq. (6.2a).

$\nu_{min} := 0.035 \cdot k^{3 \div 2} \cdot \left(f_{ck} \div MPa\right)^{1 \div 2} = 0.741$ SS-EN1992-2-2005,Eq. (6.3N).

$V_{Rd.c.min} := \left(\nu_{min} \cdot MPa + k_1 \cdot \sigma_{cp}\right) \cdot b_w \cdot d = 327 \cdot kN$ SS-EN1992-2-2005,Eq. (6.2b).

$V_{Rd.c.max} := \max\left(V_{Rd.c}, V_{Rd.c.min}\right) = 374 \cdot kN$ Shear force.

$Controll\_Shear := \text{if}\left(V_{Rd.c.max} \geq V_{Ed}, \text{"capacity sufficient"}, \text{"capacity unsufficient "}\right)$

Controll_Shear = "capacity unsufficient "

$V_{Ed} \leq 0.5 \cdot b_w \cdot d \cdot \upsilon \cdot f_{cd}$

$f_{cd} := \alpha_{cc} \cdot f_{ck} \div \gamma_c = 60 \cdot MPa$

$\upsilon := 0.6 \cdot \left[1 - \left(f_{ck} \div MPa\right) \div 250\right] = 0.384$ SS-EN1992-2-2005, Eq.(6.10.bN)

$V_{Rd.c.max} := 0.5 \cdot b_w \cdot d \cdot \upsilon \cdot f_{cd} = 4608 \cdot kN$

Design shear reinforcement

$z := 0.9 \cdot d = 0.36\,m$ $\cot(\theta) = 2.5$

$0.9 \cdot d \cdot \cot(\theta) = 0.9\,m$

The angle should be fulfilled with regard to SS-EN 1992-1-1:2005, Ch. 6.2.3.

$A_{sw} := n_{skar} \frac{1m}{cc_b} \cdot \pi \cdot \frac{\phi_b^2}{4} = 377 \cdot mm^2$ Cross-sectional area of the shear reinforcement

$s_{b.erf} := \frac{A_{sw}}{V_{Ed}} \cdot \left[z \cdot f_{ywd} \cdot (\cot(\theta) + \cot(\alpha)) \cdot \sin(\alpha) \right] = 272 \cdot mm$ Spacing of frames or stirrups.

$s_b := 245mm$

$s_{b.max} := 0.75 \cdot d \cdot (1 + \cot(\alpha)) = 300 \cdot mm \quad \geq s_b = 245 \cdot mm$

$cc_{b.max} := 1.5d = 600 \cdot mm \quad \geq cc_b = 300 \cdot mm$

$\alpha_{cw} := 1 + \frac{\sigma_{cp}}{f_{cd}} = 1.009$ For non-prestressed SS-EN1992-2-2005, Eq.(6.11.aN)

$f_{cd} := \alpha_{cc} \cdot f_{ck} \div \gamma_c = 60 \cdot MPa$

$\upsilon_1 := \max\left(0.9 - \frac{f_{ck}}{200MPa}, 0.5\right) = 0.5$ Strength reduction factor,SS-EN1992-2-2005, eq.6.6

Final shear resistance

$V_{Rd.s} := \frac{A_{sw} \cdot z \cdot f_{ywd} \cdot \cot(\theta)}{s_b} = 602.158 \cdot kN$

Max shear force:

$V_{Rd.max} := \frac{\alpha_{cw} \cdot b_w \cdot z \cdot \upsilon_1 \cdot f_{cd}}{\cot(\theta) + \tan(\theta)} = 3756 \cdot kN \quad \geq V_{Ed} = 542.84 kN$

$A_{sw.erf} := \frac{1m}{s_{b.erf}} \cdot A_{sw} = 1387 \cdot mm^2$

$A_{sw.inlagd} := \frac{1m}{s_b} \cdot A_{sw} = 1539 \cdot mm^2$

$U := A_{sw.erf} \div A_{sw.inlagd} = 0.9$

$\rho_w := A_{sw} \div \left(s_b \cdot b_w \cdot \sin(\alpha)\right) = 0.154 \cdot \%$

$\rho_{w.min1} := \left(0.08 \cdot \sqrt{f_{ck} \div MPa}\right) \div \left(f_{yk} \div MPa\right) = 0.1518 \cdot \% \quad \leq \quad \rho_w = 0.1539 \cdot \%$ SS-EN1992-2-2005, Eq.(9.5N).

$a_1 := z \cdot (\cot(\theta) - \cot(\alpha)) \div 2 = 450.032 \cdot mm$

$shear\_force\_check := if\left(s_b \leq s_{b.erf} \wedge s_{b.max} \geq s_b \wedge cc_{b.max} \geq cc_b \wedge V_{Rd.max} \geq V_{Ed}, "OK", "EJ OK"\right)$

shear_force_check = "OK"

$\eta V_{sv} := \frac{V_{Ed}}{\min\left(V_{Rd.s}, V_{Rd.max}\right)} = 90.149 \cdot \%$

B.6.4.2 Crack control

Step 3 (SLS)

Cracking will be checked at coordinate x=3600mm (middle of the bridge) where maximum moment occurs.The calculation will be made for 1m strip. First, a check is made with accordance to SS-EN 1992-1-1:2005 to determine if the cross section is cracked or not, if the cross section is cracked, the crack width will be controlled.

Frequent load combination is used to determine if the cross section is cracked while Quasi-permanent load combination is used to control the crack width.

Design moment and load combination are obtained from Case study provided by AFRY for the bridge 100-2990-1 where the moments are modified to be suitable with the new cross section dimensions (HPC cross section).

SLS new moment for optimized cross section in HPC

x=3.60m

Design moment value of applied load, obtained from SLS- Quasi-permanent load combination for conventional concrete's cross section

Input:

$M_{Ed.Q.conv.} := 130.9kN \cdot m$ (Konstructionsberäkningar Bro 100-2990-1, Appendix 4.1.B)

$M_{Ed.F.conv} := 244kN \cdot m$ (Konstructionsberäkningar Bro 100-2990-1, Appendix 4.1.B)

$M_{Ed.sw.hpc} := \frac{G_{s.HPC}}{G_{s.con}} \cdot M_{Ed.sw.conv}$ Moment due to self-weight of HPC cross section

$M_{Ed.sw.hpc} = 30.675 \cdot kN \cdot m$

New design moment value of applied load, in SLS Quasi-permanent load combination for HPC cross section with optimized thickness

$M_{Ed.Q} := M_{Ed.Q.conv.} - (M_{Ed.sw.conv}) + M_{Ed.sw.hpc} = 120.675 \cdot kN \cdot m$

New design moment value of applied load, in SLS frequent load combination for HPC cross section with optimized thickness

$M_{Ed.F} := M_{Ed.F.conv} - (M_{Ed.sw.conv}) + M_{Ed.sw.hpc} = 233.775 \cdot kN \cdot m$

Input:

$M_{Ed.Q} = 120.675 \cdot kN \cdot m$

Axial force quasi-permanent at x=3600 mm

$N_{Ed.Q} := 23.3kN$ (Konstructionsberäkningar Bro 100-2990-1, Appendix 4.1.B)

Axial force frequent at x=3600 mm

$N_{Ed.F} := -29.4kN$ (Konstructionsberäkningar Bro 100-2990-1, Appendix 4.1.B)

$M_{Ed.F} = 233.775 \cdot kN \cdot m$

$\alpha_{ef} := \frac{E_s}{E_{cm}} = 4.545$ Ratio between steel modulus of elasticity and concrete modulus of elasticity

$\varphi := 1.87$ Creep coefficient. SS-EN 1992-1-1:2005,Ch. 3.1.4 Figure 3.1.

Bottom reinforcement diameter

$\phi_{s.bot} := 20mm$ (Konstructionsberäkningar Bro 100-2990-1, Appendix 4.1.B)

$\alpha_{eff} := \frac{E_s}{E_{cm}} \cdot (1 + \varphi) = 13.045$

$f_{ctm.fl} := \max\left[\left(1.6 - \frac{h}{1000mm}\right) \cdot f_{ctm}, f_{ctm}\right]$ Mean flexural tensile strength SS-EN 1992-1-1:2005, Ch. 3.1.8 Eq. (3.23).

$f_{ctm.fl} = 5.75 \cdot MPa$

Cross section in stage I

$A_I := b \cdot h + (\alpha_{ef} - 1) \cdot A_{s.bot} = 0.457\,m^2$

$x_I := \frac{\frac{b \cdot h^2}{2} + (\alpha_{ef} - 1) \cdot A_{s.bot} \cdot d_{bot}}{A_I} = 0.228\,m$

$I_I := \frac{b \cdot h^3}{12} + b \cdot h \cdot \left(\frac{h}{2} - x_I\right)^2 + (\alpha_{ef} - 1) \cdot A_{s.bot} \cdot (d_{bot} - x_I)^2 = 7.83 \times 10^{-3}\,m^4$

Cracking moment

$M_{cr} := \frac{I_I \cdot \left(f_{ctm.fl} - \frac{N_{Ed.F}}{A_I}\right)}{h - x_I} = 205.01 \cdot kN \cdot m$

Check if cross section cracks:

$Cross\_section\_Cracks := if(M_{cr} \le M_{Ed.F}, "YES", "NO")$ Cross_section_Cracks = "YES"

Check the crack width:

Cross section in stage II

$w_{k.max} := 0.2mm$ requirement according to TRVFS 2011:12, Ch. 22 Table a.

$$A_{II.eff}(x) := b \cdot x + \alpha_{eff} \cdot A_{s.bot}$$

$$x_{tp}(x) := \frac{\frac{b \cdot x^2}{2} + \alpha_{eff} \cdot A_{s.bot} \cdot d_{bot}}{A_{II.eff}(x)}$$

$$I_{II.eff}(x) := \frac{b \cdot x^3}{12} + b \cdot x \cdot \left(x_{tp}(x) - \frac{x}{2} \right)^2 + \alpha_{eff} \cdot A_{s.bot} \cdot \left(x_{tp}(x) - d_{bot} \right)^2$$

$$\sigma_c\left(x_{II}, z\right) := \frac{N_{Ed.Q}}{A_{II.eff}\left(x_{II}\right)} + \frac{N_{Ed.Q} \cdot \left(\frac{h}{2} - x_{tp}\left(x_{II}\right) \right) + M_{Ed.Q}}{I_{II.eff}\left(x_{II}\right)} \cdot z$$

Guess $x_{II} := 0.1233\,m$

Given

$$\sigma_c\left[x_{II}, \left(x_{II} - x_{tp}\left(x_{II}\right)\right)\right] = 0.127 \cdot MPa$$

$$x := root\left[\sigma_c\left[x_{II}, \left(x_{II} - x_{tp}\left(x_{II}\right)\right)\right], x_{II}\right] = 0.12\,m$$

$$x := if\left(x < 0 \vee x > h, 10^{-6} mm, x\right)$$

$$x = 120.393 \cdot mm$$

$$A_{II.eff}(x) = 0.148\,m^2$$

$$x_{tp}(x) = 0.124\,m$$

$$I_{II.eff}(x) = 2.793 \times 10^{-3}\,m^4$$

Concrete stress in reinforcement level

$$\sigma_{cs} := \sigma_c\left[x, \left(d_{bot} - x_{tp}(x)\right)\right] = 12.537 \cdot MPa$$

Steel stress

$$\sigma_s := \alpha_{eff} \cdot \sigma_{cs} = 163.551 \cdot MPa$$

Effective area of concrete

SS-EN 1992-1-1:2005, Ch. 7.3.2.

$$h_{c.eff} := \min\left[2.5 \cdot \left(h - d_{bot}\right), \frac{h - x}{3}, \frac{h}{2}\right] = 109.869 \cdot mm$$

Effective height of concrete . SS-EN 1992-1-1:2005, Ch. 7.3.2 (3).

$$A_{c.eff} := b \cdot h_{c.eff} = 0.11 \cdot m^2$$

Effective concrete area. SS-EN 1992-1-1:2005, Ch. 7.3.2 (3).

Crack width

$$S_{r.max} := k_3 \cdot c + k_1 \cdot k_2 \cdot k_4 \cdot \frac{\phi_s}{\rho_{p.eff}}$$

Maximum crack spacing.
SS-EN 1992-1-1,
Ch. 7.3.4 Eq. (7.11).

$k_1 := 0.8$

Assume high bond bars.
SS-EN 1992-1-1, Ch. 7.3.4 (3).

$k_2 := 0.5$

Bending. SS-EN 1992-1-1,
Ch. 7.3.4 (3).

$$k_3 := \frac{7 \cdot \phi_{s.bot}}{c_{nom}} = 4.667$$

TRVFS 2011:12, Ch. 21 13§.

$k_4 := 0.425$

SS-EN 1992-1-1, Ch. 7.3.4 (3),
is used according to
TRVFS 2011:12, Ch. 21 13§

$k_t := 0.4$

SS-EN 1992-1-1, Ch. 7.3.4 (2).

$$\rho_{p.eff} := \frac{A_{s.bot}}{A_{c.eff}} = 0.019$$

SS-EN 1992-1-1, Ch. 7.3.4 Eq. (7.10)

$$\Delta\varepsilon_m := \max\left[\frac{\sigma_s - k_t \cdot f_{ctm} \cdot \frac{\left(1 + \alpha_{ef} \cdot \rho_{p.eff}\right)}{\rho_{p.eff}}}{E_s}, 0.6 \cdot \frac{\sigma_s}{E_s}\right]$$

SS-EN 1992-1-1, Ch. 7.3.4
Eq. (7.9).

$$\Delta\varepsilon_m = 4.907 \times 10^{-4}$$

$$S_{r.max} := k_3 \cdot c_{nom} + k_1 \cdot k_2 \cdot k_4 \cdot \frac{\phi_{s.bot}}{\rho_{p.eff}}$$

$S_{r.max} = 0.318\,m$

Crack width

$$w_k := S_{r.max} \cdot \Delta\varepsilon_m = 0.156 \cdot mm$$

$$\eta w := \frac{w_k}{w_{k.max}} = 78 \cdot \%$$

$$Control\_Crack\_width := if(\eta w \le 1, "OK", "Not\ OK")$$

Control_Crack_width = "OK"

B.6.4.3 Deflection Control

The control of deflection due to traffic load is obtained from the characteristic load combination.

The deformation requirement will be checked according to SS-EN 1990.
Since the deflection is linear between the cross section I (conventional concrete) and cross section II (HPC), the deflection of HPC section will be calculated by liner interpolation where the deflection of cross section I will be obtained from case study given from AFRY.
The deflection is checked in the middle of the span where maximum deflection is expected. The deflection is calculated for 1m strip.

Input Data

$L_s := 6600mm$ $f_{ctm} := 5MPa$ $h := 450mm$ $b := 1000mm$ $A_{s.bot} := 2094.4mm^2$

$E_s := 200GPa$ $E_{cm} := 44GPa$ $\alpha_{ef} := \frac{E_s}{E_{cm}} = 4.545$

Characteristic moment from LM71 (train load)

$M_{Ed.ch} := 125.70kN \cdot m$ (Konstructionsberäkningar Bro 100-2990-1, Appendix 4.1.F)

Moment of inertia of the cross section (conventional concrete), Stage II (cracked section)

$I_{Ieff} := 0.01m^4$ (Konstructionsberäkningar Bro 100-2990-1, Appendix 4.1.B)

$E_{cm.I.eff} := 34GPa$ Elastic modulus of concrete C35/45

$E_{cm.II.eff} := 44GPa$ Elastic modulus of concrete C90/105

The maximum allowed vertical deflection due to characteristic traffic load according

$\delta_{max.1} := \frac{L_s}{600} = 11 \cdot mm$ SS-EN 1990 (A2.4.4.3.2)

The maximum allowed vertical deflection due to characteristic traffic load with regard to passenger comfort according to TDOK 2016:204, ch B3.4.2.2.
The design value of train speed for this bridge is 160km/h
The studied bridge is a frame bridge and can be assumed as continuous bridge with minimum 3 spans.

Comfort level is assumed to be (Good)

$b_v := 1.3$ SS-EN 1990, Table (A2.9)

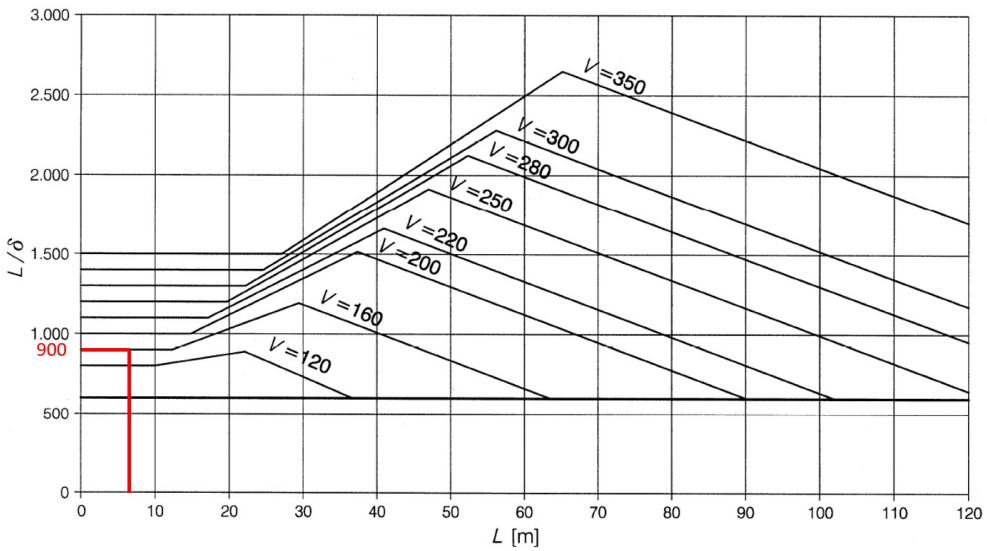

Figure. comfort level according to SS-EN 1990, Figure A2.3

$$\delta_{max} := \frac{L_s}{0.9 \cdot \frac{900}{1.3}} = 10.593 \cdot mm$$

Calculation moment of inertia for the cracked section of cross section II (HPC)

$$A_{II.eff}(x) := b \cdot x + \alpha_{eff} \cdot A_{s.bot}$$

$$x_{tp}(x) := \frac{\frac{b \cdot x^2}{2} + \alpha_{eff} \cdot A_{s.bot} \cdot d_{bot}}{A_{II.eff}(x)}$$

$$I_{II.eff}(x) := \frac{b \cdot x^3}{12} + b \cdot x \cdot \left(x_{tp}(x) - \frac{x}{2} \right)^2 + \alpha_{eff} \cdot A_{s.bot} \cdot \left(x_{tp}(x) - d_{bot} \right)^2$$

$$\sigma_c\left(x_{II}, z\right) := \frac{M_{Ed.ch}}{I_{II.eff}\left(x_{II}\right)} \cdot z$$

Guess $x_{II} := 0.12289m$

Given

$$\sigma_c\left[x_{II}, \left(x_{II} - x_{tp}\left(x_{II}\right)\right)\right] = -0.047 \cdot MPa$$

$$x := root\left[\sigma_c\left[x_{II}, \left(x_{II} - x_{tp}\left(x_{II}\right)\right)\right], x_{II}\right] = 0.124\,m$$

$$x := if\left(x < 0 \vee x > h, 10^{-6} mm, x\right)$$

$$x = 123.931 \cdot mm$$

$$A_{II.eff}(x) = 1.513 \times 10^5 \cdot mm^2$$

$$x_{tp}(x) = 123.931 \cdot mm$$

$I_{II.eff}(x) = 2.793 \times 10^{9} \cdot mm^{4}$ Moment of inertia of the cross section II (HPC)

Maximum characteristic vertical deflection due to Load model 71 (Conventional concrete)

$\delta_I := 1.72mm$ (Konstructionsberäkningar Bro 100-2990-1, Appendix 4.3)

$$\delta_{II} := \delta_I \cdot \frac{E_{cm.II.eff} \cdot I_{II.eff}(x)}{I_{Ieff} \cdot E_{cm.I.eff}} = 0.622 \cdot mm$$

Utilization ration of deflection

$$\eta_\delta := \frac{\delta_{II}}{\delta_{max}} = 5.869 \cdot \%$$ OK

B.6.4.6 Amount of concrete

$h = 450 \cdot mm$

$b_{tot} := 7670mm$

$$\rho_c = 25 \cdot \frac{kN}{m^3}$$

$$m_c := h \cdot b_{tot} \cdot \left(\rho_c - 1 \frac{kN}{m^3} \right) \cdot \frac{1}{9.81N} \cdot kg \qquad m_c = 8444.037 \frac{kg}{m}$$

Appendix C- Case 3:
Design the bridge with UHPC C200/215

C.1 Geometry

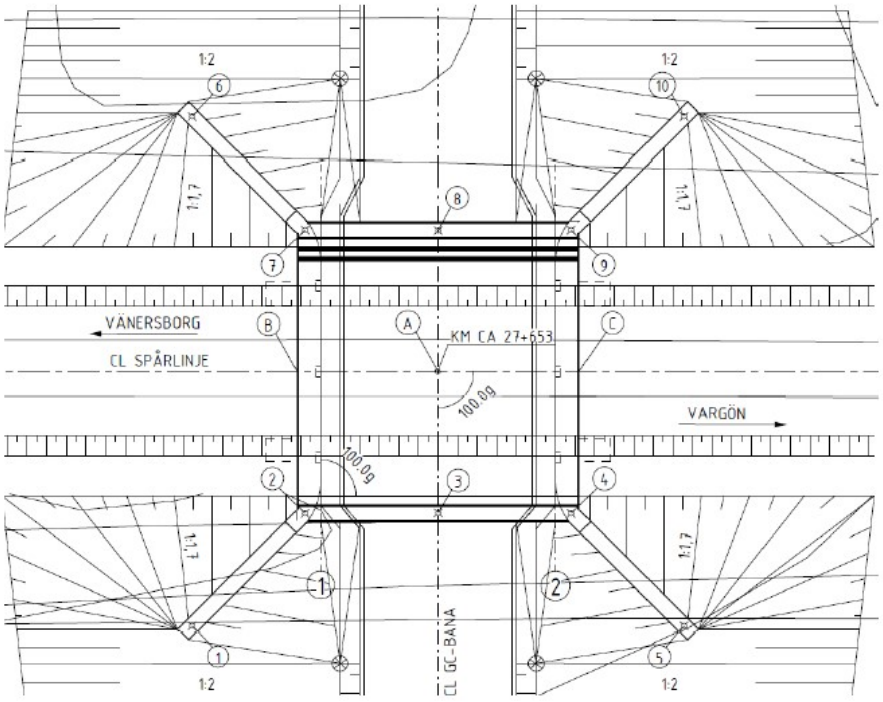

Figure Bridge plan

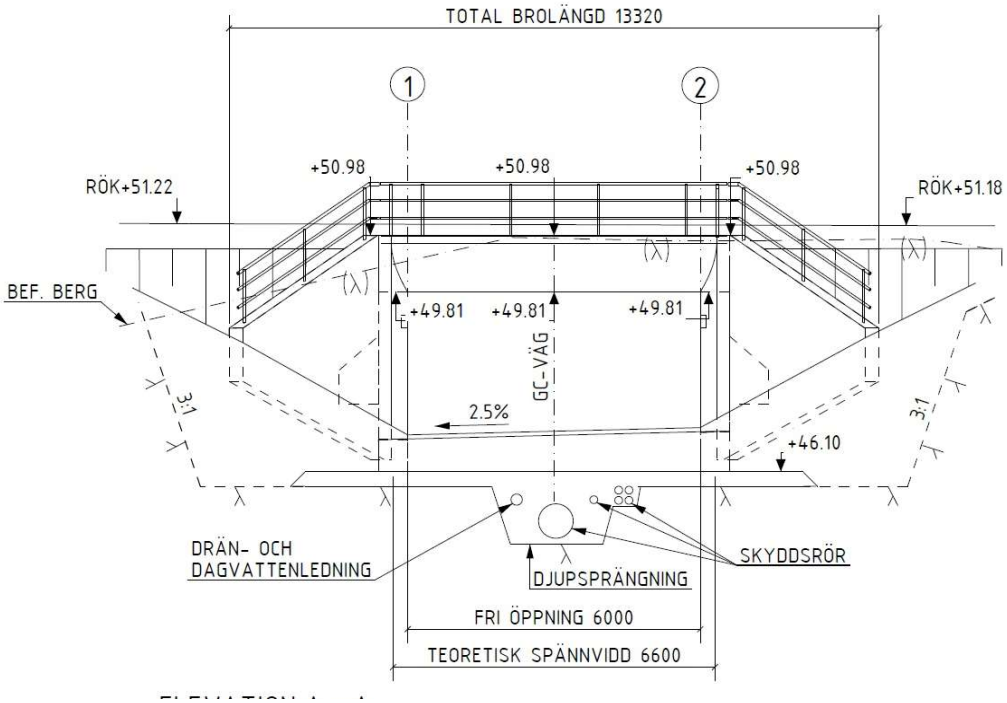

Figure Elevation

The bridge type is concrete frame bridge made from ultra high performance concrete C90/105

Dimensions

Free span 6000mm
Theoretical span
6600mm
Bridge width 7210mm
Thickness is varying between 565mm-600mm

$h := 600mm$ which is the original high

C.2 Calculation conditions

Service life: L100 (120 years)
For the bridge deck a safety class 3 is chosen. (VVFS 2004:31 and VVFS 2004:43).

Exposure classes according SS-EN 1992-1-1:2005

Construction part	Exposure class	Service life	Concrete cover[mm]	W.k[mm]	Max w/c
Bridge deck, top	XD1/XF4	L100	30	0.3	0.3
Bridge deck, botton	XC4/XF3	L100	30	0.2	0.35

C.3 Concrete cover

Concrete cover is calculated according to TRVFS 2011:12, Ch. 21 Table a:

C.3.1 Bottom

Longitudinal reinforcement diameter

$\phi_{s.bot} := 20mm$

Stirrups diameter

$\phi_{stirup} := 12mm$

$\Delta c_{dev} := 10mm$ SS-EN 1992-1-1:2005, ch.4.4.1.3

$\Delta c_{dur.st} := 0mm$ SS-EN 1992-1-1:2005, ch. 4.4.1.2.

$\Delta c_{dur.add} := 0mm$ SS-EN 1992-1-1:2005, ch. 4.4.1.2.

$\Delta c_{dur.\gamma} := 0mm$ SS-EN 1992-1-1:2005, ch. 4.4.1.2.

$c_{min.b} := \phi_{s.bot}$ SS-EN 1992-1-1:2005, ch. 4.4.1.2. table 4.2.

$c_{min.dur} := 20mm$ TRAV2011-12, table a, page 38

length of the longest fibres,

$L_f := 15mm$ NF P18-710 (2016),Table T.1,Annex T.

$D_{sup} := 0.5mm$ The nominal upper dimension of the largest aggregate Ch. 5.4.3 of standard NF P18-470.

$c_{min.p} := \max\left(1.5 \cdot L_f, 1.5 \cdot D_{sup}, \phi_{s.bot}\right) = 22.5 \cdot mm$

$c_{min} := \max\left(c_{min.b}, c_{min.dur} + \Delta c_{dur.\gamma} - \Delta c_{dur.st} - \Delta c_{dur.add}, c_{min.p}, 10mm\right)$

$c_{min} = 22.5 \cdot mm$

$c_{nom} := c_{min} + \Delta c_{dev}$ SS-EN 1992-1-1:2005, ch. 4.4.1.1. eq.(4.1)

Concrete cover bottom

$c_{nom} = 32.5 \cdot mm$

$d'_{bot} := c_{nom} + \frac{1}{2} \cdot \phi_{s.bot} + \phi_{stirup} = 54.5 \cdot mm$

$d_{bot} := h - d'_{bot} = 545.5 \cdot mm$

C.3.2 Top

$\phi_{s.top} := 16mm$

$c_{min.b} := \phi_{s.top}$ SS-EN 1992-1-1:2005, ch. 4.4.1.2. Table 4.2

$c_{min.dur} := 20mm$ TRAV2011-12, Table A

$c_{min.p} := \max\left(1.5 \cdot L_f, 1.5 \cdot D_{sup}, \phi_{s.top}\right) = 22.5 \cdot mm$

$c_{min} := \max\left(c_{min.b}, c_{min.dur} + \Delta c_{dur.\gamma} - \Delta c_{dur.st} - \Delta c_{dur.add}, c_{min.p}, 10mm\right)$

$c_{nom} := c_{min} + \Delta c_{dev}$

$c_{nom} = 32.5 \cdot mm$

$d'_{top} := c_{nom} + \frac{1}{2} \cdot \phi_{s.top} + \phi_{stirup} = 52.5 \cdot mm$

$d_{top} := h - d'_{top} = 547.5 \cdot mm$

C.4 Material properties

C.4.1 Concrete

C200/215 — Values are taken from NF P18-710 (2016),Table T.1,Annex T.

$f_{ck} := 200MPa$ — Characteristic compressive strength. NF P18-710 (2016),Table T.1, Annex T.

$f_{cm} := 230MPa$ — Mean compressive strength. NF P18-710 (2016),Table T.1,Annex T.

$f_{ctk.el} := 10MPa$ — Characteristic tensile strength. NF P18-710 (2016),Table T.1,Annex T.

$f_{ctm.el} := 12MPa$ — Mean tensile strength

$f_{ctfk} := 10MPa$ — Characteristic post-cracking strength

$f_{ctfm} := 12MPa$ — Mean post-cracking strength

$K_{global} := 1.25$ — Global fibre orientation factor

$K_{local} := 1.75$ — Local fibre orientation factor

$L_f = 0.015\,m$ — Length of fibers

$E_{cm} := 65GPa$ — Modulus of elasticity.

$\varphi_{ef} := 1$ — Creep coefficient, SS-EN 1992-1-1, 2005.figure 3.1

C.4.2 Steel K500C-T

$f_{yk} := 500MPa$ — Characteristic value for the yield strength of the reinforcement.

$E_s := 200GPa$ — Steel modulus of elasticity. SS-EN 1992-1-1,2005.

$\rho_s := 78.5\frac{kN}{m^3}$ — Density of steel. SS-EN 1991-1-1:2002,Table A.4.

$\varepsilon_{uk} := 7.5\%$ — Characteristic ultimate strain of reinforcement. SS-EN 1992-1-1:2005, Annex C Table C.1.

C.4.3 Strength

UHPC

Compressive strength

Partial factor for compressed concrete in ULS

$\gamma_{cf} := 1.3$

SS-EN 1992-1-1:2005, Ch. 2.4.2.4 Table 2.1N

Partial factor for tensioned UHPFRC in ULS.

$\gamma_c := 1.5$

coefficient which takes account of long-term effects

$\alpha_{cc} := 0.85$

NF P18-710 (2016),Ch.3.1.6.

$$f_{cd} := \frac{\alpha_{cc} \cdot f_{ck}}{\gamma_c} = 113.333 \cdot MPa$$

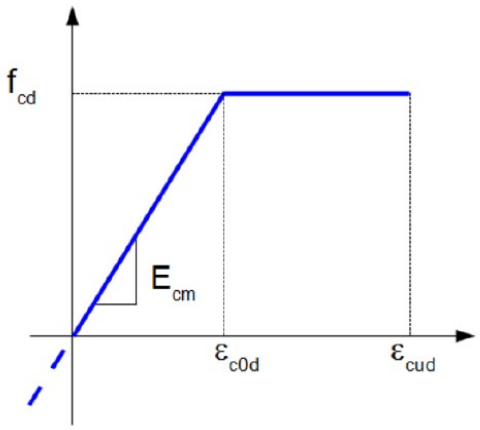

Figure Representation of the stress-strain relation of UHPFRC in compression for designs at ULS

Maximum design elastic shortingin strain at ULS

$$\varepsilon_{c0d} := \frac{f_{cd}}{E_{cm}} = 1.744 \times 10^{-3}$$

NF P18-710 (2016), Ch. 3.1.7 Eq. (3.9)

$\varepsilon_{c0d} = 0.174 \cdot \%$

Maximum design shorting in strain at ULS

$$\varepsilon_{cud} := \left(1 + 14 \cdot \frac{f_{ctfm}}{K_{global} \cdot f_{cm}}\right) \varepsilon_{c0d}$$

NF P18-710 (2016), Ch. 3.1.7 Eq. (3.208)

$\varepsilon_{cud} = 0.002762$

Tensile strength

NF P18-710 (2016), Ch 3.1.7.3

$$\text{Tensile\_CLass} := \begin{cases} \text{"T3"} & \text{if } \dfrac{f_{ctfm}}{K_{global}} \geq f_{ctm.el} \text{ and } \dfrac{f_{ctfk}}{K_{global}} < f_{ctk.el} \\ \text{"T2"} & \text{if } \dfrac{f_{ctfm}}{K_{global}} \geq f_{ctm.el} \text{ and } \dfrac{f_{ctfk}}{K_{global}} \geq f_{ctk.el} \\ \text{"T1"} & \text{otherwise} \end{cases}$$

Tensile_CLass = "T3"

$$\text{Controll\_slenderness} := \begin{cases} \text{"Thick"} & \text{if } h \geq 3 \cdot L_f \\ \text{"Thin"} & \text{otherwise} \end{cases}$$

NF P18-710 (2016), Ch 3.1.7.3

Controll_slenderness = "Thick"

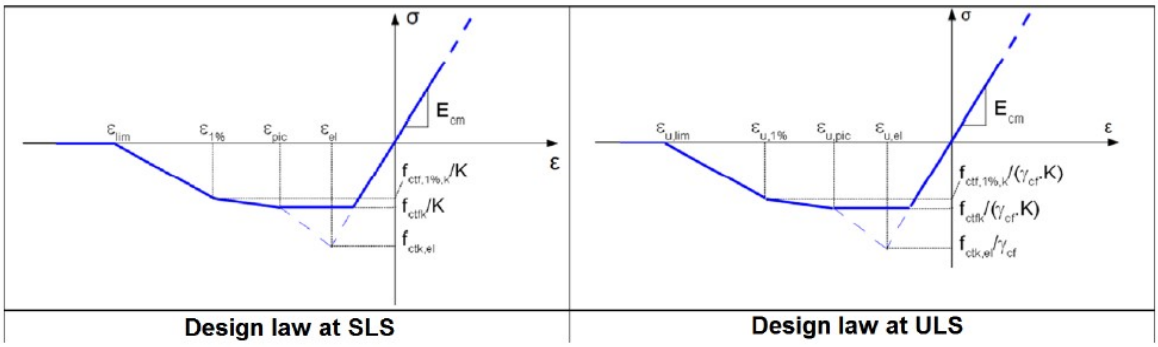

Figure Conventional law for UHPFRCs of class T2 (from σ(w) curve)

ULS

Tensile limit of elasticity design value

$$f_{ctd.el} := \frac{f_{ctk.el}}{\gamma_{cf}} = 7.692 \times 10^6\,\text{Pa}$$

NF P18-710 (2016), Chapter 3.1.7.3.2

Elastic tensile strain at ULS

$$\varepsilon_{u.el} := \frac{f_{ctd.el}}{E_{cm}} = 0.012 \cdot \%$$

NF P18-710 (2016), Chapter 3.1.7.3.2

Post-cracking strength (Design value)

$$f_{ctfd} := \frac{f_{ctfk}}{\gamma_{cf} \cdot K_{global}} = 6.154 \times 10^6\,\text{Pa}$$

NF P18-710 (2016), Chapter 3.1.7.3.2

Characteristic length which relates the crack width to an equivalent deformation where h is the height of the section

$$L_c := \frac{2 \cdot h}{3} = 400 \cdot \text{mm}$$

tensile strain limit beyond which the participation of the fibres is no longer taken into account at the ultimate limit state

$$\varepsilon_{u.lim} := \frac{L_f}{4 \cdot L_c} = 0.938 \cdot \%$$

NF P18-710 (2016), Ch 3.1.7.3

Steel

$$\gamma_s := 1.15$$

Reinforcement partial factor in ULS,SS-EN 1992-1-1, Table 2.1.

$$f_{yd} := \frac{f_{yk}}{\gamma_s} = 434.783 \cdot \text{MPa}$$

$$\varepsilon_{sy} := \frac{f_{yd}}{E_s} = 2.174 \times 10^{-3}$$

$$\varepsilon_{ud} := 0.9 \cdot \varepsilon_{uk} = 6.75 \cdot \%$$

$$\alpha_{ef} := \frac{E_s}{E_{cm}} = 3.077$$

Ratio between steel modulus of elasticity and concrete modulus of elasticity

C.5 Scenario 1

Calculation of moment resistance for bottom reinforcement $M_{Rd,max}$ (Bottom)

Cross section at x=3600mm

Input

The moment and its normal force are changed in this cas due to chanting of UHPC density, a new M_{Ed} and N_{Ed} are calculated for UHPC.

New moment due to changing of UHPC self-weight

cross-section at x=3.6m

Max design moment value of applied load, obtained from ULS load combination for conventional concrete's cross section (bottom)

$M_{Ed.con.max.uls} := 366kN \cdot m$ (Constructions Bro 100-2990-1, Appendix 4.1.B)

Minimum design moment value of applied load, obtained from ULS load combination for conventional concrete's cross section (Top)

$M_{Ed.con.min.uls} := 42.1kN \cdot m$ (Konstructionsberäkningar Bro 100-2990-1, Appendix 4.1.B)

Moment due to self-weight of conventional concrete's cross section characteristic value

$M_{Ed.sw.conv} := 40.9kN \cdot m$

$h := 600mm$ Height of conventional concrete cross section (original height)

$\rho_c := 25 \frac{kN}{m^3}$ density of conventional concrete

$\rho_{UHPC} := 24.4 \frac{kN}{m^3}$

$G_{s.con} := \rho_c \cdot h = 15 \cdot \frac{kN}{m^2}$ Self-weight of conventional cross section

$G_{s.UHPC} := h \cdot \rho_{UHPC} = 14.64 \cdot \frac{kN}{m^2}$ Self-weight of UHPC cross section

$M_{Ed.sw.uhpc} := \frac{G_{s.UHPC}}{G_{s.con}} \cdot M_{Ed.sw.conv}$ Moment due to self-weight of UHPC cross section

$M_{Ed.sw.uhpc} = 39.918 \cdot kN \cdot m$ Moment due to self-weight of UHPC cross section

$M_{Ed.max} := M_{Ed.con.max.uls} - \left(1.35M_{Ed.sw.conv}\right) + 1.35M_{Ed.sw.uhpc} = 364.675 \cdot kN \cdot m$

$M_{Ed.min} := M_{Ed.con.min.uls} - \left(1.35M_{Ed.sw.conv}\right) + 1.35M_{Ed.sw.uhpc} = 40.775 \cdot kN \cdot m$

$M_{Ed.max} = 364.675 \cdot kN \cdot m$

$N_{Ed.max} := -28.4kN$

(Konstructionsberäkningar Bro 100-2990-1, Appendix 4.1.B)

$A_{s.bot} := 2094.4mm^2$

$b := 1000mm$ $h := 600mm$ $d_{bot} = 545.5 \cdot mm$ $d'_{bot} = 54.5 \cdot mm$

Calculation of compressive zone

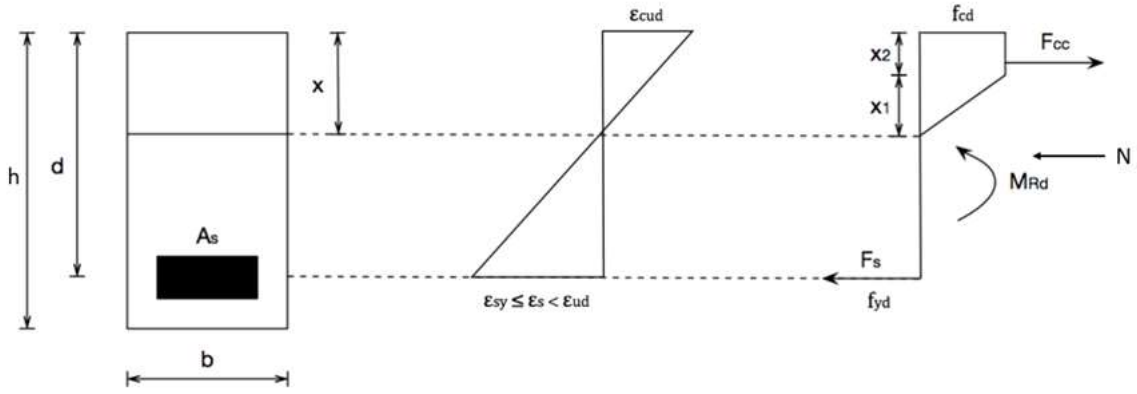

Figure Stress-strain relation with section forces for the cross-section

$x_{bot} := 12.1101009mm$ Assumed compressive depth.

$\varepsilon_{cud} = 0.276 \cdot \%$ Assume that the compressive strain reachs ultimate design strain

$$F_c := f_{cd} \cdot \left[\frac{\left(\frac{\varepsilon_{c0d}}{2}\right) + \left(\varepsilon_{cud} - \varepsilon_{c0d}\right)}{\varepsilon_{cud}}\right] \cdot x_{bot} \cdot b$$

Compressive force of UHPFRC

$F_c = 939.341 \cdot kN$

$$x_1 := \frac{\varepsilon_{c0d}}{\varepsilon_{cud}} \cdot x_{bot}$$

NF P18-710 (2016), Chapter 6.1

$x_1 = 7.644 \cdot mm$

$x_2 := x_{bot} - x_1 = 4.467 \cdot mm$

$$x_c := \frac{\left(\frac{x_1 \cdot 2}{3}\right) \cdot \frac{x_1}{2} + \left(x_1 + \frac{x_2}{2}\right) \cdot x_2}{\frac{x_1}{2} + x_2}$$

$x_c = 7.672 \cdot mm$

Reinforcement

$F_{s.bot} := f_{yd} \cdot A_{s.bot}$

$F_{s.bot} = 910.609 \cdot kN$ Force of the reinforcement

$x_{s.bot} := d_{bot} - x_{bot}$

$x_{s.bot} = 533.39 \cdot mm$ Lever arm to the neutral axis of steel force

Horizontal equilibrium

$F_c - F_{s.bot} + N_{Ed.max} = 0.333 \cdot kN$ Close to Zero

Assume yielding $\varepsilon_{s.bot} > \varepsilon_{sy}$

$$\varepsilon_{s.bot} := \text{if}\left(x_{bot} > 0, \frac{d_{bot} - x_{bot}}{x_{bot}} \cdot \varepsilon_{cud}, \varepsilon_{sy}\right) = 0.1217$$ Elongation in the reinforcement

$Kontroll_{\varepsilon.s.bot} := \text{if}\left(\varepsilon_{s.bot} > \varepsilon_{sy}, \text{"OK"}, \text{"Not OK"}\right)$

$Kontroll_{\varepsilon.s.bot} = \text{"OK"}$

Con troll of strain limit in reinforcement

$$Control\_Strain := \begin{cases} \text{"Normal reinforced"} & \text{if } \varepsilon_{sy} < \varepsilon_{s.bot} < \varepsilon_{ud} \\ \text{"Not normal Reinforced"} & \text{otherwise} \end{cases}$$

$Control\_Strain = \text{"Not normal Reinforced"}$

$$M_{Rd.bot} := F_c \cdot x_c + F_{s.bot} \cdot x_{s.bot} - N_{Ed.max} \cdot \left(\frac{h}{2} - x_{bot}\right)$$

$M_{Rd.bot} = 501.092 \cdot kN \cdot m$

Check moment capacity

$$\eta_{bot} := \frac{M_{Ed.max}}{M_{Rd.bot}} = 72.776 \cdot \%$$

Ductility

$$xd_{bot} := \frac{x_{bot}}{d_{bot}} = 0.022$$

C.5.2 Calculation of moment resistance for top reinforcement MRd, top

Input

$M_{Ed.min} = 40.775 \cdot kN \cdot m$

$N_{Ed.min} := -260.5kN$ (Konstructionsberäkningar Bro 100-2990-1, Appendix 4.1.B)

$A_{s.top} := 1340.4mm^2$ (Konstructionsberäkningar Bro 100-2990-1, Appendix 4.1.B)

$d_{top} = 547.5 \cdot mm$ $d'_{top} = 52.5 \cdot mm$

Calculation of compressive zone

$x_{top} := 10.8717mm$ Assumed compressive depth.

$\varepsilon_{cud} = 0.276 \cdot \%$ Assume that the compressive strain reachs ultimate design strain

$$F_c := f_{cd} \cdot \left[\frac{\left(\frac{\varepsilon_{c0d}}{2} \right) + \left(\varepsilon_{cud} - \varepsilon_{c0d} \right)}{\varepsilon_{cud}} \right] \cdot x_{top} \cdot b$$

$F_c = 843.283 \cdot kN$

$$x_1 := \frac{\varepsilon_{c0d}}{\varepsilon_{cud}} \cdot x_{top} \qquad x_1 = 6.862 \cdot mm$$

$x_2 := x_{top} - x_1 = 4.01 \cdot mm$

$$x_c := \frac{\left(\frac{x_1 \cdot 2}{3} \right) \cdot \frac{x_1}{2} + \left(x_1 + \frac{x_2}{2} \right) \cdot x_2}{\frac{x_1}{2} + x_2}$$

$x_c = 6.888 \cdot mm$

Reinforcement

$F_{s.top} := f_{yd} \cdot A_{s.top}$

$F_{s.top} = 582.783 \cdot kN$ Force of the reinforcement

$x_{s.top} := d_{top} - x_{top}$

$x_{s.top} = 536.628 \cdot mm$ Lever arm to the neutral axis of steel force

Horizontal equilibrium

$F_c - F_{s.top} + N_{Ed.min} = 0.115 \cdot N$ Close to Zero

Assume yielding $\varepsilon_{s.top} > \varepsilon_{sy}$

$$\varepsilon_{s.top} := \text{if}\left(x_{top} > 0, \frac{d_{top} - x_{top}}{x_{top}} \cdot \varepsilon_{cud}, \varepsilon_{sy}\right) = 13.6355 \cdot \%$$

$$\text{Kontroll}_{\varepsilon.s.top} := \text{if}\left(\varepsilon_{s.top} > \varepsilon_{sy}, \text{"OK"}, \text{"Not OK"}\right)$$

$\text{Kontroll}_{\varepsilon.s.top} = \text{"OK"}$

Con troll of strain limit in reinforcement

$$\text{Control\_Strain} := \begin{cases} \text{"Normal reinforced"} & \text{if } \varepsilon_{sy} < \varepsilon_{s.top} < \varepsilon_{ud} \\ \text{"Not Normal Reinforced"} & \text{otherwise} \end{cases}$$

$\text{Control\_Strain} = \text{"Not Normal Reinforced"}$

$$M_{Rd.top} := F_c \cdot x_c + F_{s.top} \cdot x_{s.top} - N_{Ed.min} \cdot \left(\frac{h}{2} - x_{top}\right)$$

$M_{Rd.top} = 393.864 \cdot kN \cdot m$

Check moment capacity

$$\eta_{bot} := \frac{M_{Ed.min}}{M_{Rd.top}} = 10.353 \cdot \%$$

$$xd_{top} := \frac{x_{top}}{d_{top}} = 0.02$$

Ductility

$xd_{max} := 0.3$ According to SS-EN 1992-2:2005 section 5.6.3 , $\frac{x}{d}$ should not be larger than 0.3

$$\eta_{xd} := \frac{\max\left(xd_{top}, xd_{bot}\right)}{xd_{max}} = 7 \cdot \%$$ Ductility

C.5.3 Shear reinforcement

Shear force must always be checked against the shear capacity or shear stress capacity of the section. But according to SS-EN 1992-1-1:2005, Ch. 6.2.1. Shear force have not to be checked at distance less than d from the support when a uniformly distributed load is applied on the member. The shear force depends on the support conditions of the beam and the location of the load on the member. The first axle force is located at a distance d from the support, while the shear reinforcement is designed for the shear force at the support because the shear force is maximum.

In this case the shear reinforcement is designed at x= 1200mm.

ULS new Shear for optimized cross section in UHPC

(Konstructionsberäkningar Bro 100-2990-1, Appendix 4.1.B)

$V_{Ed.conv} := 555.9kN$

$L := 6000mm$

$\rho_c = 25 \cdot \frac{kN}{m^3}$ Density of NC

$\rho_{UHPC} = 24.4 \cdot \frac{kN}{m^3}$ Density of UHPC

$h_1 := 579mm$ Height of conventional concrete cross section (original height)

$b := 1000mm$

$q_c := h_1 \cdot \rho_{UHPC} = 14.128 \cdot \frac{kN}{m^2}$ Load coming from UHPC

$V_c := \frac{q_c \cdot L \cdot b}{2} = 42.383 \cdot kN$ Shear force from UHPC

$q_{c1} := h_1 \cdot \rho_c = 1.447 \times 10^4 Pa$ Load coming from conventional concrete

$V_{c.1} := \frac{q_{c1} \cdot L \cdot b}{2} = 43.425 \cdot kN$ Shear coming from conventional concrete

$V_{Ed.ULS.max} := \left[V_{Ed.conv} - \left(V_{c.1} \cdot 1.35\right)\right] + V_c \cdot 1.35 = 554.493 \cdot kN$ New shear force of UHPC cross section

Input:

$V_{Ed} := V_{Ed.ULS.max} = 554.493 \cdot kN$ $N_{Ed} := 231kN$ (compression)

$h = 600 \cdot mm$ $b_w := 1m$ $d_{bot} = 545.5 \cdot mm$ $A_{sl} := 3272.5mm^2$ $f_{yd} = 434.783 \cdot MPa$

$f_{ck} = 200 \cdot MPa$

$f_{ctfd} = 6.154 \cdot MPa$ Design post-cracking strength

$f_{ctd.el.SLS} := f_{ctk.el} = 10 \cdot MPa$ Design tensile limit of elasticity,

$\varepsilon_{el} := \frac{f_{ctd.el.SLS}}{E_{cm}}$ $\varepsilon_{el} = 0.000154$ Strain at the maximum limit of elasticity

$\varepsilon_{u.lim} = 0.009375$ Ultimate strain in tension

Calculation of $V_{Rd.c}$

$\gamma_E := 1.1538$

$\gamma_{cf} \cdot \gamma_E = 1.5$ NF P18-710 (2016), Ch 6.2

$\sigma_{cp} := \frac{N_{Ed}}{h \cdot b} = 0.385 \cdot MPa$

$Control_{\sigma.cp} := if\left(0 \le \sigma_{cp} \le 0.4 \cdot f_{ck}, "OK", "Not\ OK"\right)$ NF P18-710 (2016), Ch 6.2

$Control_{\sigma.cp} = "OK"$

$k := 1 + 3 \cdot \frac{\sigma_{cp}}{f_{ck}}$

$V_{Rd.c} := \frac{0.18}{\left(\gamma_{cf} \cdot \gamma_E\right)} \cdot k \cdot \left(\frac{f_{ck}}{MPa}\right)^{\frac{1}{2}} \cdot MPa \cdot b \cdot h$ UHPC contribution term $V_{Rd.c} = 1.024 \times 10^3 \cdot kN$

Calculation of $V_{Rd.s}$

Assume no shear reinforcement

$V_{Rd.s} := 0$

Calculation of $V_{Rd.f}$

$d := \frac{7}{8} \cdot h$

lever arm of the internal forces

$z := 0.9 \cdot d$ $z = 472.5 \cdot mm$ NF-P-18-710 Eq (6.203)

$A_{fv} := b \cdot z = 0.473\,m^2$ For a rectangular section NF-P-18-710 Eq (6.203)

$\varepsilon := \varepsilon_{u.lim} = 0.938 \cdot \%$ NF-P-18-710 Eq (6.214)

$\varepsilon_{ud} = 0.068$ $\varepsilon_{u.lim} = 0.938 \cdot \%$

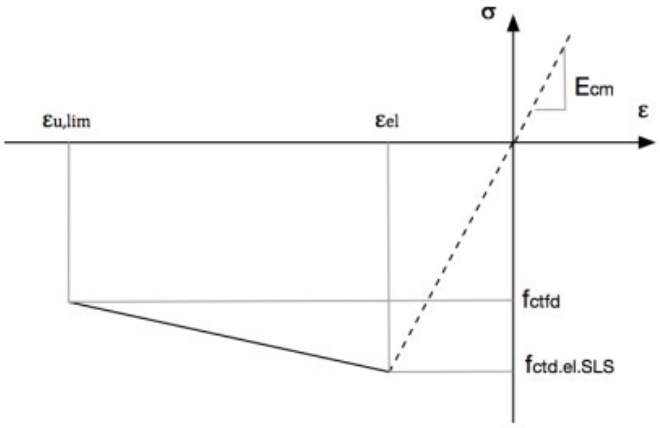

Figure Law for UHPFRCs of class T3

$$\sigma_{Rd.f} := \frac{1}{K_{global}\cdot\gamma_{cf}}\cdot\frac{1}{\varepsilon-\varepsilon_{el}}\cdot\int_{\varepsilon_{el}}^{\varepsilon}\sigma_f(\varepsilon)\,d\varepsilon$$

NF-P-18-710 Eq (6.214)

$$\int_{\varepsilon_{el}}^{\varepsilon}\sigma_f(\varepsilon)\,d\varepsilon := f_{ctfd}\cdot\left(\frac{\varepsilon_{u.lim}-\varepsilon_{el}}{\varepsilon_{u.lim}}\right)+\left(f_{ctd.el.SLS}-f_{ctfd}\right)\cdot\left(\frac{\varepsilon_{u.lim}-\varepsilon_{el}}{2\varepsilon_{u.lim}}\right)$$

$$f_{ctfd}\cdot\left(\frac{\varepsilon_{u.lim}-\varepsilon_{el}}{\varepsilon_{u.lim}}\right)+\left(f_{ctd.el.SLS}-f_{ctfd}\right)\cdot\left(\frac{\varepsilon_{u.lim}-\varepsilon_{el}}{2\varepsilon_{u.lim}}\right) = 7.944\cdot MPa$$

$$\sigma_{Rd.f} := \frac{1}{K_{global}\cdot\gamma_{cf}}\cdot\frac{1}{\frac{(\varepsilon-\varepsilon_{el})}{\%}}\cdot\left[f_{ctfd}\cdot\left(\frac{\varepsilon_{ud}-\varepsilon_{el}}{\varepsilon_{ud}}\right)+\left(f_{ctd.el.SLS}-f_{ctfd}\right)\cdot\left(\frac{\varepsilon_{ud}-\varepsilon_{el}}{2\varepsilon_{ud}}\right)\right]$$

$\sigma_{Rd.f} = 5.378\cdot MPa$

Inclination of the main compression stress on the longitudinal axis

$\theta := 30°$

NF-P-18-710 Eq (6.208)

$V_{Rd.f} := A_{fv}\cdot\sigma_{Rd.f}\cdot\cot(\theta)$ Shear resistance from fibres $V_{Rd.f} = 4401.278\cdot kN$

Total shear resistance

$V_{Rd} := V_{Rd.c} + V_{Rd.s} + V_{Rd.f}$

$V_{Rd} = 5425.433\cdot kN$

Calculation of $V_{Rd.max}$

$$V_{Rd.max} := 2.3\cdot b\cdot z\cdot\left(\frac{f_{ck}}{MPa}\right)^{\frac{2}{3}}\cdot MPa\cdot\tan(\theta)$$

NF-P-18-710 Eq (6.215)

$V_{Rd.max} = 21457.989 \cdot kN$

Design of shear force resistance

$V_{Rd} := \min(V_{Rd.max}, V_{Rd})$

$V_{Rd} = 5425.433 \cdot kN$

Control_Shear := if$(V_{Rd} > V_{Ed}$, "Sufficient capacity" , "NOT Sufficient cappacity"$)$

Control_Shear = "Sufficient capacity"

$\eta_{Shear} := \frac{V_{Ed}}{V_{Rd}} = 10 \cdot \%$

NO shear reinforcement needed.

C.6 Scenario 2

The cross section is optimized by reducing the thickness and making required controls in ULS and SLS. The amount of reinforcement is unchanged (same reinforcement amount used in provided bridge input).

New thickness is assumed to be 450mm, a new design value of the applied internal bending moment (M_{Ed}) is obtained due to reduction of the thickness where a new design moment of self-weight is considered.

ULS new moment for optimized cross section in UHPC

cross-section at x=3.6m

Max design moment value of applied load, obtained from ULS load combination for conventional concrete's cross section (bottom)

$M_{Ed.con.max.uls} := 366kN \cdot m$ (Konstructionsberäkningar Bro 100-2990-1, Appendix 4.1.B)

Minimum design moment value of applied load, obtained from ULS load combination for conventional concrete's cross section (Top)

$M_{Ed.con.min.uls} := 42.1kN \cdot m$ (Konstructionsberäkningar Bro 100-2990-1, Appendix 4.1.B)

Moment due to self-weight of conventional concrete's cross section characteristic value

$M_{Ed.sw.conv} := 40.9kN \cdot m$

$h_{conv} := 600mm$ Height of conventional concrete cross section (original height)

$h_{uhpc} := 365mm$ Height of UHPC cross section (assumed)

$\rho_{c} := 25 \frac{kN}{m^3}$ density of conventional concrete

$\rho_{UHPC} := 24.4 \frac{kN}{m^3}$

$G_{s.con} := \rho_c \cdot h_{conv} = 15 \cdot \frac{kN}{m^2}$ Self-weight of conventional cross section

$G_{s.UHPC} := h_{uhpc} \cdot \rho_{UHPC} = 8.906 \cdot \frac{kN}{m^2}$ Self-weight of UHPC cross section

$M_{Ed.sw.uhpc} := \frac{G_{s.UHPC}}{G_{s.con}} \cdot M_{Ed.sw.conv}$ Moment due to self-weight of UHPC cross section

$M_{Ed.sw.uhpc} = 24.284 \cdot kN \cdot m$ Moment due to self-weight of UHPC cross section

$M_{Ed.max} := M_{Ed.con.max.uls} - \left(1.35 M_{Ed.sw.conv}\right) + 1.35 M_{Ed.sw.uhpc} = 343.568 \cdot kN \cdot m$

$M_{Ed.min} := M_{Ed.con.min.uls} - \left(1.35 M_{Ed.sw.conv}\right) + 1.35 M_{Ed.sw.uhpc} = 19.668 \cdot kN \cdot m$

C.6.1 Calculation of moment resistance for bottom edge MRd,max (Bottom)

Step 2 (ULS)

Input

$b := 1000mm$ $h := h_{uhpc} = 365 \cdot mm$ $N_{Ed.max} := -28.4kN$ $M_{Ed.max} = 343.568\ m \cdot kN$

$d'_{bot} := c_{nom} + \frac{1}{2} \cdot \phi_{s.bot} + \phi_{stirup} = 54.5 \cdot mm$ $d'_{bot} = 54.5 \cdot mm$ $A_{s.bot} := 3200mm^2$ Increased

$d_{bot} := h - d'_{bot} = 310.5 \cdot mm$ $d_{bot} = 310.5 \cdot mm$

Calculation of compressive zone

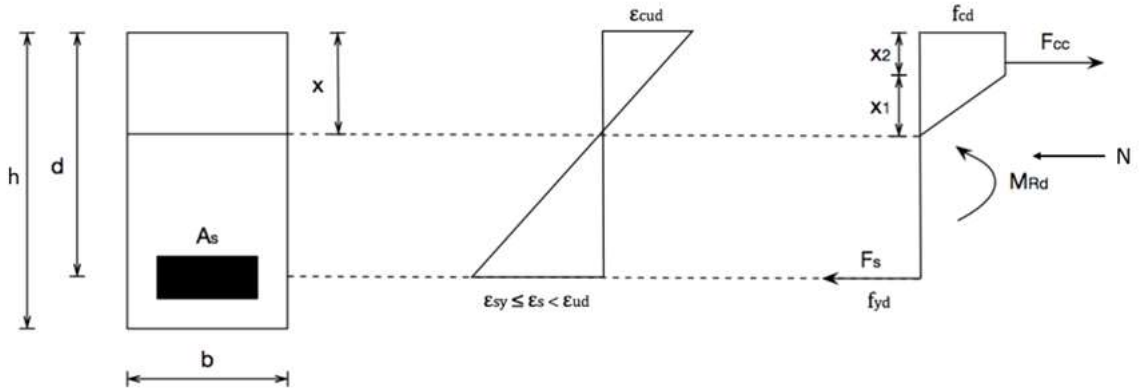

Figure Stress-strain relation with section forces for the cross-section

$x_{bot} := 18.303mm$ Assumed compressive depth.

$\varepsilon_{cud} = 0.002762$ Assume that the compressive strain reachs ultimate design strain

$$F_c := f_{cd} \cdot \left[\frac{\left(\frac{\varepsilon_{c0d}}{2}\right) + \left(\varepsilon_{cud} - \varepsilon_{c0d}\right)}{\varepsilon_{cud}} \right] \cdot x_{bot} \cdot b$$

$F_c = 1.42 \times 10^3 \cdot kN$

$x_1 := \frac{\varepsilon_{c0d}}{\varepsilon_{cud}} \cdot x_{bot}$ $x_1 = 11.552 \cdot mm$

$x_2 := x_{bot} - x_1 = 6.751 \cdot mm$

$$x_c := \frac{\left(\frac{x_1 \cdot 2}{3}\right) \cdot \frac{x_1}{2} + \left(x_1 + \frac{x_2}{2}\right) \cdot x_2}{\frac{x_1}{2} + x_2}$$

$x_c = 6.888 \cdot mm$

Reinforcement

$F_{s.bot} := f_{yd} \cdot A_{s.bot}$

$F_{s.bot} = 1.391 \times 10^{3} \cdot kN$ Force of the reinforcement

$x_{s.bot} := d_{bot} - x_{bot}$

$x_{s.bot} = 292.197 \cdot mm$ Lever arm to the neutral axis of steel force

Horizontal equilibrium

$F_c - F_{s.bot} + N_{Ed.max} = 0.361 \cdot N$ Close to Zero

Assume yielding $\varepsilon_{s.bot} > \varepsilon_{sy}$

$$\varepsilon_{s.bot} := if\left(x_{bot} > 0, \frac{d_{bot} - x_{bot}}{x_{bot}} \cdot \varepsilon_{cud}, \varepsilon_{sy}\right) = 0.0441$$

Elongation in the reinforcement

$Kontroll_{\varepsilon.s.bot} := if\left(\varepsilon_{s.bot} > \varepsilon_{sy}, "OK", "Not\ OK"\right)$ $\varepsilon_{sy} = 2.174 \times 10^{-3}$

$Kontroll_{\varepsilon.s.bot} = "OK"$

Con troll of strain limit in reinforcement

$$Control\_Strain := \begin{cases} "Normal\ reinforced" & if\ \varepsilon_{sy} < \varepsilon_{s.bot} < \varepsilon_{ud} \\ "Over\ Reinforced" & otherwise \end{cases}$$

$h = 365 \cdot mm$

$Control\_Strain = "Normal\ reinforced"$ $\varepsilon_{ud} = 0.068$

C.6.3 Minimum and surface reinforcement

According to NF-P-18-710 ch (7.3.2), the minimum reinforcement is not required in structural member of UHPFRC because it is assumed that UHPFRC is sufficiently ductile under tension where UHPFRC fulfill the following condition:

$$\frac{1}{w_{0.3}} \int_0^{w_{0.3}} \frac{\sigma(w)}{1.25} dw \geq \max(0.4 f_{ctmel}; 3\ MPa)$$

NF P18-710 ch 1.1

Surface reinforcement is not apply according to NF P-18-710 ch 9.2.4

$M_{Rd.bot} := F_c \cdot x_c + F_{s.bot} \cdot x_{s.bot} - N_{Ed.max} \cdot \left(\frac{h}{2} - x_{bot} \right)$

$M_{Rd.bot} = 427.661 \cdot kN \cdot m$

Check moment capacity

$\eta_{bot} := \frac{M_{Ed.max}}{M_{Rd.bot}} = 80 \cdot \%$

$s_b := \frac{\pi \cdot \phi_{s.bot}^2}{4 \cdot A_{s.bot}} \cdot m = 98.175 \cdot mm$

Ductility

$xd_{bot} := \frac{x_{bot}}{d_{bot}} = 0.059$

C.6.4 Calculation of moment resistance for top edge MRd, top

$M_{Ed.min} := 28.29kN \cdot m$ $N_{Ed.min} := -260.5kN$ $A_{s.top} := 1340.4mm^2$

$d'_{top} := c_{nom} + \frac{1}{2} \cdot \phi_{s.top} + \phi_{stirup}$ $d_{top} := h - d'_{top}$

$d_{top} = 312.5 \cdot mm$ $d'_{top} = 52.5 \cdot mm$

Calculation of compressive zone

$x_{top} := 10.8717mm$ Assumed compressive depth.

$\varepsilon_{cud} = 0.276 \cdot \%$ Assume that the compressive strain reachs ultimate design strain

$F_c := f_{cd} \cdot \left[\frac{\left(\frac{\varepsilon_{c0d}}{2} \right) + \left(\varepsilon_{cud} - \varepsilon_{c0d} \right)}{\varepsilon_{cud}} \right] \cdot x_{top} \cdot b$ $F_c = 843.283 \cdot kN$

$x_1 := \frac{\varepsilon_{c0d}}{\varepsilon_{cud}} \cdot x_{top}$ $x_1 = 6.862 \cdot mm$

$x_2 := x_{top} - x_1 = 4.01 \cdot mm$

$x_c := \frac{\left(\frac{x_1 \cdot 2}{3} \right) \cdot \frac{x_1}{2} + \left(x_1 + \frac{x_2}{2} \right) \cdot x_2}{\frac{x_1}{2} + x_2}$ $x_c = 6.888 \cdot mm$

Reinforcement

$F_{s.top} := f_{yd} \cdot A_{s.top}$

$F_{s.top} = 582.783 \cdot kN$ Force of the reinforcement

$x_{s.top} := d_{top} - x_{top}$

$x_{s.top} = 301.628 \cdot mm$ Lever arm to the neutral axis of steel force

Horizontal equilibrium

$F_c - F_{s.top} + N_{Ed.min} = 0.115 \cdot N$ Close to Zero

Assume yielding $\varepsilon_{s.top} > \varepsilon_{sy}$

$\varepsilon_{s.top} := \text{if}\left(x_{top} > 0, \frac{d_{top} - x_{top}}{x_{top}} \cdot \varepsilon_{cud}, \varepsilon_{sy}\right) = 0.0766$

$\text{Control}_{\varepsilon.s.top} := \text{if}\left(\varepsilon_{s.top} > \varepsilon_{sy}, \text{"OK"}, \text{"Not OK"}\right)$

$\text{Control}_{\varepsilon.s.top} = \text{"OK"}$

Con troll of strain limit in reinforcement

$\text{Control\_Strain} := \begin{cases} \text{"Normal reinforced"} & \text{if } \varepsilon_{sy} < \varepsilon_{s.top} < \varepsilon_{ud} \\ \text{"Not Normal Reinforced"} & \text{otherwise} \end{cases}$

$\varepsilon_{ud} = 0.068$

$\text{Control\_Strain} = \text{"Not Normal Reinforced"}$

$M_{Rd.top} := F_c \cdot x_c + F_{s.top} \cdot x_{s.top} - N_{Ed.min} \cdot \left(\frac{h}{2} - x_{top}\right)$

$M_{Rd.top} = 226.301 \cdot kN \cdot m$

Check moment capacity

$\eta_{bot} := \frac{M_{Ed.min}}{M_{Rd.top}} = 12.501 \cdot \%$

Ductility

$xd_{top} := \frac{x_{top}}{d_{top}} = 0.035$

$xd_{max} := 0.3$ According to SS-EN 1992-2:2005 section 5.6.3 , $\frac{x}{d}$ should not be larger than 0.3

$\eta_{xd} := \frac{\max\left(xd_{top}, xd_{bot}\right)}{xd_{max}} = 20 \cdot \%$

Shear reinforcement

Shear force must always be checked against the shear capacity or shear stress capacity of the section. But according to SS-EN 1992-1-1:2005, Ch. 6.2.1. Shear force have not to be checked at distance less than d from the support when a uniformly distributed load is applied on the member. The shear force depends on the support conditions of the beam and the location of the load on the member. The first axle force is located at a distance d from the support, while the shear reinforcement is designed for the shear force at the support because the shear force is maximum.

In this case the shear reinforcement is designed at x= 1200mm.

ULS new Shear for optimized cross section in UHPC

$V_{Ed.conv} := 555.9kN$ (Konstructionsberäkningar Bro 100-2990-1, Appendix 4.1.B)

$L := 6000mm$ Free span length

$h = 365 \cdot mm$ Height of UHPC cross section (optimized)

$\rho_c = 25 \cdot \frac{kN}{m^3}$

$\rho_{UHPC} = 24.4 \cdot \frac{kN}{m^3}$ density of concrete

$b := 1000mm$

$q_c := h \cdot \rho_{UHPC} = 8.906 \cdot \frac{kN}{m^2}$ Load coming from UHPC

$V_c := \frac{q_c \cdot L \cdot b}{2} = 26.718 \cdot kN$ Shear force from UHPC

$h_1 := 579mm$ Height of conventional concrete cross section (original height)

$q_{c1} := h_1 \cdot \rho_c = 1.447 \times 10^4 Pa$ Load coming from conventional concrete

$V_{c.1} := \frac{q_{c1} \cdot L \cdot b}{2} = 43.425 \cdot kN$ Shear coming from conventional concrete

$V_{Ed.ULS.max} := \left[V_{Ed.conv} - \left(V_{c.1} \cdot 1.35\right)\right] + V_c \cdot 1.35 = 533.346 \cdot kN$ New shear force of UHPC cross section

Input:

$V_{Ed} := V_{Ed.ULS.max} = 533.346 \cdot kN$ $N_{Ed} := 231kN$ (compression)

$h = 365 \cdot mm$ $b_w := 1m$ $d_{bot} = 310.5 \cdot mm$ $A_{sl} := 3272.5mm^2$ $f_{yd} = 434.783 \cdot MPa$

$f_{ck} = 200 \cdot MPa$

$f_{ctfd} = 6.154 \cdot MPa$ Design post-cracking strength

$f_{ctd.el.SLS} := f_{ctk.el} = 10 \cdot MPa$ Design tensile limit of elasticity,

$\varepsilon_{el} := \frac{f_{ctd.el.SLS}}{E_{cm}}$ $\varepsilon_{el} = 0.000154$ Strain at the maximum limit of elasticity

$\varepsilon_{u.lim} = 0.009375$ Ultimate strain in tension

Calculation of $V_{Rd.c}$

$\gamma_E := 1.1538$

$\gamma_{cf} \cdot \gamma_E = 1.5$

$\sigma_{cp} := \frac{N_{Ed}}{h \cdot b} = 0.633 \cdot MPa$

$Control_{\sigma.cp} := if\left(0 \le \sigma_{cp} \le 0.4 \cdot f_{ck}, "OK" , "Not\ \ OK"\right)$ NF-P-18-710, Ch 6.2

$Control_{\sigma.cp} = "OK"$

$k := 1 + 3 \cdot \frac{\sigma_{cp}}{f_{ck}}$

$V_{Rd.c} := \frac{0.18}{\left(\gamma_{cf} \cdot \gamma_E\right)} \cdot k \cdot \left(\frac{f_{ck}}{MPa}\right)^{\frac{1}{2}} \cdot MPa \cdot b \cdot h$ UHPC contribution term $V_{Rd.c} = 625.331 \cdot kN$

Calculation of $V_{Rd.s}$

Assume no shear reinforcement

$V_{Rd.s} := 0$

Calculation of $V_{Rd.f}$

$d := \frac{7}{8} \cdot h$

lever arm of the internal forces

$z := 0.9 \cdot d$ $z = 287.437 \cdot mm$ NF-P-18-710 Eq (6.203)

$A_{fv} := b \cdot z = 0.287\,m^2$ For a rectangular section NF-P-18-710 Eq (6.203)

$\varepsilon := \varepsilon_{u.lim} = 0.938 \cdot \%$ NF-P-18-710 Eq (6.214)

$\varepsilon_{ud} = 0.068$ $\varepsilon_{u.lim} = 0.938 \cdot \%$

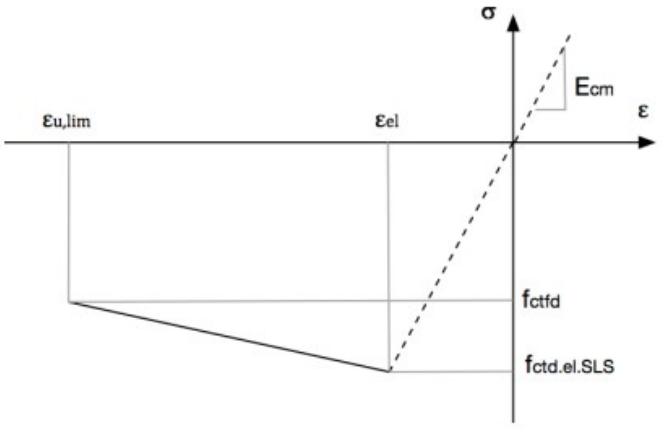

Figure Law for UHPFRC

$$\sigma_{Rd.f} := \frac{1}{K_{global} \cdot \gamma_{cf}} \cdot \frac{1}{\varepsilon - \varepsilon_{el}} \cdot \int_{\varepsilon_{el}}^{\varepsilon} \sigma_f(\varepsilon)\, d\varepsilon$$ NF-P-18-710 Eq (6.214)

$$\int_{\varepsilon_{el}}^{\varepsilon} \sigma_f(\varepsilon)\, d\varepsilon := f_{ctfd} \cdot \left(\frac{\varepsilon_{u.lim} - \varepsilon_{el}}{\varepsilon_{u.lim}} \right) + \left(f_{ctd.el.SLS} - f_{ctfd} \right) \cdot \left(\frac{\varepsilon_{u.lim} - \varepsilon_{el}}{2\varepsilon_{u.lim}} \right)$$

$$f_{ctfd} \cdot \left(\frac{\varepsilon_{u.lim} - \varepsilon_{el}}{\varepsilon_{u.lim}} \right) + \left(f_{ctd.el.SLS} - f_{ctfd} \right) \cdot \left(\frac{\varepsilon_{u.lim} - \varepsilon_{el}}{2\varepsilon_{u.lim}} \right) = 7.944 \cdot MPa$$

$$\sigma_{Rd.f} := \frac{1}{K_{global} \cdot \gamma_{cf}} \cdot \frac{1}{\frac{(\varepsilon - \varepsilon_{el})}{\%}} \cdot \left[f_{ctfd} \cdot \left(\frac{\varepsilon_{ud} - \varepsilon_{el}}{\varepsilon_{ud}} \right) + \left(f_{ctd.el.SLS} - f_{ctfd} \right) \cdot \left(\frac{\varepsilon_{ud} - \varepsilon_{el}}{2\varepsilon_{ud}} \right) \right]$$

$\sigma_{Rd.f} = 5.378 \cdot MPa$

Inclination of the main compression stress on the longitudinal axis

$\theta := 30°$ NF-P-18-710 Eq (6.208)

$V_{Rd.f} := A_{fv} \cdot \sigma_{Rd.f} \cdot \cot(\theta)$ shear resistance from fibres $V_{Rd.f} = 2677.444 \cdot kN$

Total shear resistance

$V_{Rd} := V_{Rd.c} + V_{Rd.s} + V_{Rd.f}$

$V_{Rd} = 3302.775 \cdot kN$

Calculation of $V_{Rd.max}$

$$V_{Rd.max} := 2.3 \cdot b \cdot z \cdot \left(\frac{f_{ck}}{MPa} \right)^{\frac{2}{3}} \cdot MPa \cdot \tan(\theta)$$

NF-P-18-710 Eq (6.215)

$V_{Rd.max} = 13053.610 \cdot kN$

Design of shear force resistance

$V_{Rd} := \min(V_{Rd.max}, V_{Rd})$

$V_{Rd} = 3302.775 \cdot kN$

$Control\_Shear := \text{if}(V_{Rd} > V_{Ed}, \text{"Sufficient capacity"}, \text{"NOT Sufficient cappacity"})$

Control_Shear = "Sufficient capacity"

$$\eta_{Shear} := \frac{V_{Ed}}{V_{Rd}} = 16 \cdot \%$$

NO shear reinforcement needed.

C.6.5 Crack control

Cracking will be checked at coordinate x=3600mm (middle of the bridge) where maximum moment occurs.The calculation will be made for 1m strip. First, a check is made with accordance to SS-EN 1992-1-1:2005 to determine if the cross section is cracked or not, if the cross section is cracked, the crack width will be controlled.

Frequent load combination is used to determine if the cross section is cracked while Quasi-permanent load combination is used to con troll the crack width.

Design moment and load combination are obtained from Case study provided by AFRY for the bridge 100-2990-1 where the moments are modified to be suitable with the new cross section dimensions (HPC cross section).

SLS new moment for optimized cross section in UHPC

x=3.60m

Design moment value of applied load, obtained from SLS- Quasi-permanent load combination for conventional concrete's cross section

Input:

$M_{Ed.Q.conv.} := 130.9kN \cdot m$ (Konstructionsberäkningar Bro 100-2990-1, Appendix 4.1.B)

$M_{Ed.F.conv} := 244kN \cdot m$ (Konstructionsberäkningar Bro 100-2990-1, Appendix 4.1.B)

$M_{Ed.sw.uhpc} := \frac{G_{s.UHPC}}{G_{s.con}} \cdot M_{Ed.sw.conv}$ Moment due to self-weight of HPC cross section

$M_{Ed.sw.uhpc} = 24.284 \cdot kN \cdot m$

New design moment value of applied load, in SLS Quasi-permanent load combination for HPC cross section with optimized thickness

$M_{Ed.Q} := M_{Ed.Q.conv.} - (M_{Ed.sw.conv}) + M_{Ed.sw.uhpc} = 114.284 \cdot kN \cdot m$

New design moment value of applied load, in SLS frequent load combination for HPC cross section with optimized thickness

$M_{Ed.F} := M_{Ed.F.conv} - (M_{Ed.sw.conv}) + M_{Ed.sw.uhpc} = 227.384 \cdot kN \cdot m$

Input:

$M_{Ed.Q} = 114.284 \cdot kN \cdot m$

Axial force quasi-permanent at x=3600 mm

$N_{Ed.Q} := 23.3kN$

(Konstructionsberäkningar Bro 100-2990-1, Appendix 4.1.B)

Axial force frequent at x=3600 mm

$N_{Ed.F} := -29kN$

(Konstructionsberäkningar Bro 100-2990-1, Appendix 4.1.B)

$M_{Ed.F} = 227.384 \cdot kN \cdot m$

$\alpha_{ef} := \frac{E_s}{E_{cm}} = 3.077$

Ratio between steel modulus of elasticity and concrete modulus of elasticity

$\varphi := 1$

Creep coefficient. SS-EN 1992-1-1:2005,Ch. 3.1.4 Figure 3.1.

Bottom reinforcement diameter

$\phi_{s.bot} := 20mm$

(Konstructionsberäkningar Bro 100-2990-1, Appendix 4.1.B)

$E_s = 200 \cdot GPa$ $E_{cm} = 65 \cdot GPa$ $b := 1000mm$ $d_{bot} = 310.5 \cdot mm$

$A_{s.bot} = 3200 \cdot mm^2$ $h := 365mm$ $f_{ctd.el.SLS} = 10 \cdot MPa$

$\alpha_{ef} := \frac{E_s}{E_{cm}} = 3.077$ $\alpha_{eff} := \frac{E_s}{E_{cm}} \cdot (1 + \varphi) = 6.154$

Transformed moment of inertia

$A_I := b \cdot h + (\alpha_{ef} - 1) \cdot A_{s.bot} = 0.372\,m^2$

$x_I := \frac{\frac{b \cdot h^2}{2} + (\alpha_{ef} - 1) \cdot A_{s.bot} \cdot d_{bot}}{A_I} = 184.789 \cdot mm$

$I_I := \frac{b \cdot h^3}{12} + b \cdot h \cdot \left(\frac{h}{2} - x_I\right)^2 + (\alpha_{ef} - 1) \cdot A_{s.bot} \cdot (d_{bot} - x_I)^2 = 4.159 \times 10^{-3}\,m^4$

Cracking moment

$M_{cr} := \frac{I_I \cdot \left(f_{ctd.el.SLS} - \frac{N_{Ed.F}}{A_I}\right)}{h - x_I} = 232.597 \cdot kN \cdot m$

$$\alpha_{eff} := \frac{E_s}{E_{cm}} \cdot (1 + \varphi) = 6.154$$

Check if cross section cracks:

Cross_section_Cracks := if$\left(M_{cr} \le M_{Ed.F}, \text{"YES"}, \text{"NO"}\right)$

Cross_section_Cracks = "NO"

C.6.6 Deflection Control

The control of deflection due to traffic load is obtained from the characteristic load combination.
The deformation requirement will be checked according to SS-EN 1990.

Since the deflection is linear between the cross section I (conventional concrete) and cross section II (HPC), the deflection of HPC section will be calculated by liner interpolation where the deflection of cross section I will be obtained from case study given from AFRY. The cross section in the middle of the span does not cracks according to calculation in previous section, thus the deflection is obtained from the cross section properties on stage I of UHPC.

The deflection is checked in the middle of the span where maximum deflection is expected. The deflection is calculated for 1m strip.

Input Data

$L_s := 6600mm$ $E_s := 200GPa$ $h = 365 \cdot mm$ $b := 1000mm$ $A_{s.bot} = 3200.000 \cdot mm^2$

Characteristic moment from LM71 (train load)

$M_{Ed.ch} := 125.70kN \cdot m$ (Konstructionsberäkningar Bro 100-2990-1, Appendix 4.1.F)

Moment of inertia of the cross section (conventional concrete), Stage II (cracked section)

$I_{Ieff} := 0.01m^4$ (Konstructionsberäkningar Bro 100-2990-1, Appendix 4.1.B)

$E_{cm.1} := 34GPa$ Elastic modulus of concrete C35/45

$E_{cm.2} := 65GPa$ Elastic modulus of UHPC

$$\alpha_{eff} := \frac{E_s}{E_{cm.2}} = 3.077$$

The maximum allowed vertical deflection due to characteristic traffic load according to

$$\delta_{max.1} := \frac{L_s}{600} = 11\cdot mm$$ SS-EN 1990 (A2.4.4.3.2)

The maximum allowed vertical deflection due to characteristic traffic load with regard to passenger comfort according to TDOK 2016:204, ch B3.4.2.2.
The design value of train speed for this bridge is 160km/h

The studied bridge is a frame- bridge and can be assumed as continuous bridge with minimum 3 spans.

Comfort level is assumed to be (Good)

$b_v := 1.3$ SS-EN 1990, Table (A2.9)

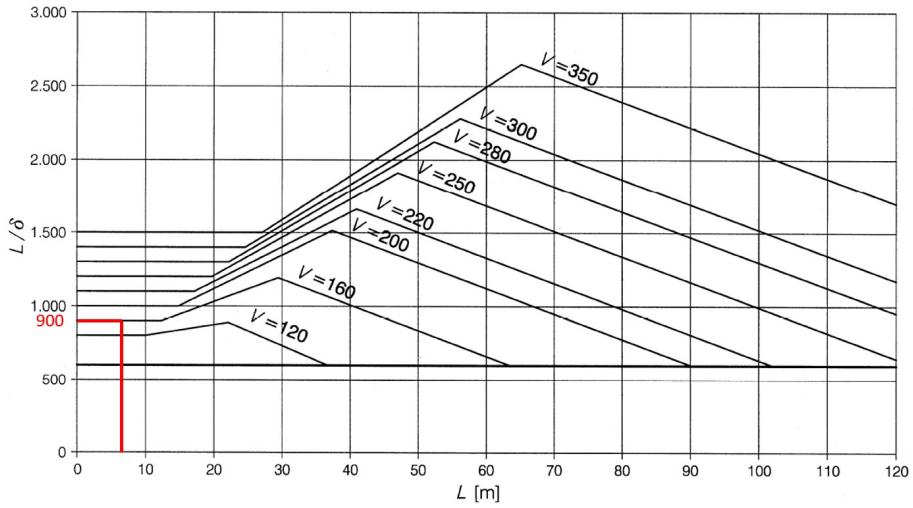

Figure Comfort level

$$\delta_{max.2} := \frac{L_s}{0.9\cdot\frac{900}{1.3}} = 10.593\cdot mm$$

Calculation moment of inertia for the uncracked section of (UHPC), stage I

Transformed cross-section area of UHPC

$$A_{I.2} := b\cdot h + (\alpha_{ef} - 1)\cdot A_{s.bot}$$ $A_{I.2} = 0.372\,m^2$

Transformed centre of gravity from the top.

$$x_{I.2} := \frac{\frac{b\cdot h^2}{2} + (\alpha_{ef} - 1)\cdot A_{s.bot}\cdot d_{bot}}{A_{I.2}}$$ $x_{I.2} = 184.789\cdot mm$

Moment of inertia.

$$I_{I.2} := \frac{b\cdot h^3}{12} + b\cdot h\cdot\left(\frac{h}{2} - x_I\right)^2 + (\alpha_{ef} - 1)\cdot A_{s.bot}\cdot(d_{bot} - x_I)^2$$ $I_{I.2} = 4.159\times 10^9\cdot mm^4$

Maximum characteristic vertical deflection due to Load model 71 (Conventional concrete)

$\delta_I := 1.72mm$ (Konstructionsberäkningar Bro 100-2990-1, Appendix 4.3)

$$\delta_{II} := \delta_I \cdot \frac{E_{cm.2} \cdot I_{I.2}}{I_{Ieff} \cdot E_{cm.1}} = 1.368 \cdot mm$$

Utilization ration of deflection

$$\eta_\delta := \frac{\delta_{II}}{\delta_{max.2}} = 12.911 \cdot \%$$ OK

C.6.7 Amount of concrete

$h = 365 \cdot mm$

$b_{tot} := 7670mm$

$$\rho_{UHPC} = 24.4 \cdot \frac{kN}{m^3}$$

$$m_c := h \cdot b_{tot} \cdot \left(\rho_{UHPC} - 1 \frac{kN}{m^3} \right) \cdot \frac{1}{9.81N} \cdot kg \qquad m_c = 6677.826 \frac{kg}{m}$$